# Lecture Notes on Condensed Matter Physics

*Course PH 208*

---


## Aveek Bid


These notes draw on the following excellent references:

1. N. W. Ashcroft and N. D. Mermin, *Solid State Physics*
2. J. Sólyom, *Fundamentals of the Physics of Solids*


Department of Physics
Indian Institute of Science, Bangalore, India

# Contents

# List of Figures

# Chapter 1

# Crystal lattice

## 1.1 Introduction

**How does one construct a crystal?** The construction of a crystal proceeds through three fundamental steps:

1. Define the lattice
2. Specify the lattice constants
3. Define the basis

### Definition of a Lattice

A **lattice** is a mathematical construct: an ideally infinite, periodic arrangement of points in space. It contains no physical content by itself—it merely encodes translational symmetry.

A particularly important class is the **Bravais lattice**, defined as an infinite array of discrete points such that the local environment of every point is identical.

Mathematically, a Bravais lattice consists of points with position vectors

$$\mathbf{R} = n_1\mathbf{a}_1 + n_2\mathbf{a}_2 + n_3\mathbf{a}_3 \tag{1.1}$$

where:

- $\mathbf{a}_1, \mathbf{a}_2, \mathbf{a}_3$ are three non-coplanar vectors (primitive vectors),
- $n_1, n_2, n_3 \in \mathbb{Z}$ span all integers.

Associated with a Bravais lattice is a set of **primitive vectors** $\{\mathbf{a}_i\}$, which generate all lattice points through integer linear combinations.

A key property of the Bravais lattice is **translational symmetry**. Any point $\mathbf{r}$ in the lattice can be translated to another equivalent point $\mathbf{r}'$ via

$$\mathbf{r}' = \mathbf{r} + n_1\mathbf{a}_1 + n_2\mathbf{a}_2 + n_3\mathbf{a}_3 \tag{1.2}$$

This symmetry implies that the lattice looks identical from every lattice point.

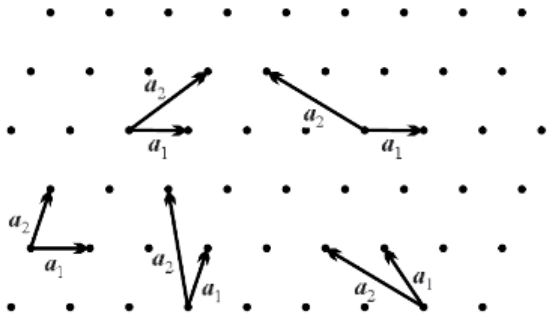


Figure 1.1: Non-universality of primitive vectors

**Important remark:** The choice of primitive vectors is **not unique**. Different sets of $\{\mathbf{a}_i\}$ can generate the same lattice.

## Primitive Cell

The volume defined by the primitive vectors $\mathbf{a}_1, \mathbf{a}_2, \mathbf{a}_3$ is called the **primitive cell** (or unit cell). It is the smallest volume that can tile space through lattice translations.

A defining property is that each primitive cell contains **exactly one lattice point**.

## Definition of Basis

While the lattice is an abstract construct, the **basis** introduces physical content.

The basis is the set of atoms, ions, or molecules attached to each lattice point. Each lattice point carries an identical basis, and the repetition of this combined object generates the full crystal.

## Crystal Structure

The complete crystal is obtained as:

$$\text{Crystal structure} = \text{Lattice} + \text{Basis} \tag{1.1}$$

Thus:

- The lattice encodes symmetry,
- The basis encodes material-specific properties.

### Coordination Number

The **coordination number** is defined as the number of nearest neighbours of a lattice point.

For example, in a simple cubic lattice, the coordination number is 6.

## 1.2 Examples of some important crystal structures

**Simple cubic:** Co-ordination number 6; extremely rare in nature, only one element ($\alpha$-phase of Pollonium) crystallizes in this form.

**Body-centered cubic (BCC):** Co-ordination number 8; quite common in nature, e.g., alkali metals. One can treat it as a simple cubic with a 2-atom basis or a lattice with a single atom basis with primitive lattice vectors defined as $\mathbf{a}_1 = \frac{a}{2}(\hat{y} + \hat{z} - \hat{x})$ and so on.

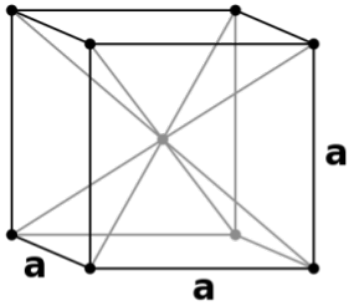


Figure 1.2: BCC structure

**Face-centered cubic (FCC):** Co-ordination number 12; quite common in nature, e.g., noble metals, Ni. One can treat it as a simple cubic with a 4-atom basis or a lattice with a single atom basis with primitive lattice vectors defined as $\mathbf{a}_1 = \frac{a}{2}(\hat{y} + \hat{z})$ and so on.

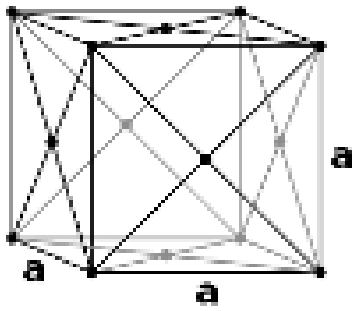


Figure 1.3: FCC structure

**Hexagonal close-packed (HCP):** *Not a Bravais lattice* – many elements ($\sim 30$) crystallize in this form.

Think of stacking balls on top of each other – in some sense, it is the most natural arrangement. In the a-b plane, it forms a close-packed triangular lattice; stack them up

along the c-axis by placing atoms on the alternate voids formed in the lower layer. If the arrangement is ABAB... then we get HCP; the arrangement ABCABC... gives FCC!

Both FCC and HCP are close-packed structures – they can achieve the highest packing density of $\frac{\pi}{3\sqrt{2}} \sim 0.74$. Both have a co-ordination number of 12.

**NaCl structure:** NaCl crystallizes with $Na^+$ and $Cl^-$ placed at alternate sites in a simple cubic lattice. Describe the structure as FCC with a two-point basis – $Na^+$ at the origin and $Cl^-$ at $\frac{a}{2}(\hat{x} + \hat{y} + \hat{z})$.

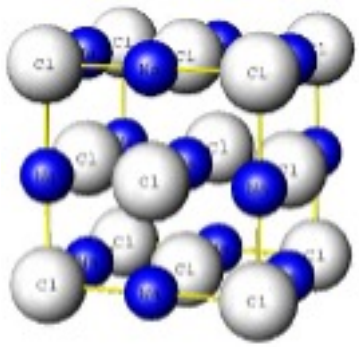

Figure 1.4: NaCl structure

## 1.3 Wigner-Seitz cell

A common choice of unit cell that reflects the full symmetry of the underlying lattice is the Wigner-Seitz cell.

1. Choose a zero point of the lattice.
2. Draw lines from your zero point to all neighboring lattice points.
3. Draw a plane (in two-dimensional systems, a line) that exactly bisects all of your lines at a right angle.
4. A subset of all your planes will form some closed body, and that is your Wigner-Seitz elementary cell.

## 1.4 Reciprocal Lattice

Consider a Bravais lattice consisting of points $\mathbf{R}$. A plane wave with an arbitrary wave-vector $\mathbf{K}$ will, in general, not share the periodicity of the lattice. For the wave to be lattice-periodic, it must satisfy

$$e^{i\mathbf{K}\cdot(\mathbf{R}+\mathbf{r})} = e^{i\mathbf{K}\cdot\mathbf{r}} \tag{1.2}$$

for any position $\mathbf{r}$ and for all lattice vectors $\mathbf{R}$.

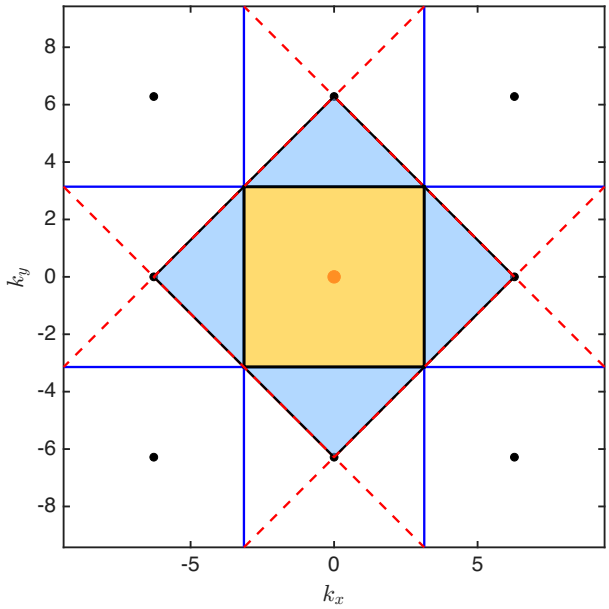


Figure 1.5: Wigner-Seitz cell construction

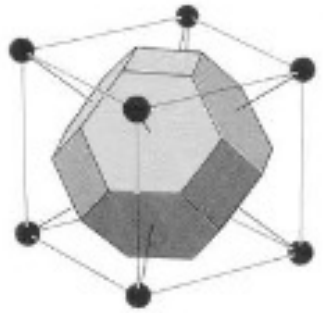

Figure 1.6: Wigner-Seitz cell for BCC structure

This immediately implies the condition

$$e^{i\mathbf{K}\cdot\mathbf{R}} = 1, \tag{1.3}$$

which defines the **reciprocal lattice**.

**Construction of the reciprocal lattice:**

Given a direct lattice with primitive vectors $\mathbf{a}_1, \mathbf{a}_2, \mathbf{a}_3$, the primitive vectors of the reciprocal lattice are defined as

$$\mathbf{b}_i = 2\pi \frac{\mathbf{a}_j \times \mathbf{a}_k}{\mathbf{a}_i \cdot (\mathbf{a}_j \times \mathbf{a}_k)}, \tag{1.4}$$

where $(i, j, k)$ are cyclic permutations of $(1, 2, 3)$.

These vectors satisfy the fundamental orthogonality relation

$$\mathbf{a}_i \cdot \mathbf{b}_j = 2\pi\delta_{ij}, \tag{1.5}$$

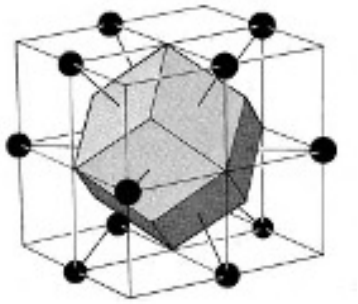

Figure 1.7: Wigner-Seitz cell for FCC structure

which ensures the correct periodicity condition in Eq. (1.3).

**Proof:**

Any reciprocal lattice vector $\mathbf{K}$ can be written as a linear combination of the primitive reciprocal vectors:

$$\mathbf{K} = \sum_i k_i \mathbf{b}_i.$$

Similarly, any direct lattice vector can be written as

$$\mathbf{R} = \sum_i n_i \mathbf{a}_i,$$

where $n_i \in \mathbb{Z}$.

Using the orthogonality relation $\mathbf{a}_i \cdot \mathbf{b}_j = 2\pi\delta_{ij}$, we obtain

$$\mathbf{K} \cdot \mathbf{R} = \sum_{i,j} k_i n_j \mathbf{b}_i \cdot \mathbf{a}_j = 2\pi \sum_i k_i n_i.$$

The condition $e^{i\mathbf{K}\cdot\mathbf{R}} = 1$ for all $\mathbf{R}$ requires

$$\mathbf{K} \cdot \mathbf{R} = 2\pi \times (\text{integer}),$$

which is satisfied for all integers $n_i$ only if all coefficients $k_i$ are integers.

Thus, every reciprocal lattice vector can be written as an integer linear combination of $\mathbf{b}_i$. This shows that:

- The reciprocal lattice is itself a Bravais lattice,
- $\mathbf{b}_i$ are its primitive vectors.

**Note:** The reciprocal of the reciprocal lattice is the original (direct) Bravais lattice.

**Examples of reciprocal lattices:**

1. **Simple cubic (SC):** The reciprocal lattice of a simple cubic lattice with lattice constant $a$ is also simple cubic, with lattice constant $2\pi/a$.

2. **Face-centered cubic (FCC):** The reciprocal lattice of an FCC lattice with a conventional cubic cell of side $a$ is a body-centered cubic (BCC) lattice with a cubic cell of side $4\pi/a$, and vice versa.

**First Brillouin zone:** The Wigner–Seitz cell of the reciprocal lattice is called the **first Brillouin zone**. It plays a central role in the description of electronic states and wave propagation in periodic solids.

## 1.5 Relation between lattice planes and reciprocal lattice points

The direct lattice can be decomposed into families of lattice planes: parallel, equally spaced planes that collectively contain all lattice points.

A fundamental correspondence exists between such families of planes and reciprocal lattice vectors. For every reciprocal lattice vector $\mathbf{K}$, there is an associated family of lattice planes perpendicular to $\mathbf{K}$ with spacing $d$, where

$$|\mathbf{K}| = \frac{2\pi}{d}.$$

Conversely, for every family of lattice planes with spacing $d$, there exist reciprocal lattice vectors perpendicular to the planes, the shortest of which has magnitude $2\pi/d$.

### Proof

Recall that a vector $\mathbf{K}$ belongs to the reciprocal lattice if

$$e^{i\mathbf{K}\cdot\mathbf{R}} = 1$$

for all Bravais lattice vectors $\mathbf{R}$.

Consider a family of equally spaced planes with separation $d$, and let $\mathbf{n}$ be a unit vector normal to these planes. Define

$$\mathbf{K} = \frac{2\pi}{d}\,\mathbf{n}.$$

The plane wave $e^{i\mathbf{K}\cdot\mathbf{r}}$ is constant on any plane perpendicular to $\mathbf{K}$, since $\mathbf{K}\cdot\mathbf{r}$ is constant over such a plane. Moreover, adjacent planes differ in phase by

$$\Delta(\mathbf{K}\cdot\mathbf{r}) = \mathbf{K}\cdot(d\,\mathbf{n}) = 2\pi,$$

so the wave takes the same value on all planes in the family.

Choosing the origin to lie on one of these planes, it follows that for any lattice vector $\mathbf{R}$ (which lies on one of the planes),

$$e^{i\mathbf{K}\cdot\mathbf{R}} = 1.$$

Thus $\mathbf{K}$ is a reciprocal lattice vector.

Furthermore, this is the *shortest* reciprocal lattice vector perpendicular to the planes: any smaller vector would correspond to a wavelength larger than $d$, and hence would not reproduce the periodicity of the lattice planes.

## 1.6 Miller indices

### Definition

A convenient way to label families of lattice planes is to exploit their correspondence with reciprocal lattice vectors. Each family of planes is associated with a *unique* reciprocal lattice vector.

If the shortest reciprocal lattice vector perpendicular to a given family of planes is

$$\mathbf{K} = h\mathbf{b}_1 + k\mathbf{b}_2 + l\mathbf{b}_3,$$

then the planes are labeled by the **Miller indices** $(hkl)$.

### Physical interpretation

A plane with Miller indices $(hkl)$ is perpendicular to the reciprocal lattice vector

$$\mathbf{K} = h\mathbf{b}_1 + k\mathbf{b}_2 + l\mathbf{b}_3,$$

and can be written as

$$\mathbf{K}\cdot\mathbf{r} = C,$$

where $C$ is a constant.

Suppose the plane intersects the real-space lattice axes at

$$n_1\mathbf{a}_1, \quad n_2\mathbf{a}_2, \quad n_3\mathbf{a}_3.$$

Since these points lie on the plane, they satisfy

$$\mathbf{K}\cdot(n_1\mathbf{a}_1) = \mathbf{K}\cdot(n_2\mathbf{a}_2) = \mathbf{K}\cdot(n_3\mathbf{a}_3) = C.$$

Using the orthogonality relation $\mathbf{a}_i\cdot\mathbf{b}_j = 2\pi\delta_{ij}$, we obtain

$$\mathbf{K}\cdot(n_1\mathbf{a}_1) = 2\pi h n_1 = C,$$

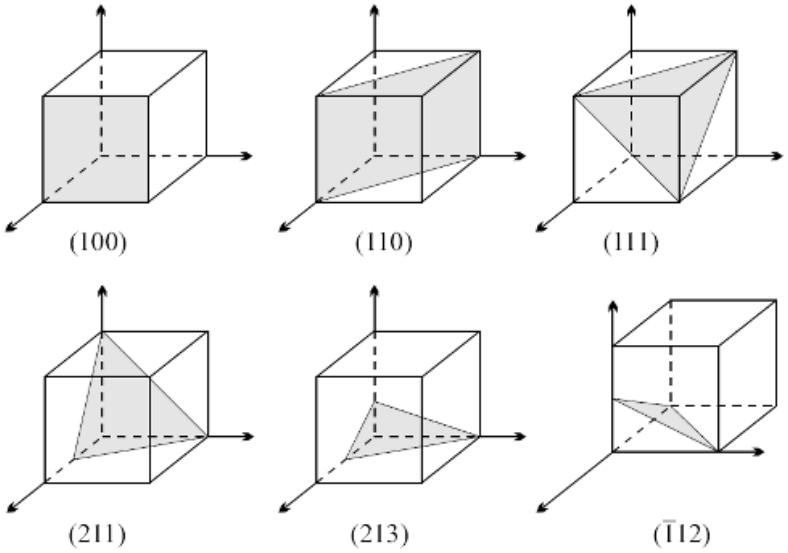


Figure 1.8: Miller indices of some planes for a simple cubic lattice

and similarly for $n_2$ and $n_3$. Hence,

$$n_1 = \frac{C}{2\pi h}, \quad n_2 = \frac{C}{2\pi k}, \quad n_3 = \frac{C}{2\pi l}.$$

Thus, the Miller indices $(hkl)$ are inversely proportional to the intercepts of the plane on the real-space lattice axes.

**Conclusion:** Miller indices provide a compact and physically meaningful labeling of lattice planes, directly tied to reciprocal lattice vectors and therefore to diffraction and wave phenomena in crystals.

# Chapter 2

# Crystal structure from X-ray diffraction

## 2.1 Crystal Structure from X-ray Diffraction

Atomic length scales in solids are of order $\sim 1$ Å. To probe such length scales, one requires radiation with comparable wavelength. X-rays, with wavelengths in the range $\sim 0.1$–$10$ Å, are ideally suited for this purpose.

There are two equivalent formulations of X-ray diffraction in crystals:

- Bragg condition (real-space picture)
- Laue condition (reciprocal-space formulation)

### 2.1.1 Bragg Condition

Bragg interpreted X-ray diffraction as arising from specular reflection of waves from families of lattice planes in a crystal. Constructive interference between waves reflected from successive planes leads to diffraction peaks at specific incident angles and wavelengths.

**Conditions for sharp reflected intensity:**

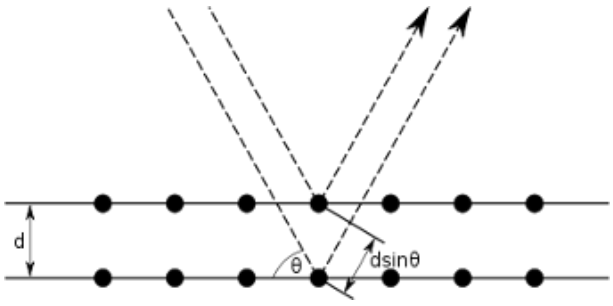


Figure 2.1: Bragg reflection

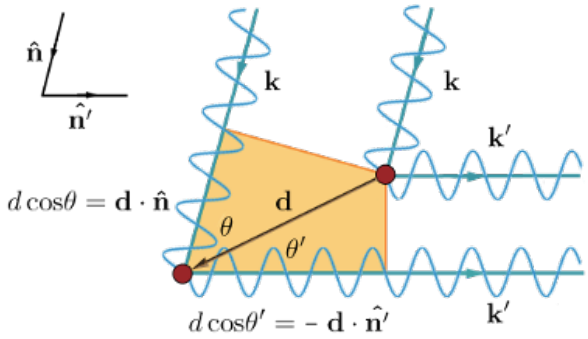


Figure 2.2: Laue scattering

1. The scattering is elastic (no energy loss), so $|\mathbf{k}| = |\mathbf{k}'|$.
2. Waves reflected from adjacent planes interfere constructively.

Consider two rays reflected from adjacent lattice planes separated by a distance $d$. The path difference between them is

$$\Delta = 2d \sin\theta.$$

Constructive interference requires

$$2d \sin\theta = n\lambda,$$

which is the **Bragg condition**.

### 2.1.2 Laue Condition

The Bragg formulation relies on decomposing the crystal into families of lattice planes. A more general formulation is obtained in terms of reciprocal lattice vectors.

Consider an incident plane wave with wave vector $\mathbf{k}$ scattered into $\mathbf{k}'$ by atoms located at lattice sites $\mathbf{R}$.

The phase difference between waves scattered from two lattice sites separated by $\mathbf{R}$ is

$$\Delta\phi = (\mathbf{k}' - \mathbf{k}) \cdot \mathbf{R}.$$

Constructive interference requires

$$(\mathbf{k}' - \mathbf{k}) \cdot \mathbf{R} = 2\pi m, \quad m \in \mathbb{Z},$$

for all lattice vectors $\mathbf{R}$.

Thus,

$$e^{i(\mathbf{k}'-\mathbf{k})\cdot\mathbf{R}} = 1 \quad \forall \mathbf{R}.$$

This implies

$$\mathbf{K} = \mathbf{k}' - \mathbf{k}$$

must be a **reciprocal lattice vector**. Therefore, the Laue condition is

$$\mathbf{k}' - \mathbf{k} = \mathbf{K}.$$

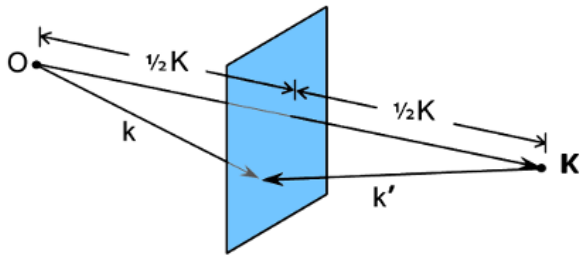


Figure 2.3: Geometrical interpretation of Laue scattering

**Geometrical Interpretation**

From $\mathbf{k}' = \mathbf{k} + \mathbf{K}$ and $|\mathbf{k}| = |\mathbf{k}'|$, we obtain

$$|\mathbf{k} + \mathbf{K}|^2 = |\mathbf{k}|^2.$$

Expanding,

$$|\mathbf{k}|^2 + 2\mathbf{k} \cdot \mathbf{K} + |\mathbf{K}|^2 = |\mathbf{k}|^2,$$

which gives

$$\mathbf{k} \cdot \mathbf{K} = -\frac{|\mathbf{K}|^2}{2}.$$

Equivalently,

$$\mathbf{k} \cdot \mathbf{K} = \frac{|\mathbf{K}|^2}{2}$$

(depending on sign convention).

This implies that diffraction occurs when the tip of $\mathbf{k}$ lies on a plane perpendicular to $\mathbf{K}$ and bisecting the segment joining the origin to $\mathbf{K}$. This plane is called the **Bragg plane**.

### 2.1.3 Equivalence of Bragg and Laue Pictures

The Laue condition $\mathbf{k}' - \mathbf{k} = \mathbf{K}$ can be interpreted as Bragg reflection from planes perpendicular to $\mathbf{K}$.

The magnitude of $\mathbf{K}$ is related to the spacing $d$ between these planes by

$$|\mathbf{K}| = \frac{2\pi}{d}.$$

From the scattering geometry,

$$|\mathbf{K}| = 2|\mathbf{k}| \sin\theta = \frac{4\pi}{\lambda} \sin\theta.$$

Combining,

$$\frac{2\pi}{d} = \frac{4\pi}{\lambda} \sin\theta \quad \Rightarrow \quad 2d \sin\theta = \lambda.$$

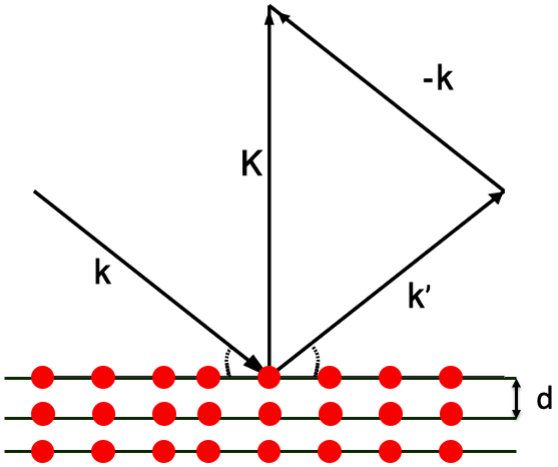


Figure 2.4: Equivalence of Bragg and Laue pictures

This is the Bragg condition for $n = 1$. Higher orders correspond to $\mathbf{K}$ being multiples of the shortest reciprocal lattice vector.

Thus:

- Laue scattering corresponds to momentum transfer $\mathbf{K}$
- Bragg reflection corresponds to diffraction from planes perpendicular to $\mathbf{K}$

### 2.1.4 Ewald Construction

The reciprocal lattice consists of discrete points. The Laue condition is therefore not satisfied for arbitrary $\mathbf{k}$ and $\mathbf{k}'$.

A convenient geometrical construction to determine allowed diffraction conditions is the **Ewald construction**.

Procedure:

- Draw the incident wave vector $\mathbf{k}$ from the origin.
- Construct a sphere of radius $|\mathbf{k}|$ centered at the tip of $\mathbf{k}$.
- Any reciprocal lattice point lying on the surface of this sphere satisfies

$$\mathbf{k}' - \mathbf{k} = \mathbf{K},$$

  and hence produces a diffraction peak.

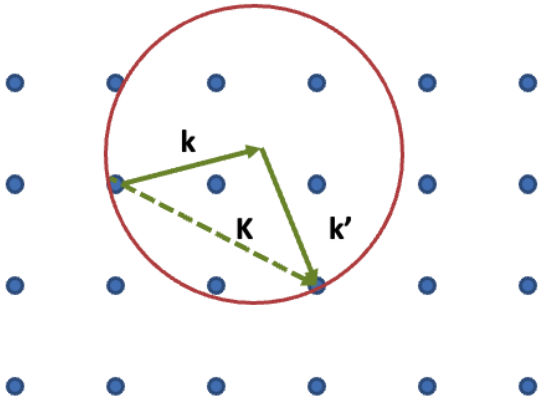


Figure 2.5: Ewald Construction

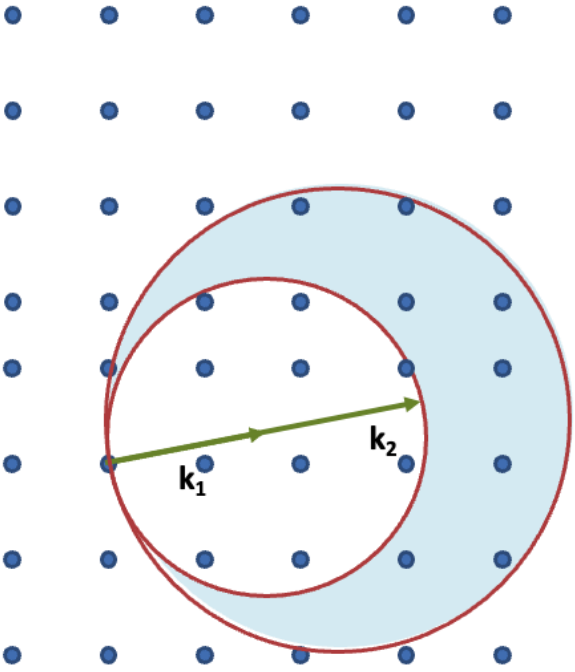


Figure 2.6: Laue method

### 2.1.5 Experimental Methods for Observing Diffraction

**Laue Method**

- Incident direction fixed
- Wavelength varied (polychromatic radiation)
- Ewald sphere sweeps a range of radii
- All reciprocal lattice points within this range produce diffraction

Best suited for single crystals.

**Rotating Crystal Method**

- Wavelength fixed
- Crystal rotated about an axis
- Reciprocal lattice rotates accordingly
- Diffraction occurs when reciprocal points intersect the Ewald sphere

**Debye–Scherrer (Powder) Method**

- Powder sample with randomly oriented crystallites
- Fixed wavelength and incident direction
- Equivalent to sampling all crystal orientations
- Produces concentric diffraction rings

## 2.2 Geometrical structure factor

In kinematic diffraction (X-ray, neutron, electron), the intensity of a Bragg peak at reciprocal lattice vector $\mathbf{G}$ is proportional to

$$I(\mathbf{G}) \propto |F(\mathbf{G})|^2, \tag{2.1}$$

where $F(\mathbf{G})$ is the structural structure factor defined as

$$F(\mathbf{G}) = \sum_j f_j \exp(-i\mathbf{G} \cdot \mathbf{r}_j), \tag{2.2}$$

with $f_j$ the atomic form factors and $\mathbf{r}_j$ the positions of the atoms within the unit cell. The structure factor encodes interference between atoms in the basis and is responsible for extinction rules in diffraction patterns.

### 2.2.1 Simple Cubic (SC) Lattice

#### Lattice and Basis

The simple cubic lattice has primitive vectors

$$\mathbf{a}_1 = a\hat{x}, \quad \mathbf{a}_2 = a\hat{y}, \quad \mathbf{a}_3 = a\hat{z}, \tag{2.3}$$

and a single-atom basis

$$\mathbf{r}_1 = (0, 0, 0). \tag{2.4}$$

#### Structure Factor

For SC:

$$F_{\mathrm{SC}}(\mathbf{G}) = f. \tag{2.5}$$

There are no systematic absences. All reciprocal lattice vectors give non-zero intensity (modulo the form factor decay).

### 2.2.2 Body-Centered Cubic (BCC) Lattice

#### Basis

The BCC lattice can be written as SC Bravais lattice with basis

$$\mathbf{r}_1 = (0, 0, 0), \qquad \mathbf{r}_2 = \frac{a}{2}(1, 1, 1). \tag{2.6}$$

#### Structure Factor

$$F_{\mathrm{BCC}}(\mathbf{G}) = f\left[\exp(-i\mathbf{G}\cdot\mathbf{r}_1) + \exp(-i\mathbf{G}\cdot\mathbf{r}_2)\right]. \tag{2.7}$$

With $\mathbf{G} = \frac{2\pi}{a}(h, k, l)$,

$$\mathbf{G}\cdot\mathbf{r}_2 = \pi(h + k + l). \tag{2.8}$$

Thus

$$F_{\mathrm{BCC}} = f\left[1 + (-1)^{h+k+l}\right]. \tag{2.9}$$

#### Selection Rule

- $h + k + l$ even $\Rightarrow F_{\mathrm{BCC}} = 2f$ (allowed)
- $h + k + l$ odd $\Rightarrow F_{\mathrm{BCC}} = 0$ (extinct)

### 2.2.3 Face-Centered Cubic (FCC) Lattice

#### Basis

FCC basis:

$$\mathbf{r}_1 = (0,0,0), \tag{2.10}$$
$$\mathbf{r}_2 = \frac{a}{2}(0,1,1), \tag{2.11}$$
$$\mathbf{r}_3 = \frac{a}{2}(1,0,1), \tag{2.12}$$
$$\mathbf{r}_4 = \frac{a}{2}(1,1,0). \tag{2.13}$$

#### Structure Factor

$$F_{\text{FCC}}(\mathbf{G}) = f\left[1 + e^{-i\pi(k+l)} + e^{-i\pi(h+l)} + e^{-i\pi(h+k)}\right]. \tag{2.14}$$

Since $e^{-i\pi n} = (-1)^n$, we obtain:

#### Selection Rule

- $h, k, l$ all even or all odd $\Rightarrow F_{\text{FCC}} = 4f$
- mixed parity $\Rightarrow F_{\text{FCC}} = 0$

## Comparison

| Lattice | Structure Factor | Allowed Reflections |
|---|---|---|
| SC | $f$ | all $(hkl)$ |
| BCC | $2f$ | $h+k+l$ even |
| FCC | $4f$ | $h, k, l$ all even or all odd |

## 2.3 Example Diffraction Calculations

We illustrate how selection rules manifest in experimentally observable powder diffraction patterns.

### 2.3.1 Bragg Condition and $d$-Spacing

For cubic systems,

$$d_{hkl} = \frac{a}{\sqrt{h^2 + k^2 + l^2}}, \tag{2.15}$$

and Bragg's law yields

$$2d_{hkl}\sin\theta = \lambda. \tag{2.16}$$

Powder diffractometers report $2\theta$.

We use Cu K$\alpha$ radiation with wavelength $\lambda = 1.5406\,\text{Å}$.

### 2.3.2 Simple Cubic Example: Po ($a = 3.345\,\text{Å}$)

Reflections (all allowed):

$$\begin{aligned}(100): &\quad 2\theta = 26.56^\circ,\\ (110): &\quad 2\theta = 38.04^\circ,\\ (111): &\quad 2\theta = 46.84^\circ,\\ (200): &\quad 2\theta = 54.72^\circ.\end{aligned}$$

### 2.3.3 BCC Example: $\alpha$-Fe ($a = 2.866\,\text{Å}$)

BCC selection rule: $h + k + l$ even.

Allowed reflections and peak positions:

$$\begin{aligned}(110): &\quad 2\theta = 44.18^\circ,\\ (200): &\quad 2\theta = 64.94^\circ,\\ (211): &\quad 2\theta = 82.48^\circ,\\ (220): &\quad 2\theta = 103.56^\circ.\end{aligned}$$

Forbidden examples:

$$(100), (111) \quad \text{extinct.}$$

### 2.3.4 FCC Example: Cu ($a = 3.615\,\text{Å}$)

FCC rule: $(hkl)$ all even or all odd.

Allowed reflections:

$$\begin{aligned}(111): &\quad 2\theta = 43.34^\circ,\\ (200): &\quad 2\theta = 49.90^\circ,\\ (220): &\quad 2\theta = 65.48^\circ,\\ (311): &\quad 2\theta = 88.18^\circ.\end{aligned}$$

Mixed parity examples such as (100), (110), (210) are extinct.

### 2.3.5 Diagnostic First Peak Rule

A common identification shortcut:

$$\begin{aligned} \text{SC}: &\quad (100) \text{ first peak}, \\ \text{BCC}: &\quad (110) \text{ first peak}, \\ \text{FCC}: &\quad (111) \text{ first peak}. \end{aligned}$$

## 2.4 Intensity Considerations

True peak intensities in experiments depend also on:

- atomic form factors $f(\mathbf{G})$,
- multiplicity of crystallographic planes,
- Lorentz–polarization factors,
- Debye–Waller factors $e^{-2W}$,
- instrumental resolution.

## 2.5 Conclusion

Structure factors control extinction rules and enable rapid lattice symmetry identification from powder diffraction. SC shows no systematic absences; BCC enforces $h + k + l$ even; FCC enforces identical parity. Real diffraction patterns obey these rules and enable phase identification in crystallography and materials characterization.

# Chapter 3

# Drude model

## 3.1 Recap of Kinetic Theory of Gases

The kinetic theory treats gas molecules as neutral solid spheres. The gas molecules are thought to move in straight lines until collisions occur. During this free motion, no forces act on them. The average time between collisions is the **relaxation time** (mean free time).

Collisions randomize velocity completely — all memory is erased. After a collision, particles emerge with speeds determined by the local temperature.

## Application to Classical Electron Gas

In the Drude model, the ion cores of atoms are considered immobile, with core electrons remaining tightly bound to the nucleus. In contrast, the valence electrons are loosely bound and can wander throughout the entire metal, forming what are referred to as conduction electrons. It is important to note that these electrons differ from standard gas molecules because they are charged and move within a background of other charged entities. Additionally, electron densities in metals are quite large, approximately $10^{28}/\mathrm{m}^3$. Despite the fact that kinetic theory is typically valid only for neutral, dilute classical gases, Drude applied these principles to the study of electrons in metals.

### 3.1.1 Basic Assumptions of Drude Model

Between collisions, electrons move in a straight line in the absence of any electromagnetic field. The model ignores the effect of electron-electron interaction (independent electron approximation—reasonably valid assumption) and the effect of electron-ion interaction (independent-electron approximation — completely invalid assumption). The mean free time between collisions is $\tau$, such that the probability of an electron suffering a collision per unit time is $1/\tau$, and the probability of having a collision in an infinitesimal time interval $dt$ is $dt/\tau$. This relaxation time $\tau$ is assumed to be independent of an electron's

position or velocity.

Furthermore, electrons achieve thermal equilibrium through collisions with the lattice. They emerge after each collision in a random direction with a speed appropriate to the temperature of the region where the collision happened; effectively, the hotter the region, the higher the speed of the emerging electrons.

## What the Model Attempts to Explain

The model specifically tries to tackle the distinction between metals and insulators, the nature of electrical transport in metals, and the thermal conductivity of metals. It stands as a pre-quantum mechanical semi-classical model that remains roughly applicable for simple alkaline metals.

## DC Electrical Conductivity

$$V = IR, \quad \mathbf{E} = \rho \mathbf{J}$$

The number of electrons crossing area $A$ in time $dt$ is $nvAdt$. Each electron carries a charge $-e$. The current density is then $\mathbf{j} = -ne\mathbf{v}$.

Electrons in a metal are constantly undergoing random thermal motion. Therefore, the instantaneous velocity $\mathbf{v}$ differs from electron to electron, and we must consider the *average velocity* in order to determine the current.

In equilibrium $\langle \mathbf{v} \rangle = 0$. Consequently, there is no net electrical current in the absence of an applied field.

In the presence of a finite electric field $\mathbf{E}$, $\mathbf{v} = \mathbf{v}_0 - (e\mathbf{E}t)/m$ where

- $\mathbf{v}_0$ is the velocity immediately after the last collision (random in direction),
- $t$ is the time elapsed since the last collision.

Each electron acquires a systematic velocity component due to the electric field, superimposed on the random thermal motion. Averaging over all electrons, the random component vanishes $\langle \mathbf{v}_0 \rangle = 0$. Consequently,

$$\langle \mathbf{v} \rangle = -\frac{e\mathbf{E}}{m} \langle t \rangle$$

The time $t$ since the last collision is a random variable. In the Drude model, collisions occur with a constant probability per unit time, leading to an exponential distribution of $t$. The average time since the last collision is therefore equal to the relaxation time:

$$\langle t \rangle = \tau$$

Therefore, the average (drift) velocity is:

$$\mathbf{v}_d = -\frac{e\mathbf{E}\tau}{m}$$

Substituting into the expression for current density $\mathbf{j} = -ne\mathbf{v}_d$, we obtain:

$$\mathbf{j} = \frac{ne^2\tau}{m}\mathbf{E}$$

$$\boxed{\sigma = \frac{ne^2\tau}{m}}$$

This result shows that the electric field does not produce large velocities, but only a small systematic drift superimposed on otherwise random thermal motion. The magnitude of the current is controlled not by how fast electrons move, but by how long they retain their momentum between collisions.

## Mean Free Path

The mean free path $\ell$ is defined as the average distance an electron travels between successive collisions, $\ell = v\tau$. Using thermal velocity:

$$\frac{1}{2}mv^2 = \frac{3}{2}k_BT \Rightarrow v \sim 10^5 \text{ m/s}$$

$$\ell \sim 1 - 10 \text{ Å}$$

This estimate yields a mean free path comparable to the interatomic spacing. This was initially seen as a success of the Drude model, since it suggested that electrons travel distances of the order of atomic separations between collisions. However, experimentally, $\ell_{exp} \sim \text{cm}, \quad v_{exp} \sim 10^6$ m/s.

The discrepancy between the predictions of the model and experimentally obtained values arises because the Drude model uses the thermal velocity to estimate $\ell$, whereas in real metals the relevant velocity scale is the Fermi velocity, which is significantly larger.

The mean free path represents the distance over which an electron retains memory of its momentum before being randomized by scattering. It is difficult to determine the microscopic origin of the relaxation time $\tau$, since it depends on various scattering mechanisms (impurities, phonons, defects). This motivates the search for physical phenomena whose behavior does not depend explicitly on $\tau$, as such quantities provide more robust insight into the underlying electronic structure.

## 3.1.2 Equations of Motion

We now derive the effective equation of motion for an electron in the Drude model by incorporating the probabilistic nature of collisions. Consider an electron with momentum $\mathbf{p}(t)$ at time $t$. Over a short time interval $dt$, two possibilities arise:

- With probability $1 - \frac{dt}{\tau}$, the electron does *not* undergo a collision and continues to evolve under the applied force.

- With probability $\frac{dt}{\tau}$, the electron undergoes a collision, after which its momentum is completely randomized.

If no collision occurs:

$$\mathbf{p} \to \mathbf{p}(t) + \mathbf{F}(t)\, dt$$

If a collision occurs, the electron loses memory of its previous momentum. On average, the post-collision momentum is zero, and the only contribution comes from the force acting during $dt$:

$$\mathbf{p} \to \mathbf{F}(t)\, dt$$

Combining both possibilities:

$$\mathbf{p}(t + dt) = \left(1 - \frac{dt}{\tau}\right) [\mathbf{p}(t) + \mathbf{F}(t)\, dt] + \frac{dt}{\tau} [\mathbf{F}(t)\, dt]$$

Expanding and neglecting terms of order $dt^2$:

$$\mathbf{p}(t + dt) = \mathbf{p}(t) + \mathbf{F}(t)\, dt - \frac{dt}{\tau}\mathbf{p}(t)$$

or,

$$\boxed{\frac{d\mathbf{p}}{dt} = \mathbf{F}(t) - \frac{\mathbf{p}}{\tau}}$$

This equation has the form of Newton's second law with an additional damping term. The first term represents acceleration due to external forces, while the second term describes the loss of momentum due to collisions. Thus, collisions act as an effective *frictional force* that opposes motion.

## Steady-State Balance

In the steady state, the acceleration vanishes, $\frac{d\mathbf{p}}{dt} = 0$. Hence,

$$\mathbf{F}(t) = \frac{\mathbf{p}}{\tau}$$

This expresses a balance between the driving force and the rate at which momentum is dissipated through collisions.

## Remark

The relaxation time $\tau$ encapsulates all microscopic scattering processes in a single parameter. While its detailed origin is complex, its role in determining transport properties is central in the Drude model.

- Impurity scattering: $\tau \sim$ const (dominates at low temperature)

- Phonon scattering: $\tau^{-1} \propto T$ (high temperature regime)
- Electron-electron scattering: $\tau^{-1} \propto T^2$ (Fermi liquid behavior)

The net scattering time is determined by Matthiessen's Rule:

$$\frac{1}{\tau_{total}} = \frac{1}{\tau_{imp}} + \frac{1}{\tau_{ph}} + \frac{1}{\tau_{ee}}$$

### 3.1.3 Hall Effect and Magnetoresistance

We now consider the motion of electrons in the presence of both an electric field and a magnetic field. This allows us to probe not just conductivity, but also the *sign* and dynamics of charge carriers.

Suppose the current flows along the $x$-direction, and a magnetic field is applied along the $z$-direction:

$$\mathbf{E} = (E_x, E_y, 0), \qquad \mathbf{B} = (0, 0, B_z)$$

The Lorentz force on an electron is:

$$\mathbf{F} = -e(\mathbf{E} + \mathbf{v} \times \mathbf{B})$$

Including relaxation, the equation of motion becomes:

$$m\frac{d\mathbf{v}}{dt} = -e(\mathbf{E} + \mathbf{v} \times \mathbf{B}) - \frac{m\mathbf{v}}{\tau}$$

In component form, the equations of motion are:

$$m\frac{dv_x}{dt} = -e(E_x + v_y B_z) - \frac{mv_x}{\tau} \tag{3.1}$$

$$m\frac{dv_y}{dt} = -e(E_y - v_x B_z) - \frac{mv_y}{\tau} \tag{3.2}$$

Rearranging the terms,

$$\sigma_0 E_x = j_x + \omega_c \tau j_y \tag{3.3}$$

$$\sigma_0 E_y = -\omega_c \tau j_x + j_y \tag{3.4}$$

or,

$$\mathbf{E} = \frac{1}{\sigma_0} \begin{pmatrix} 1 & \omega_c\tau \\ -\omega_c\tau & 1 \end{pmatrix} \mathbf{j} = \boldsymbol{\rho}\mathbf{j} \tag{3.5}$$

Eqn. 3.5 gives the **resistivity tensor**

$$\boldsymbol{\rho} = \frac{1}{\sigma_0} \begin{pmatrix} 1 & \omega_c\tau \\ -\omega_c\tau & 1 \end{pmatrix} \tag{3.6}$$

The conductivity tensor is $\boldsymbol{\sigma} = \boldsymbol{\rho}^{-1}$.:

$$\boldsymbol{\sigma} = \frac{\sigma_0}{1 + (\omega_c \tau)^2} \begin{pmatrix} 1 & \omega_c \tau \\ -\omega_c \tau & 1 \end{pmatrix}$$

where $\sigma_0 = ne^2\tau/m$ and $\omega_c = eB/m$ is the cyclotron frequency.

In a Hall experiment, a current is applied along the x-direction. Since there is an open circuit along the y-direction, the transverse current $j_y$ vanishes, $j_y = 0$. This yields the transverse electric field:

$$E_y = -\omega_c \tau j_x / \sigma_0 \tag{3.7}$$

The longitudinal current density is:

$$j_x = \sigma_0 E_x = \frac{ne^2\tau}{m} E_x \tag{3.8}$$

## Hall coefficient

The Hall coefficient is defined as:

$$R_H = \frac{E_y}{j_x B_z}$$

Substituting Eqn. 3.7 and Eqn. 3.8 in the above definition of $R_H$, we get:

$$\boxed{R_H = -\frac{1}{ne}}$$

The magnetic field bends electron trajectories sideways. This causes charges to accumulate on one side of the sample, generating a transverse electric field that cancels further sideways motion. Thus, the Hall effect is a *self-consistent equilibrium* between Lorentz deflection and electrostatic buildup.

**Electrons vs Holes: Same Deflection, Opposite Voltage** It is important to note that electrons and holes are deflected toward the *same physical edge* of the sample under the Lorentz force. This is because the direction of the Lorentz force depends on the product of charge and velocity, and holes (which have positive charge) drift in the opposite direction to electrons under an applied electric field.

Consequently:

- Electrons $(-e)$ moving with drift velocity $\boldsymbol{v}_e$ and holes $(+e)$ moving with drift velocity $\boldsymbol{v}_h = -\boldsymbol{v}_e$ experience Lorentz forces

  $$\boldsymbol{F} = q\,\boldsymbol{v} \times \boldsymbol{B}$$

  that point toward the same side of the sample. For example, if the magnetic field is $\mathbf{B} = B\hat{z}$ and the current is $\mathbf{j} = j\hat{x}$, then the charge carriers (both electrons and holes will be deflected towards $-\hat{y}$.

- However, the *charge that accumulates* on that edge is opposite:
  - Electrons → negative charge accumulation
  - Holes → positive charge accumulation
- Therefore, the resulting Hall voltage has *opposite sign* for electrons and holes.

Thus, the Hall effect distinguishes carrier type not through the direction of deflection, but through the *sign of the accumulated charge*, i.e., the sign of the Hall voltage.

## Magnetoresistance

Magnetoresistance refers to the change in the longitudinal resistivity of a material upon application of a magnetic field:

$$\Delta\rho_{xx}(B) = \rho_{xx}(B) - \rho_{xx}(0)$$

Within the Drude model, one finds that the longitudinal conductivity is:

$$\sigma_{xx} = \frac{ne^2\tau}{m}$$

which is *independent of magnetic field*. Consequently,

$$\Delta\rho_{xx}(B) = 0$$

This result can be understood as follows. The magnetic field enters the equations of motion through the Lorentz force:

$$\boldsymbol{F} = -e(\boldsymbol{E} + \boldsymbol{v} \times \boldsymbol{B})$$

The term $\boldsymbol{v} \times \boldsymbol{B}$ is always perpendicular to the velocity $\boldsymbol{v}$, and therefore does *no work* on the electrons:

$$\boldsymbol{F} \cdot \boldsymbol{v} = 0$$

As a result, the magnetic field cannot change the magnitude of the electron velocity, and hence does not directly affect the dissipative processes responsible for resistivity.

More formally, solving the steady-state equations of motion yields a conductivity tensor:

$$\boldsymbol{\sigma} = \frac{\sigma_0}{1 + (\omega_c\tau)^2} \begin{pmatrix} 1 & \omega_c\tau \\ -\omega_c\tau & 1 \end{pmatrix}$$

where $\sigma_0 = ne^2\tau/m$ and $\omega_c = eB/m$ is the cyclotron frequency.

Inverting the conductivity tensor to obtain the resistivity tensor:

$$\boldsymbol{\rho} = \boldsymbol{\sigma}^{-1} = \frac{1}{\sigma_0} \begin{pmatrix} 1 & -\omega_c\tau \\ \omega_c\tau & 1 \end{pmatrix}$$

Thus,

$$\rho_{xx} = \frac{1}{\sigma_0}$$

is independent of $B$, while the off-diagonal component $\rho_{xy}$ gives the Hall effect.

Therefore, within the Drude model, a magnetic field only redistributes current between longitudinal and transverse directions, but does not change the total dissipation. This leads to the prediction of *zero magnetoresistance*.

In real materials:

- Multiple bands exist
- Fermi surface is anisotropic
- Orbital motion modifies transport

These effects produce finite magnetoresistance and can even change the sign of the Hall coefficient.

### 3.1.4 AC Electrical Conductivity

We now consider the response of electrons to a time-dependent electric field. This introduces a competition between:

- Driving by the external field
- Relaxation due to scattering

#### Equation of motion

$$m\frac{d\mathbf{v}}{dt} = -e\mathbf{E}(t) - \frac{m\mathbf{v}}{\tau}$$

Assume a harmonic field:

$$\mathbf{E}(t) = \mathbf{E}_0 e^{-i\omega t}$$

We look for a steady-state solution of the form:

$$\mathbf{v}(t) = \mathbf{v}_0 e^{-i\omega t}$$

#### Substitution into equation

$$m(-i\omega)\mathbf{v}_0 = -e\mathbf{E}_0 - \frac{m}{\tau}\mathbf{v}_0$$

Rearrange:

$$\left(\frac{m}{\tau} - i\omega m\right)\mathbf{v}_0 = -e\mathbf{E}_0$$

Factor out $m$:

$$m\left(\frac{1}{\tau} - i\omega\right)\mathbf{v}_0 = -e\mathbf{E}_0$$

Solve for $\mathbf{v}_0$:

$$\mathbf{v}_0 = -\frac{e}{m}\frac{1}{\frac{1}{\tau} - i\omega}\mathbf{E}_0$$

Multiply numerator and denominator by $\tau$:

$$\mathbf{v}_0 = -\frac{e\tau}{m}\frac{1}{1 - i\omega\tau}\mathbf{E}_0$$

## Current density

$$\mathbf{j} = -ne\mathbf{v}$$

$$\mathbf{j}_0 = \frac{ne^2\tau}{m}\frac{1}{1 - i\omega\tau}\mathbf{E}_0$$

Thus:

$$\boxed{\sigma(\omega) = \frac{ne^2\tau}{m}\frac{1}{1 - i\omega\tau}}$$

The conductivity is now complex:

$$\sigma(\omega) = \sigma_1(\omega) + i\sigma_2(\omega)$$

- Real part $\sigma_1$: dissipative response (energy loss)
- Imaginary part $\sigma_2$: reactive response (energy storage)

## Limiting Regimes

Starting from the Drude conductivity:

$$\sigma(\omega) = \frac{ne^2\tau}{m}\frac{1}{1 - i\omega\tau} = \sigma_0\frac{1}{1 - i\omega\tau} \quad \text{where } \sigma_0 = \frac{ne^2\tau}{m}$$

It is useful to separate real and imaginary parts:

$$\sigma(\omega) = \frac{\sigma_0}{1 + (\omega\tau)^2}\left[1 + i\omega\tau\right]$$

$$\Rightarrow \begin{cases} \sigma_1(\omega) = \dfrac{\sigma_0}{1 + (\omega\tau)^2} \\ \sigma_2(\omega) = \dfrac{\sigma_0\,\omega\tau}{1 + (\omega\tau)^2} \end{cases}$$

**Low-frequency limit ($\omega\tau \ll 1$):**

$$\sigma_1(\omega) \approx \sigma_0, \qquad \sigma_2(\omega) \approx \sigma_0\,\omega\tau$$

Thus,

$$\sigma(\omega) \approx \sigma_0(1 + i\omega\tau)$$

This corresponds to the DC regime where electrons relax rapidly and follow the field adiabatically.

**High-frequency limit ($\omega\tau \gg 1$):**

$$\sigma_1(\omega) \approx \frac{\sigma_0}{(\omega\tau)^2}, \qquad \sigma_2(\omega) \approx \frac{\sigma_0}{\omega\tau}$$

Thus,

$$\sigma(\omega) \approx \frac{\sigma_0}{-i\omega\tau} = \frac{ne^2}{m}\frac{1}{-i\omega}$$

In this regime, the response is predominantly imaginary, indicating that electrons cannot dissipate energy efficiently and instead exhibit an inertial (reactive) response.

**Summary:**

- $\omega\tau \ll 1$: dissipative (Ohmic) response dominates
- $\omega\tau \gg 1$: reactive (inductive) response dominates

### Physical Picture

At low frequencies, electrons experience many collisions within one oscillation cycle, so they relax quickly and follow the field.

At high frequencies, the field changes direction before scattering occurs. Electrons behave like nearly free particles and cannot respond efficiently, leading to reduced dissipation.

This frequency dependence is the origin of the optical properties of metals.

## 3.2 Electromagnetic Waves in Metals

We now study how electromagnetic waves propagate inside a metal within the Drude model. This connects transport to optical response and reveals the origin of metallic reflectivity.

## Maxwell's Equations in a Conducting Medium

We begin with Maxwell's equations in a medium:

$$\nabla \times \mathbf{E} = -\frac{\partial \mathbf{B}}{\partial t} \tag{3.9}$$

$$\nabla \times \mathbf{B} = \mu_0 \mathbf{J} + \mu_0 \epsilon_0 \frac{\partial \mathbf{E}}{\partial t} \tag{3.10}$$

In a metal, the current density is related to the electric field through the Drude conductivity:

$$\mathbf{J} = \sigma(\omega)\mathbf{E}$$

Substitute into Ampère's law:

$$\nabla \times \mathbf{B} = \mu_0 \sigma(\omega)\mathbf{E} + \mu_0 \epsilon_0 \frac{\partial \mathbf{E}}{\partial t}$$

## Derivation of the Wave Equation

Take the curl of Faraday's law:

$$\nabla \times (\nabla \times \mathbf{E}) = -\frac{\partial}{\partial t}(\nabla \times \mathbf{B})$$

Using the vector identity:

$$\nabla \times (\nabla \times \mathbf{E}) = \nabla(\nabla \cdot \mathbf{E}) - \nabla^2 \mathbf{E}$$

In a homogeneous medium with no free charge density:

$$\nabla \cdot \mathbf{E} = 0$$

Thus:

$$-\nabla^2 \mathbf{E} = -\frac{\partial}{\partial t}\left(\mu_0 \sigma(\omega)\mathbf{E} + \mu_0 \epsilon_0 \frac{\partial \mathbf{E}}{\partial t}\right)$$

Rearranging:

$$\nabla^2 \mathbf{E} = \mu_0 \sigma(\omega) \frac{\partial \mathbf{E}}{\partial t} + \mu_0 \epsilon_0 \frac{\partial^2 \mathbf{E}}{\partial t^2}$$

## Plane Wave Solution

We look for solutions of the form:

$$\mathbf{E}(x,t) = \mathbf{E}_0 e^{i(kx - \omega t)}$$

Substitute derivatives:

$$\frac{\partial}{\partial t} \to -i\omega, \quad \nabla^2 \to -k^2$$

Thus:

$$-k^2 \mathbf{E} = \mu_0 \sigma(\omega)(-i\omega)\mathbf{E} + \mu_0 \epsilon_0 (-\omega^2)\mathbf{E}$$

Divide through:

$$k^2 = i\mu_0 \sigma(\omega)\omega + \mu_0 \epsilon_0 \omega^2$$

## Definition of Dielectric Function

We define the complex dielectric constant:

$$\epsilon(\omega) = 1 + \frac{i\sigma(\omega)}{\omega\epsilon_0}$$

Thus:

$$k^2 = \mu_0\epsilon_0\omega^2\epsilon(\omega)$$

Using $c^2 = \frac{1}{\mu_0\epsilon_0}$:

$$k^2 = \frac{\omega^2}{c^2}\epsilon(\omega)$$

## Drude Dielectric Function

Using:

$$\sigma(\omega) = \frac{ne^2\tau}{m}\frac{1}{1 - i\omega\tau}$$

we obtain:

$$\epsilon(\omega) = 1 - \frac{\omega_p^2}{\omega(\omega + i/\tau)}$$

where:

$$\boxed{\omega_p = \sqrt{\frac{ne^2}{\epsilon_0 m}}}$$

## High-Frequency Limit ($\omega\tau \gg 1$)

In this limit:

$$\epsilon(\omega) \approx 1 - \frac{\omega_p^2}{\omega^2}$$

## Spatial Dependence of Fields

Write:

$$k = \kappa$$

Thus:

$$E(x) = E_0 e^{i\kappa x}$$

If $\kappa$ is complex:

$$\kappa = \kappa_1 + i\kappa_2$$

then:

$$E(x) = E_0 e^{i\kappa_1 x} e^{-\kappa_2 x}$$

Thus, $\kappa_2$ describes decay into the material.

## Propagation Regimes

- $\omega < \omega_p$: $\epsilon(\omega) < 0 \rightarrow \kappa$ imaginary $\rightarrow$ exponential decay

  $$E(x) \sim e^{-x/\delta}$$

  The metal is reflective.

- $\omega > \omega_p$: $\epsilon(\omega) > 0 \rightarrow \kappa$ real $\rightarrow$ wave propagates The metal becomes transparent.

## Physical Insight

The plasma frequency represents the natural frequency of collective electron motion.

- Below $\omega_p$, electrons can rearrange quickly enough to screen the field $\rightarrow$ reflection.
- Above $\omega_p$, electrons cannot respond fast enough $\rightarrow$ field penetrates.

Thus, metals are mirrors in the visible range because $\omega < \omega_p$, but can become transparent in the ultraviolet.

## Experimental Connection

Typical plasma frequencies:

$$\omega_p \sim 10^{15} \text{ Hz}$$

Alkali metals become transparent above this frequency.

Gold nanoparticles exhibit strong optical effects due to surface plasmons. Their color depends sensitively on particle size and shape because these modify collective oscillation modes.

### Remark: Beyond Drude

Real metals deviate from this simple picture because:

- Interband transitions contribute to $\epsilon(\omega)$
- Bound electrons modify optical response
- Surface effects become important at the nanoscale

## 3.3 Plasma Oscillations

Plasmons can be understood as collective oscillations of the free electron density relative to the fixed positive ionic background.

### Physical Picture

Imagine a metal in an external electric field pointing to the right. Electrons shift to the left, leaving behind exposed positive ions on the right. This charge separation produces a restoring electric field.

If the external field is removed, the electrons overshoot and oscillate about equilibrium. This motion is a collective oscillation of the electron gas.

### Continuum Description

We describe the system in terms of a charge density fluctuation $\rho(\mathbf{r}, t)$.

A charge oscillation corresponds to a density wave of the form:

$$\rho(\mathbf{r}, t) = \rho_0 e^{i(\mathbf{q}\cdot\mathbf{r}-\omega t)}$$

### Continuity Equation

Charge conservation gives:

$$\frac{\partial \rho}{\partial t} + \nabla \cdot \mathbf{j} = 0$$

Assume current density:

$$\mathbf{j} = -ne\mathbf{v}$$

Thus:

$$\frac{\partial \rho}{\partial t} = ne\nabla \cdot \mathbf{v}$$

## Equation of Motion

The electron velocity obeys:

$$m\frac{d\mathbf{v}}{dt} = -e\mathbf{E}$$

Taking divergence:

$$m\frac{\partial}{\partial t}(\nabla \cdot \mathbf{v}) = -e\nabla \cdot \mathbf{E}$$

## Gauss's Law

$$\nabla \cdot \mathbf{E} = \frac{\rho}{\epsilon_0}$$

Thus:

$$m\frac{\partial}{\partial t}(\nabla \cdot \mathbf{v}) = -\frac{e}{\epsilon_0}\rho$$

## Combine Equations

Differentiate continuity equation:

$$\frac{\partial^2 \rho}{\partial t^2} = ne\frac{\partial}{\partial t}(\nabla \cdot \mathbf{v})$$

Substitute:

$$\frac{\partial^2 \rho}{\partial t^2} = ne\left(-\frac{e}{m\epsilon_0}\rho\right)$$

$$\boxed{\frac{\partial^2 \rho}{\partial t^2} + \omega_p^2 \rho = 0}$$

where:

$$\boxed{\omega_p = \sqrt{\frac{ne^2}{\epsilon_0 m}}}$$

## Physical Interpretation

This equation describes a harmonic oscillator:

$$\rho(t) \sim e^{-i\omega_p t}$$

Thus, collective charge oscillations can exist only at the plasma frequency.

### Rigid Shift Picture

Assume the entire electron gas is displaced by $x$:

Charge density:

$$\rho = -ne$$

Electric field from Gauss law:

$$E = \frac{nex}{\epsilon_0}$$

Force:

$$F = -eE = -\frac{ne^2}{\epsilon_0}x$$

Equation:

$$m\ddot{x} = -\frac{ne^2}{\epsilon_0}x$$

This gives:

$$\omega = \omega_p$$

### Experimental Observation

Plasma oscillations are observed via enhanced absorption of electromagnetic radiation.

Surface plasmons also occur at interfaces. Their frequency depends on geometry.

Gold nanoparticles exhibit different colors due to size-dependent plasmon resonances (as seen in stained glass).

## 3.4 Thermal Conductivity of Metals

Thermal transport in metals arises because electrons carry energy from hot regions to cold regions.

### Fourier's Law

$$J_Q = -\kappa\frac{dT}{dx}$$

Our goal is to derive $\kappa$ using the Drude model.

### Physical Setup

Consider a rod with temperature gradient:

$$T_2 > T_1 \quad \Rightarrow \quad \frac{dT}{dx} > 0$$

Key idea: electrons arriving at position $x$ come from regions a distance $\sim v\tau$ away.

## Energy Transport

Energy of an electron depends on temperature where its last collision occurred.
Electrons arriving from:

- Left: $E(T(x - v\tau))$
- Right: $E(T(x + v\tau))$

## Taylor Expansion

$$E(x \pm v\tau) = E(x) \pm v\tau \frac{dE}{dx}$$

Difference:

$$\Delta E = 2v\tau \frac{dE}{dx}$$

## Energy Flux

Number of electrons crossing per unit area per unit time:

$$\frac{1}{2}nv$$

Thus:

$$J_Q = \frac{1}{2}nv\Delta E$$

$$J_Q = nv^2\tau \frac{dE}{dx}$$

Using:

$$\frac{dE}{dx} = C_v \frac{dT}{dx}$$

$$J_Q = nv^2\tau C_v \frac{dT}{dx}$$

Comparing with Fourier's law:

$$\boxed{\kappa = \frac{1}{3}C_v v^2 \tau}$$

### Physical Insight

Thermal conductivity is governed by:

- Energy per particle ($C_v$)
- Velocity ($v$)
- Distance traveled between collisions ($v\tau$)

Thus:

$$\kappa \sim C_v \times (\text{velocity}) \times (\text{mean free path})$$

### Limitations of the Argument

We assumed velocity depends only on local temperature, ignoring where the last collision occurred.

This introduces second-order corrections, but the structure of the result remains robust.

## 3.4.1 Wiedemann–Franz Law

We now compare electrical and thermal transport.

### Expressions from Drude Model

$$\sigma = \frac{ne^2\tau}{m}$$

$$\kappa = \frac{1}{3}C_v v^2 \tau$$

### Substitute Classical Values

$$C_v = \frac{3}{2}nk_B$$

$$v^2 = \frac{3k_BT}{m}$$

Substitute into $\kappa$:

$$\kappa = \frac{1}{3} \cdot \frac{3}{2}nk_B \cdot \frac{3k_BT}{m}\tau$$

$$\kappa = \frac{3}{2}\frac{nk_B^2T}{m}\tau$$

## Ratio

$$\frac{\kappa}{\sigma T} = \frac{\frac{3}{2}\frac{nk_B^2 T}{m}\tau}{\frac{ne^2\tau}{m}T}$$

Cancel terms:

$$\boxed{L = \frac{\kappa}{\sigma T} = \frac{3}{2}\frac{k_B^2}{e^2}}$$

## Drude's "Luck"

Numerically:

$$L \approx 1.11 \times 10^{-8}\,\mathrm{W\Omega/K^2}$$

Experimental value:

$$L = \frac{\pi^2}{3}\frac{k_B^2}{e^2}$$

Agreement is accidental:

- $C_v$ overestimated (classical statistics)
- $v^2$ underestimated (should use $v_F^2$)

## Physical Meaning

The Wiedemann–Franz law shows that heat and charge transport are carried by the same particles.

This is a deep result: it connects two seemingly unrelated phenomena through microscopic dynamics.

## Validity

The law holds well for simple metals over a limited temperature range.

Deviations arise when:

- Inelastic scattering dominates
- Multiple bands are present
- Strong correlations exist

## 3.5 Thermoelectric Effect

Drude model assumes that the mean electronic velocity at a point vanishes – this cannot be rigorously justified. Electrons coming from the higher temperature side will have higher energy and hence a higher speed – net motion of electrons from higher temperature side to lower temperature side.

Thermal properties are measured in open circuit conditions – no net current can flow. This implies that electrons will accumulate at the low temperature end of the rod and produce an electric field that would inhibit further accumulation of electrons (similar to Hall Effect) – this is the Seebeck Effect (temperature gradient in a metallic rod is accompanied by a voltage gradient).

$$E = Q\nabla T \quad \text{where } Q \text{ is the thermopower}$$

Mean electronic velocity at a point $x$ due to the temperature gradient in a 1-D rod is:

$$v_Q = \frac{1}{2}[v(x - v\tau) - v(x + v\tau)] = -v\tau\frac{dv}{dx} = -\frac{1}{2}\tau\frac{dv^2}{dx}$$

In a 3-D system:

$$v_Q = -\frac{1}{6}\tau\frac{dv^2}{dx} = -\frac{1}{6}\tau\frac{dv^2}{dT}\nabla T$$

Mean velocity due to the induced electric field $E$ is:

$$v_E = -\frac{e\tau}{m}E$$

At equilibrium net electronic velocity should vanish (current is zero): $v_Q + v_E = 0$

$$-\frac{1}{6}\tau\frac{dv^2}{dT}\nabla T + \left(-\frac{e\tau}{m}E\right) = 0$$

$$E = -\frac{1}{3ne}c_v\nabla T \quad \text{or} \quad Q = -\frac{1}{3ne}c_v$$

Using $c_v = \frac{3}{2}nk_B$, Drude estimated $Q = -0.43 \times 10^{-4}$ V/K.

Observed values of $Q$ are $\sim \mu$V/K – about 100 times too small. This is due to over-estimation of $c_v$ by about a factor of 100 due to the use of classical statistics. Furthermore, the Drude model can't explain why $Q$ is sometimes positive (i.e., why carriers sometimes appear to be positively charged). To explain this, one needs to use the quantum mechanical theory of electrons in a metal.

## Failures of the Drude Model

While the Drude model successfully captures the structure of transport equations, it fails quantitatively and sometimes qualitatively.

These failures are not minor corrections — they reveal missing fundamental physics.

## (1) Electronic Specific Heat

Drude prediction:

$$C_v = \frac{3}{2} n k_B$$

Experiment:

$$C_v \ll \frac{3}{2} n k_B$$

**Physical reason:**

Drude assumes all electrons contribute to thermal properties. In reality, only electrons within $k_B T$ of the Fermi energy contribute.

## (2) Mean Free Path and Velocity

Drude uses thermal velocity:

$$v \sim 10^5 \text{ m/s}$$

Experiment:

$$v_F \sim 10^6 \text{ m/s}$$

Mean free path can be:

$$\ell \sim \text{mm–cm}$$

**Implication:** electrons are not classical particles but degenerate fermions.

## (3) Hall Effect

Drude predicts:

$$R_H = -\frac{1}{ne}$$

Problems:

- Some metals show positive Hall coefficient
- Carrier density extracted is often incorrect

**Missing physics:** band structure and multiple carrier types.

## (4) Magnetoresistance

Drude predicts:

$$\Delta\rho = 0$$

Experiment:

$$\Delta\rho \neq 0$$

**Reason:**

- Fermi surface anisotropy
- Orbital motion in a magnetic field

## (5) Thermal Conductivity and Lorentz Number

Agreement with experiments is accidental (Drude's luck).

**Reason:**

- Overestimates $C_v$
- Underestimates velocity

## (6) Thermoelectric Effect

Drude predicts:

$$Q \sim \frac{k_B}{e}$$

Experiment:

$$Q \sim \mu\text{V/K}$$

**Reason:**

- Only Fermi surface electrons contribute
- Energy-dependent transport is crucial

## (7) Fundamental Conceptual Issue

Drude assumes:

- Classical statistics
- Free particles

Real metals:

- Obey Fermi-Dirac statistics
- Have band structure

## Summary

| Quantity | Drude | Experiment |
|---|---|---|
| $C_v$ | large | small |
| $R_H$ | always negative | sign varies |
| Magnetoresistance | zero | finite |
| $Q$ | large | small |

The Drude model fails microscopically but succeeds structurally.

> It gives the correct *form* of transport equations, but with incorrect microscopic inputs.

This is why it remains foundational: it provides the framework upon which quantum transport theory is built.

## What Comes Next

To resolve these failures, we must introduce:

- Fermi-Dirac statistics (Sommerfeld model)
- Band structure
- Quantum scattering theory

# Chapter 4

# Sommerfeld model

## 4.1 Introduction

### 4.1.1 Recap of the Drude Model

In the Drude model, conduction electrons in a metal are treated as free particles moving in a constant potential background provided by the ionic lattice. The complicated periodic potential of the crystal is thus replaced by a spatially uniform potential, allowing the electrons to be described as classical particles undergoing random scattering events.

Within this framework, electrons are assumed to be identical but *distinguishable*, and their statistical behavior is described using classical Maxwell–Boltzmann statistics. This leads to a simple kinetic theory of transport, which successfully explains several qualitative features such as Ohm's law and the order of magnitude of electrical conductivity.

### Drawbacks of the Drude Model

Despite its successes, the Drude model suffers from several fundamental limitations. First, electrons cannot be treated as classical particles: they are quantum mechanical entities with wave-like properties. More importantly, electrons are Fermions and hence are *identical and indistinguishable* particles, in contrast to the assumptions of classical statistics.

A crucial consequence of their fermionic nature is that electrons obey the *Pauli exclusion principle*, which forbids multiple electrons from occupying the same quantum state. This has profound implications for their statistical distribution and physical properties.

These observations necessitate a quantum statistical description of electrons. In particular, the electron gas in a metal must be described using *Fermi–Dirac statistics*, which correctly incorporates indistinguishability and the Pauli exclusion principle. This forms the foundation of the Sommerfeld model, which provides a quantum-mechanical refinement of the Drude picture.

### Sommerfeld (Drude–Sommerfeld) Model

The Sommerfeld model retains most of the central assumptions of the Drude model, but incorporates essential quantum-mechanical principles that are required for a correct description of electrons in a metal.

The key modification is the replacement of classical Maxwell–Boltzmann statistics with *Fermi–Dirac (FD) statistics*. Electrons are treated as a gas of non-interacting Fermions, and their statistical distribution reflects their indistinguishable nature and the constraints imposed by quantum mechanics.

In addition, the model recognizes that the allowed energy states of electrons are *discrete*. These states are obtained by treating electrons as particles confined within a three-dimensional box with a constant potential, leading to quantized energy levels. This is equivalent to solving the Schrödinger equation for free electrons subject to appropriate boundary conditions.

The occupation of these energy levels is then determined using the *Pauli exclusion principle*, which allows at most one electron per quantum state (or two, when spin is included). As a result, electrons fill the available states starting from the lowest energy, building up a distribution that is sharply defined at low temperatures.

Thus, the Sommerfeld model can be viewed as a quantum-mechanical refinement of the Drude picture: it preserves the idea of free electrons moving in a constant potential, but replaces the classical description with a quantum statistical framework based on Fermi–Dirac statistics and the Pauli principle.

## 4.2 Ground state of ideal electron gas

The electrons are confined in a cube of sides $L$ at $T = 0$, the potential inside the cube is constant (take it to be zero). Assume non-interacting electrons, i.e.,

$$\psi(r_1, r_2, \ldots, r_N) = \psi(r_1)\psi(r_2)\ldots\psi(r_N)$$

For non-interacting electrons, the many-body wavefunction is constructed as a Slater determinant of single-particle states to satisfy antisymmetry. The Hamiltonian is:

$$-\frac{\hbar^2}{2m}\nabla^2\psi = \varepsilon\psi$$

Using the periodic boundary condition $\psi(x + L, y, z) = \psi(x, y, z)$ and so on,

$$\psi(\mathbf{r}) = \frac{1}{\sqrt{V}}e^{i\mathbf{k}\cdot\mathbf{r}}$$

with the energy eigenvalues $\varepsilon(k) = \frac{\hbar^2 k^2}{2m}$ — this is the dispersion relation for free electrons (Fig. 4.1).

$k$ is a position-independent wave vector; each value of $k$ labels a distinct state $\mathbf{p}\psi = \hbar\mathbf{k}\psi$ implying that $k$ plays the role of wave-vector for the free electrons.

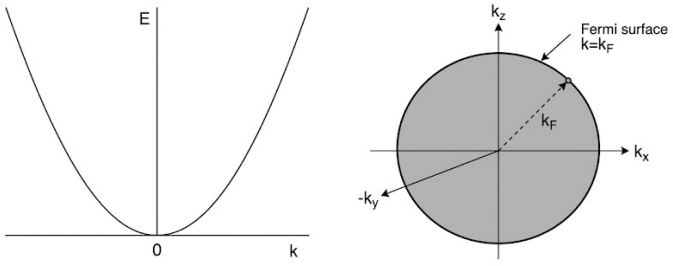


Figure 4.1: Left panel: Dispersion relation for free electrons. Bottom panel: Fermi sphere at $T = 0$.

The allowed values of $k$ are given by the quantization condition $\psi(x + L, y, z) = \psi(x, y, z)$ to be $k_x = \frac{2\pi}{L} n_x$, where $n_x$ is an integer.

For large $N$, the filled states form a sphere in $k$-space (remember $\varepsilon(k) \propto k^2$) – its radius is $k_F$ (this is called the Fermi wave-vector) and volume $\frac{4}{3}\pi k_F^3$. This is the Fermi sphere. $k_F$ is given by:

$$2 \times \frac{4}{3}\pi k_F^3 \times \frac{1}{(2\pi/L)^3} = N$$

or,

$$k_F = (3\pi^2 n)^{1/3} \tag{4.1}$$

The highest occupied energy level in the ground state is called the Fermi energy. This separates the completely filled states from the completely empty ones in the ground state. For free electrons $\varepsilon_F = \frac{\hbar^2 k_F^2}{2m}$. For metallic systems, Fermi energy $\varepsilon_F \sim$ eV and Fermi velocity $v_F = \frac{\hbar k_F}{m} \sim 10^6$ m/s.

The total ground state energy is:

$$E = 2 \sum_{k<k_F} \frac{\hbar^2 k^2}{2m}$$

For large $N$, the values of $k$ are arbitrarily close to each other – can be treated as a continuum:

$$\sum_{\mathbf{k}} \longrightarrow \frac{V}{8\pi^3} \int d\mathbf{k}$$

Thus, the total energy of the electronic system is:

$$E = 2\frac{V}{8\pi^3} \int \frac{\hbar^2 k^2}{2m} d\mathbf{k} = 2\frac{V}{8\pi^3} \int \frac{\hbar^2 k^2}{2m} 4\pi k^2 dk = \frac{V}{10} \frac{\hbar^2}{\pi^2 m} k_F^5$$

The average energy per particle is:

$$\frac{E}{N} = \frac{E/V}{N/V} = \frac{\frac{1}{10}\frac{\hbar^2}{\pi^2 m} k_F^5}{k_F^3/3\pi^2} = \frac{3}{5}\varepsilon_F = \frac{3}{5} k_B T_F$$

In contrast to a classical gas, the degenerate quantum mechanical electron gas has appreciable ground-state energy. The Fermi temperature $T_F \sim 10^5$ K; hence, compared to a classical gas at room temperature, the average energy of electrons is about 100 times higher.

### Pressure of the Electron Gas

The ground-state pressure can be obtained from the energy:

$$P = -\left(\frac{\partial E}{\partial V}\right)_N = \frac{2}{5} n\varepsilon_F$$

This pressure arises purely from the Pauli exclusion principle and persists even at $T = 0$, unlike a classical gas.

**Physical meaning of $\varepsilon_F$:** The Fermi energy sets the natural energy scale of the electron gas. It represents the kinetic energy of the highest occupied state at $T = 0$, and determines:

- The characteristic velocity scale ($v_F$),
- The degeneracy pressure of the electron gas,
- The temperature scale $T_F = \varepsilon_F / k_B$ below which quantum effects dominate.

## 4.2.1 Ideal electron gas at finite temperatures

The probability that a state with energy $\varepsilon$ is occupied at temperature $T$ is

$$f(\varepsilon) = \frac{1}{e^{(\varepsilon-\mu)/k_B T} + 1}$$

where $\mu$ is the chemical potential and equals $\varepsilon_F$ at $T = 0$. At finite temperature, it is the energy at which the occupation probability is 1/2.

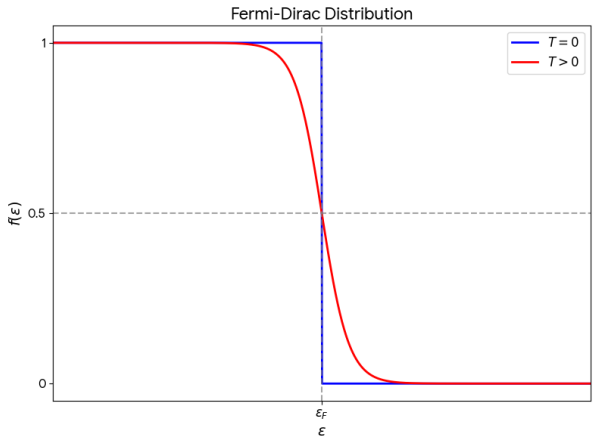


Figure 4.2: Fermi distribution function

The energy density $u = E/V$ is:

$$u = \frac{1}{4\pi^3} \int f(\varepsilon)\varepsilon(k) d\mathbf{k}$$

Similarly, the number density $n$ is:

$$n = \frac{1}{4\pi^3}\int f(\varepsilon) d\mathbf{k}$$

Changing the integral form from over $\mathbf{k}$ to over energy:

$$\frac{d\mathbf{k}}{4\pi^3} = \frac{1}{4\pi^3}4\pi k^2 dk = \frac{1}{\pi^2}k^2 dk = \frac{1}{\pi^2}\frac{2m\varepsilon}{\hbar^2}\sqrt{\frac{m}{2\hbar^2}}\frac{d\varepsilon}{\sqrt{\varepsilon}}$$

or

$$n = \int_0^\infty f(\varepsilon)g(\varepsilon)d\varepsilon$$

where

$$g(\varepsilon) = \frac{1}{2\pi^2}\left(\frac{2m}{\hbar^2}\right)^{3/2}\sqrt{\varepsilon} = \frac{3}{2}\frac{n}{\varepsilon_F}\sqrt{\frac{\varepsilon}{\varepsilon_F}}$$

is the density of states. Similarly,

$$u = \int_0^\infty \varepsilon f(\varepsilon)g(\varepsilon)d\varepsilon$$

## Sommerfeld Expansion

For integrals of the form:

$$\int_0^\infty \phi(\varepsilon)f(\varepsilon)d\varepsilon$$

at low temperatures ($T \ll T_F$), one can expand:

$$\int_0^\infty \phi(\varepsilon)f(\varepsilon)d\varepsilon = \int_0^{\varepsilon_F}\phi(\varepsilon)\,d\varepsilon + \frac{\pi^2}{6}(k_BT)^2\phi'(\varepsilon_F) + \dots$$

This provides a systematic way to compute thermodynamic quantities of a degenerate electron gas.

The number density in the Sommerfeld model is given by:

$$n = \int_0^\infty f(\varepsilon)g(\varepsilon)\,d\varepsilon = \frac{1}{2\pi^2}\left(\frac{2m}{\hbar^2}\right)^{\frac{3}{2}}\int_0^\infty \sqrt{\varepsilon}f(\varepsilon)\,d\varepsilon$$

or,

$$n = 2\left(\frac{mk_BT}{2\pi\hbar^2}\right)^{3/2}F_{1/2}\left(\frac{\mu}{k_BT}\right)$$

where $F_{1/2}(x) = \frac{2}{\sqrt{\pi}}\int_0^\infty \frac{y^{1/2}}{e^{(y-x)}+1}dy$ is the Fermi integral of order 1/2.

1. $\frac{\mu}{k_BT} \ll 1$ (valid for low-density systems like semiconductors):

$$n = 2\left(\frac{mk_BT}{2\pi\hbar^2}\right)^{3/2}e^{\frac{\mu}{k_BT}}$$

2. $\frac{\mu}{k_B T} \gg 1$ (valid for high-density systems like metals):

$$F_{1/2}(x) \approx \frac{4}{3\sqrt{\pi}} x^{3/2} \left[1 + \frac{\pi^2}{8}\frac{1}{x^2} + \dots\right]$$

$$n = \frac{1}{3\pi^2}\left(\frac{2m\mu}{\hbar^2}\right)^{3/2}\left[1 + \frac{\pi^2}{8}\left(\frac{k_B T}{\mu}\right)^2 + \dots\right] \tag{4.2}$$

From Eqn 4.1, we have

$$n = \frac{1}{3\pi^2}k_F^3 = \frac{1}{3\pi^2}\left(\frac{2m\varepsilon_F}{\hbar^2}\right)^{\frac{3}{2}}$$

Using this in Eq. 4.2 we get,

$$\varepsilon_F = \mu\left[1 + \frac{\pi^2}{8}\left(\frac{k_B T}{\mu}\right)^2 + \dots\right]^{\frac{2}{3}}$$

The expression for $\mu$ in terms of $\varepsilon_F$ (for $\frac{\mu}{k_B T} \gg 1$) is:

$$\mu = \varepsilon_F\left[1 - \frac{\pi^2}{12}\left(\frac{k_B T}{\varepsilon_F}\right)^2 + \dots\right] \tag{4.3}$$

The energy density in the Sommerfeld model:

$$u = \int_0^\infty \varepsilon f(\varepsilon) g(\varepsilon) d\varepsilon = u_0 + \frac{\pi^2}{6}(k_B T)^2 g(\varepsilon_F) \tag{4.4}$$

The specific heat:

$$C_V = \frac{du}{dT} = \frac{\pi^2}{3}k_B^2 T g(\varepsilon_F) = \frac{\pi^2}{2}\frac{k_B T}{\varepsilon_F} n k_B \tag{4.5}$$

## Role of the Fermi Surface

A key consequence of Fermi–Dirac statistics is that, at low temperatures ($T \ll T_F$), only electrons within an energy window of order $k_B T$ around the Fermi energy $\varepsilon_F$ can be thermally excited. All states deep below $\varepsilon_F$ are Pauli blocked and do not participate in transport or thermodynamic processes. Thus, although the total electron density is large, only a small fraction $\sim \frac{k_B T}{\varepsilon_F} \ll 1$ of electrons are active. This explains why:

- The electronic specific heat is small ($C_V \propto T$),
- Electrical transport is governed by properties at the Fermi surface,
- Metals behave very differently from classical gases.

## Implication for Electrical Transport

In the Sommerfeld model, electrical conduction is dominated by electrons near the Fermi surface. The conductivity retains the Drude form:

$$\sigma = \frac{ne^2\tau}{m}$$

However, only electrons within an energy window of order $k_BT$ around $\varepsilon_F$ contributes effectively. Thus, the relaxation time $\tau$ should be interpreted as a property of electrons at the Fermi surface.

### What about the other properties?

- Thermal conductivity:
$$\kappa = \frac{1}{3}vlc_V$$
retains the same form as in the Drude model within the semiclassical relaxation-time approximation. However, in the Sommerfeld picture, the specific heat $c_V$ is dominated by electrons near the Fermi surface, leading to a much smaller thermal conductivity than predicted classically.

- Thermopower:
$$Q = -\frac{\pi^2}{6}\left(\frac{k_B}{e}\right)\left(\frac{k_BT}{\varepsilon_F}\right) \sim 10^{-4}\,\mathrm{V/K}$$
is small in metals because only a narrow energy window of width $\sim k_BT$ around the Fermi energy contributes to transport. The linear temperature dependence reflects the asymmetry of carrier transport near $\varepsilon_F$.

- The Wiedemann–Franz law still remains theoretically valid:
$$\frac{\kappa}{\sigma T} = L_0 = \frac{\pi^2}{3}\left(\frac{k_B}{e}\right)^2,$$
where $L_0$ is the Lorenz number. This result follows naturally in the Sommerfeld model since both electrical and thermal transport are governed by electrons at the Fermi surface.

## Drude vs Sommerfeld Model

| | Drude Model | Sommerfeld Model |
|---|---|---|
| Statistics | Maxwell–Boltzmann | Fermi–Dirac |
| Particles | Classical | Quantum Fermions |
| Pauli principle | Ignored | Included |
| Energy distribution | $\sim k_BT$ | $\sim \varepsilon_F$ |
| Specific heat | $\frac{3}{2}nk_B$ | $\propto T$ |
| Transport carriers | All electrons | Near $\varepsilon_F$ |

### 4.2.2 Limitations of the Sommerfeld Model

Despite its successes, the Sommerfeld model neglects several important effects:

- The periodic crystal potential (band structure effects),
- Electron–electron interactions,
- Electron–phonon interactions beyond the relaxation-time approximation.

These limitations are addressed in more advanced treatments, such as the nearly free electron model and full band theory.

# Chapter 5

# Electrons in a Weak Periodic Potential

## 5.1 Electrons in a weak periodic potential

**Assumptions:**

1. Static defect-free lattice – perfectly periodic potential.
2. Weak potential – perturbative effect on the free electron states.

Perfect periodicity of the lattice potential implies that any electronic property we deduce will also be influenced by this periodicity.

### 5.1.1 Bloch states

Average potential at a point is $U(\mathbf{r})$. Assume an independent electron picture, the single particle Schrödinger equation is

$$\left[-\frac{\hbar^2}{2m}\nabla^2 + U(\mathbf{r})\right]\psi(\mathbf{r}) = E\psi(\mathbf{r}). \tag{5.1}$$

Using Bloch's theorem,

$$\psi_{\mathbf{k}}(\mathbf{r}) = e^{i\mathbf{k}\cdot\mathbf{r}}u_{\mathbf{k}}(\mathbf{r}), \quad u_{\mathbf{k}}(\mathbf{r}+\mathbf{R}) = u_{\mathbf{k}}(\mathbf{r}) \tag{5.2}$$

Note that $e^{i\mathbf{k}\cdot\mathbf{r}}$ is not periodic in the real lattice. But any measurable property will depend on

$$|\psi_{\mathbf{k}}(\mathbf{r})|^2 = |u_{\mathbf{k}}(\mathbf{r})|^2$$

which is periodic in the real lattice.

$u_{\mathbf{k}}(\mathbf{r})$ is called the Bloch function.

In terms of the Bloch function the Schrödinger equation becomes

$$\left[-\frac{\hbar^2}{2m}\nabla^2 + U(\mathbf{r})\right] e^{i\mathbf{k}\cdot\mathbf{r}} u_{\mathbf{k}}(\mathbf{r}) = E e^{i\mathbf{k}\cdot\mathbf{r}} u_{\mathbf{k}}(\mathbf{r}) \tag{5.3}$$

or

$$\left[\frac{1}{2m}(-i\hbar\nabla + \hbar\mathbf{k})^2 + U(\mathbf{r})\right] u_{\mathbf{k}}(\mathbf{r}) = E u_{\mathbf{k}}(\mathbf{r}) \tag{5.4}$$

or equivalently

$$\left[-\frac{\hbar^2}{2m}(\nabla + i\mathbf{k})^2 + U(\mathbf{r})\right] u_{\mathbf{k}}(\mathbf{r}) = E u_{\mathbf{k}}(\mathbf{r}) \tag{5.5}$$

This equation is difficult to solve for any general potential $U(\mathbf{r})$. However, the periodicity of the lattice lets us infer general features of the solution even without solving it explicitly.

### 5.1.2 General consequences of periodicity

## A. Quantization of k

Because of lattice periodicity it is enough to solve the equation in one primitive cell of the reciprocal lattice. Thus independent $\mathbf{k}$ values are confined to the first Brillouin zone.

The allowed values of $\mathbf{k}$ are quantized as

$$\mathbf{k} = \frac{2\pi}{L} n, \quad n \in \mathbb{Z}$$

## B. Number of k values

The total number of independent values of $\mathbf{k}$ is

$$\frac{L}{a} = N$$

i.e., equal to the number of lattice sites.

## C. Significance of k

$$\hat{p}\psi_{\mathbf{k}} \neq \hbar\mathbf{k}\psi_{\mathbf{k}}$$

Thus Bloch states are not eigenstates of the momentum operator. This is expected since translational invariance is broken by the lattice potential.

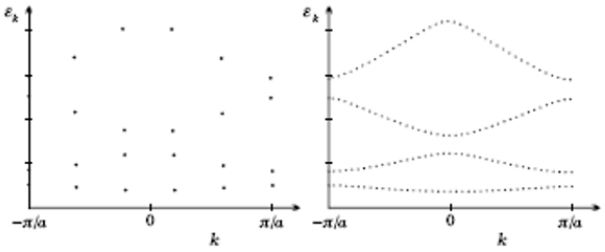


Figure 5.1: Energy levels of electrons in periodic potential for 1D chains

**k** is called the **crystal momentum**. It:

- determines selection rules in scattering processes
- determines the phase factor under lattice translations:

$$\psi_{\mathbf{k}}(\mathbf{r}+\mathbf{R}) = e^{i\mathbf{k}\cdot\mathbf{R}}\psi_{\mathbf{k}}(\mathbf{r})$$

## D. Formation of energy bands

Equation (1) is an eigenvalue problem in a box (primitive lattice) with periodic boundary conditions:

$$u_{\mathbf{k}}(\mathbf{r}+\mathbf{R}) = u_{\mathbf{k}}(\mathbf{r})$$

For each **k** there are infinitely many discrete energy eigenvalues:

$$E = E_n(\mathbf{k})$$

The set of energies for fixed $n$ and varying **k** forms an **energy band**.

## Equivalence of k and k + G

For a reciprocal lattice vector **G**,

$$\psi_{\mathbf{k}+\mathbf{G}}(\mathbf{r}) = e^{i(\mathbf{k}+\mathbf{G})\cdot\mathbf{r}}u_{\mathbf{k}}(\mathbf{r})$$

$$= e^{i\mathbf{k}\cdot\mathbf{r}}\left(e^{i\mathbf{G}\cdot\mathbf{r}}u_{\mathbf{k}}(\mathbf{r})\right)$$

Since $e^{i\mathbf{G}\cdot\mathbf{r}}$ is lattice periodic,

$$|\psi_{\mathbf{k}+\mathbf{G}}(\mathbf{r})|^2 = |\psi_{\mathbf{k}}(\mathbf{r})|^2$$

Thus, the two states are physically equivalent.

Energy:

$$E(\mathbf{k}+\mathbf{G}) = \frac{\hbar^2}{2m}|\mathbf{k}+\mathbf{G}|^2 \tag{5.6}$$

Expanding:

$$= \frac{\hbar^2}{2m}(k^2 + G^2 + 2\mathbf{k}\cdot\mathbf{G})$$

Using periodicity:

$$E(\mathbf{k}+\mathbf{G}) = E(\mathbf{k})$$

## 5.2 Nearly Free Electron Approximation

**Nearly free electron viewpoint:** We begin with the Sommerfeld free-electron states and treat the periodic lattice potential as a weak perturbation. As the potential is adiabatically turned on, the free-electron eigenstates evolve continuously into Bloch states, in accordance with Bloch's theorem.

For a weak periodic potential, this evolution is smooth over most of reciprocal space, and the resulting dispersion remains approximately free-electron-like. However, this correspondence breaks down near special points where the free-electron energies satisfy Bragg reflection conditions, i.e., when $\mathbf{k}$ lies near a Brillouin zone boundary.

At these points, degenerate (or nearly degenerate) free-electron states are strongly mixed by the periodic potential, leading to the opening of energy gaps and a qualitative reconstruction of the spectrum. In contrast, states far from these regions are only weakly perturbed.

Thus, the nearly free electron model provides a controlled framework: it reproduces free-electron behavior over most of $k$-space, while systematically incorporating band gaps at the Brillouin zone boundaries. The validity of starting from free-electron states is therefore justified *a posteriori*.

### Empty lattice approximation

Writing the potential and the Bloch function in terms of their Fourier components:

$$U(\mathbf{r}) = \sum_{\mathbf{G}} U_{\mathbf{G}} e^{i\mathbf{G}\cdot\mathbf{r}}$$

$$u_{\mathbf{k}}(\mathbf{r}) = \sum_{\mathbf{G}} C_{\mathbf{k}-\mathbf{G}} e^{i\mathbf{G}\cdot\mathbf{r}}$$

Substitute into Eqn. 5.4, multiply by $e^{-i(\mathbf{k}-\mathbf{G})\cdot\mathbf{r}}$ and integrate over primitive cell:

$$\left[\frac{\hbar^2}{2m}|\mathbf{k}-\mathbf{G}|^2 - E\right] C_{\mathbf{k}-\mathbf{G}} + \sum_{\mathbf{G}'} U_{\mathbf{G}-\mathbf{G}'} C_{\mathbf{k}-\mathbf{G}'} = 0 \tag{5.7}$$

In the limit $U \to 0$; the solutions are either

$$c_{\mathbf{nk}}\left(\mathbf{G}_i\right) = 0$$

or

$$\varepsilon_{nk} = \frac{\hbar^2}{2m}\left(\mathbf{k} + \mathbf{G}_n\right)^2$$

for a particular value of $G_i = G_n$

The solution in the empty lattice for the band of index n is therefore particularly simple: apart from a single $\mathbf{G_n}$, all reciprocal-lattice vectors have vanishing coefficients in the expansion. The normalized Bloch function of this state is then

$$\psi_{nk}\left(\mathbf{r}\right) = \frac{1}{\sqrt{V}} e^{i\mathbf{k}.\mathbf{r}} e^{i\mathbf{G}_n.\mathbf{r}}$$

Thus, there is a direct one-to-one correspondence between the band indices $n$ and the reciprocal lattice vectors $\mathbf{G_n}$.

## 5.3 Band structure of electrons in a 1-D lattice

Consider a lattice of length $L$ with lattice spacing $a = L/N$. The allowed values of $k = m\frac{2\pi}{L}$ with $-\frac{\pi}{a} < k < \pi/a$; with $-\frac{N}{2} < m < \frac{N}{2}$.

The reciprocal lattice vector is $G_n = n\frac{2\pi}{a}$.

In the empty lattice approximation:

$$\varepsilon_{nk} = \frac{\hbar^2}{2m}\left(\mathbf{k} + \mathbf{G}_n\right)^2 = \frac{\hbar^2}{2m}\left(\frac{2\pi}{L}\right)^2 \left(m + nN\right)^2$$

This looks different from the free electron energy derived using the Sommerfeld model,

$$\varepsilon_k = \frac{\hbar^2}{2m}k^2 = \frac{\hbar^2}{2m}\left(\frac{2\pi}{L}\right)^2 m^2$$

The apparent difference becomes clear once we consider the bands in the different zone schemes.

- **Reduced zone scheme:** All the bands are drawn in the first Brillouin zone.
- **Repeated/periodic zone scheme:** Every band is drawn in every Brillouin zone.
- **Extended zone scheme:** Different bands are drawn in different Brillouin zones

The infinite number of solutions associated with a given $\mathbf{k}$ can also be distributed among the infinite number of vectors $\mathbf{k} + \mathbf{G}$ in such a way that one solution belongs to each equivalent vector. The reciprocal lattice can be broken up into Brillouin zones of different orders using the same procedure for creating a Wigner-Seitz cell. The assignment of the

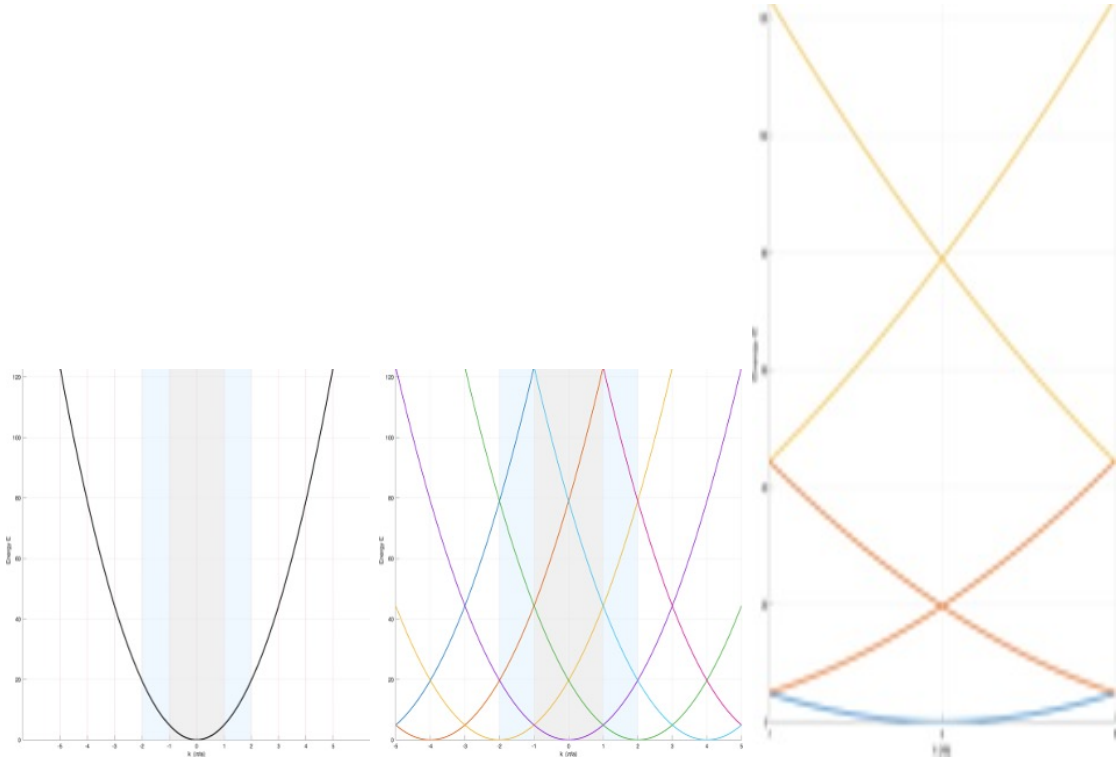

Figure 5.2: Dispersion relation of free electrons in empty lattice approx in (a) extended zone scheme, (b) repeated one scheme, and (c) Reduced zone scheme.

states to the zones is then done simply by assigning the states of the first band to the wave vectors in the first Brillouin zone, the states of the second band to the wave vectors in the second Brillouin zone, and so forth. This is how the **extended-zone** scheme is obtained.

Conversely, energy eigenvalues of the electrons moving through the empty lattice for a given **k** value in the **reduced zone scheme** can be got from the free-electron dispersion curve by finding the equivalent **k** values inside the first Brillouin zone for each wave number outside of it, and then shifting the energy eigenvalue to this **k** value. This procedure is called **zone folding**.

**Fermi surface in empty lattice approximation:** Fermi-Dirac statistics determine the filling of the energy levels – Fermi surface important as properties of metals are determined by the electronic density of states at these points - dispersion relation obtained in the extended-zone scheme in the empty lattice approximation is identical to the quadratic dispersion relation of free electrons - the $n^{th}$ band is the part of the free-electron spectrum that falls into the $n^{th}$ Brillouin zone.

Assignment of states:

- first band → first BZ
- second band → second BZ

## 5.4 Band structure of electrons in a 2-D lattice

Lattice constant $a$, $z$ electrons per site, $N$ sites – total number of electrons $N_e = zN$.

In two dimensions, the number of allowed $k$-states inside a circle of radius $k_F$ is given by

$$\text{Number of states} = 2 \times \frac{\text{Area of circle}}{\text{area per state}},$$

where the factor of 2 accounts for spin degeneracy.

The area of the Fermi circle is

$$\pi k_F^2,$$

and the area per state in $k$-space is

$$\left(\frac{2\pi}{L}\right)^2 = \frac{(2\pi)^2}{L^2}.$$

Thus,

$$N_e = 2 \times \frac{\pi k_F^2}{(2\pi)^2/L^2} = 2 \times \pi k_F^2 \times \frac{L^2}{(2\pi)^2} = \frac{L^2 k_F^2}{2\pi}.$$

**Relating to electron density:**

The total number of electrons is

$$N_e = zN = z\frac{L^2}{a^2}.$$

**Final result:**

$$k_F = \frac{\sqrt{2\pi z}}{a}.$$

In two dimensions, the electron density is

$$n = \frac{z}{a^2},$$

so that

$$k_F = \sqrt{2\pi n}.$$

Thus, the Fermi wave-vector scales as the square root of the electron density.

**Case $z = 1$:**

For $z = 1$,

$$k_F = \frac{\sqrt{2\pi}}{a} < \frac{\pi}{a},$$

the boundary of the 1st Brillouin zone. Hence, the Fermi surface lies entirely inside the 1st Brillouin zone.

**Case $z = 2$:**

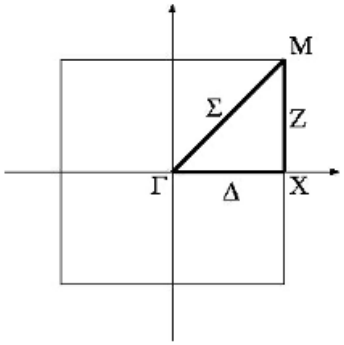


Figure 5.3: Brillouin zone for a 2-D square lattice

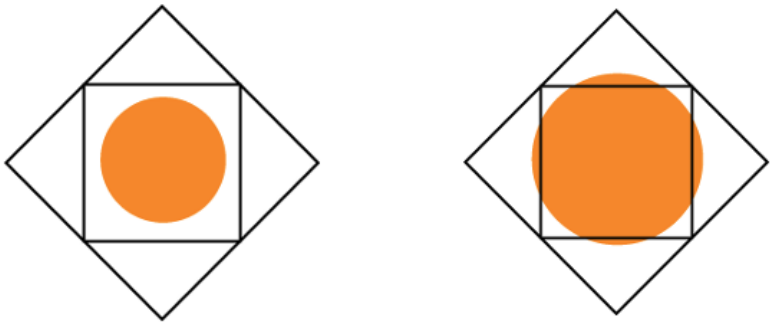

Figure 5.4: Fermi surface for left panel: $z = 1$, and right panel: $z = 2$

For $z = 2$,

$$k_F = \frac{2\sqrt{\pi}}{a} > \frac{\pi}{a}.$$

In this case, $k_F$ is larger than the distance $\Gamma X = \frac{\pi}{a}$ but smaller than $\Gamma M = \frac{\sqrt{2}\pi}{a}$.

Thus, when the lowest-energy states are filled gradually by electrons in the ground state (as required by Fermi–Dirac statistics), the lowest-lying states in the second band become occupied before the highest-lying states in the first band.

### 5.4.1 Electron-like and hole-like surfaces

For the case $z = 2$, in reduced zone representation, the Fermi surfaces forms discontinuous structure for the 1st and 2nd bands. If the wave vectors are reduced about the points $M$ or $X$ rather than $\Gamma$, then the 1st and 2nd bands form continuous Fermi surfaces – the 1st band is hole-like, and the 2nd band is electron-like (Fig. 5.5).

In the repeated/periodic zone scheme, the nth band is formed of those regions where circles from at least $n$ different zones overlap (Fig. 5.6).

The bands thus formed can be electron-like or hole-like, depending on whether they enclose a filled area or an empty area. Note that in a magnetic field, electrons will move along a constant energy surface (remember: magnetic field does not do any work on a moving

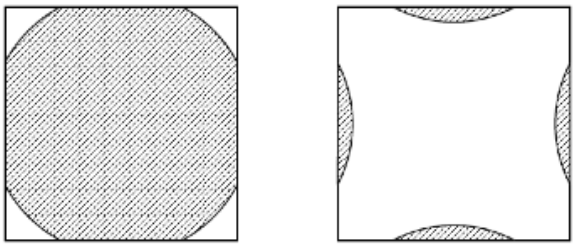

Figure 5.5: Band structure for $z = 2$ in a 2-D lattice in the reduced zone scheme

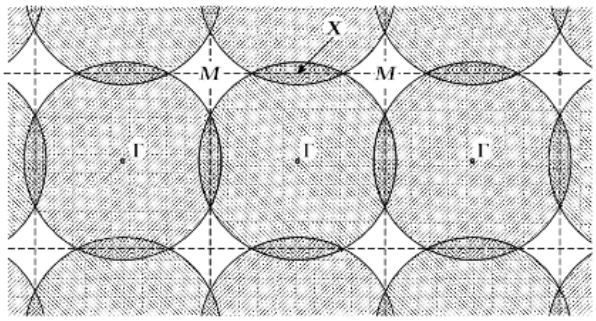


Figure 5.6: Band structure for z=2 in 2-D lattice in repeated zone scheme

charge). For a free electron

$$\hbar \frac{d\mathbf{k}}{dt} = -e\mathbf{v} \times \mathbf{B} = -\frac{e}{\hbar} \nabla_k \varepsilon \times \mathbf{B}$$

Particles in electron-like Fermi surface move in a sense opposite to that in hole-like orbits.

## 5.5 Band structure of simple cubic lattice with monatomic basis

Fig. 5.7 left panel is for wave vectors along the line $\Delta$ connecting the center $\Gamma = (0, 0, 0)$ of the Brillouin zone and $X = (\pi/a)(0, 0, 1)$. The numbers represent the degeneracy of the bands. We will calculate the energy of the state associated with the wave vector $\left(\frac{\pi}{a}\right)(0,\ 0,\ k)\,;\, 0 < k < 1$.

Remember the energy is given by $\varepsilon_{nk} = \frac{\hbar^2}{2m}\left(\mathbf{k} + \mathbf{G}_n\right)^2$ The various bands are:

Band A: $G = 0$ $\varepsilon_A = \frac{\hbar^2}{2m}\left(\mathbf{k} + \mathbf{G}_n\right)^2 = \frac{\hbar^2}{2m}\left(\frac{\pi}{a}\right)^2\ k^2$

Band B: $G = \frac{2\pi}{a}\left(0, 0, \bar{1}\right)\ \varepsilon_B = \frac{\hbar^2}{2m}\left(\mathbf{k} + \mathbf{G}_n\right)^2 = \frac{\hbar^2}{2m}\left(\frac{\pi}{a}\right)^2\ (k-2)^2$

Band C: $G = \frac{2\pi}{a}\left(0, 0, 1\right)\ \varepsilon_C = \frac{\hbar^2}{2m}\left(\mathbf{k} + \mathbf{G}_n\right)^2 = \frac{\hbar^2}{2m}\left(\frac{\pi}{a}\right)^2\ (k+2)^2$

Band D,E,F,G: $G = \frac{2\pi}{a}\left(1, 0, 0\right), \frac{2\pi}{a}\left(\bar{1}, 0, 0\right), \frac{2\pi}{a}\left(0, 1, 0\right), \frac{2\pi}{a}\left(0, \bar{1}, 0\right) \varepsilon_C = \left(\frac{\pi}{a}\right)^2\ (k^2 + 4)$. This band is 4-fold degenerate.

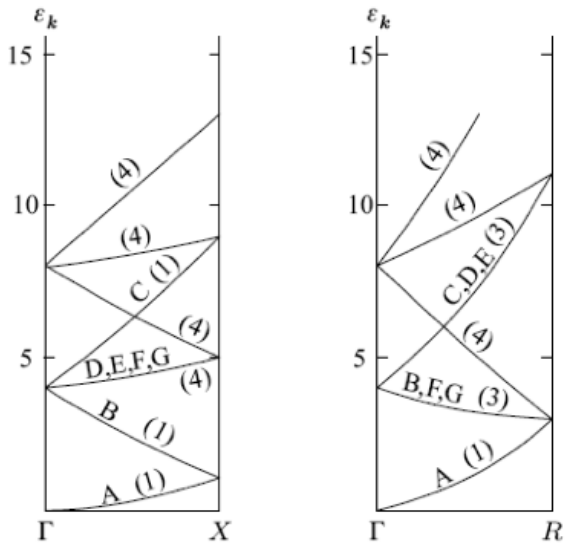


Figure 5.7: Band diagram for simple cubic along two symmetry directions

Similarly, Fig. 5.7 right panel is for wave vectors along the line $\Lambda$ connecting the center $\Gamma = (0, 0, 0)$ of the Brillouin zone and $R = (\pi/a)(1, 1, 1)$.

## 5.6 Effect of weak lattice potential on the free electron dispersion relation

Treat $U$ to be a weak perturbation – need not solve the equation – can get the result applying perturbation theory to the $U = 0$ case of free electrons. The results vary appreciably from the free electron model only near the centre and the edges of the Brillouin zones. Take the simple example of system of electrons in a very weak 1-D periodic lattice. At the edge of the Brillouin zone ($k = \pm n\frac{\pi}{a}$) the condition for Bragg reflection is satisfied. [Recall: Bragg condition $k = |k - G|$ in 1-D is $k = \pm G/2 = \pm n\pi/a$.] Hence electrons with wave vector at the Brillouin zone edge ($k = \pm\frac{n\pi}{a}$) form standing waves – solutions linear superposition of left moving and right moving waves – two different solutions can be formed from the linear combination of the left-moving $e^{ikx} = e^{i\frac{\pi x}{a}}$ and the right-moving waves $e^{-ikx} = e^{-i\frac{\pi x}{a}}$ –

$$\psi_+ = \frac{e^{i\frac{\pi x}{a}} + e^{-i\frac{\pi x}{a}}}{\sqrt{2}} = \sqrt{2}\cos\left(\frac{\pi x}{a}\right)$$

$$\psi_- = \frac{e^{i\frac{\pi x}{a}} - e^{-i\frac{\pi x}{a}}}{\sqrt{2}} = \sqrt{2}i\sin\left(\frac{\pi x}{a}\right)$$

$\psi_+$ and $\psi_-$ are the symmetric and anti-symmetric solutions respectively. Charge density associated with $\psi_+$ is

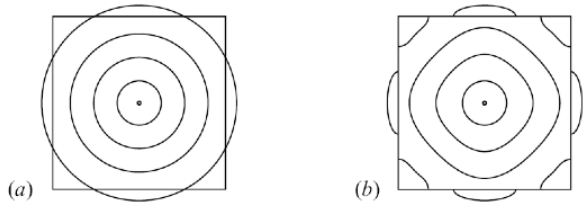


Figure 5.8: Constant energy surfaces for (a) free electrons and (b) electrons in a weak periodic potential

$$\rho_+ \propto |\psi_+|^2 \propto \cos^2\left(\frac{\pi x}{a}\right)$$

Similarly

$$\rho_- \propto |\psi_-|^2 \propto \sin^2\left(\frac{\pi x}{a}\right)$$

Density of electrons for $\psi_+$ maximum near $x = 0, a, \ldots$ i.e. at the lattice sites where the potential energy is minimum. Similarly density of electrons for $\psi_-$ maximum near $x = \frac{a}{2}, \frac{3a}{2} \ldots$ i.e. in between the lattice sites where the potential energy is maximum. So the energies of the two states at the Brillouin zone edge are no longer degenerate – they differ in energies – a band gap opens up of magnitude $E_g$ just below the gap the state is $\psi_+$ and just above the gap the state is $\psi_-$.

**Estimate of $E_g$:** Write the potential energy of the electrons as $U(x) = -U_0 \cos\left(\frac{2\pi x}{a}\right)$. The first-order difference in the energy between the two states is

$$E_g = \int_0^a dx\, U(x) \left(|\psi_-|^2 - |\psi_+|^2\right) = U_0$$

So the band gap is the Fourier component of the potential energy.

**Note:** At zone boundaries, we have standing waves – group velocity $v_g = \partial\varepsilon/\partial k = 0$, implying that the slope of the dispersion relation vanishes at the zone boundary.

The constant energy surfaces are spherical in the free-electron approximation. In the case of electrons in a weak periodic potential, the surfaces are no longer spherical – they are distorted as the Brillouin edge is approached (Fig. 5.8).

# Chapter 6

# Semiclassical Model of electron dynamics

## 6.1 Introduction

The Semiclassical model was an attempt to bridge the gap between classical and quantum descriptions. The Sommerfeld model is justified if a description at the atomic distance is not needed. Under this model, the equations of motion are:

$$\frac{d\mathbf{r}}{dt} = \frac{\hbar\mathbf{k}}{m}, \tag{6.1}$$

$$\hbar\frac{d\mathbf{k}}{dt} = -e\left(\mathbf{E} + \dot{\mathbf{r}} \times \mathbf{B}\right) \tag{6.2}$$

In reality, electrons are described by wavefunctions:

$$(r,t) = \sum_{k'} g\left(\mathbf{k}'\right) e^{i(\mathbf{k}'.\mathbf{r} - E't/\hbar)};\ E' = \frac{\hbar^2 k^{2'}}{2m} \tag{6.3}$$

with $g\left(\mathbf{k}'\right) \approx 0$ for $|\mathbf{k} - \mathbf{k}'| > \Delta\mathbf{k}$

We can generalize the approach to electrons in a general periodic potential. This will lead to the Semi-classical model of Bloch electrons. As in the Sommerfeld and Drude model, two main questions arise:

- What is the nature of collisions?
- How do electrons move between collisions?

As far as the first point goes, electrons in a perfectly periodic lattice cannot be scattered by collision with static ions—Bloch states are stationary solutions in the presence of the ions. This implies that the electronic conductivity of a perfect lattice at absolute zero of temperature is infinite. Resistance in a normal metal arises due to:

- Imperfections, defects, impurities

- Thermal lattice vibrations

The semi-classical model does not inquire about the source of the scattering – it assumes there is scattering of the Bloch electrons, which is parameterized by the relaxation time $\tau$.

### 6.1.1 Why Semiclassical?

To have a well-defined wave vector $\Delta\mathbf{k}$ must be small compared to the length of the Brillouin zone, implying the size of the wave-packet (in some sense the uncertainty in the position of the electron) must be of the order of a few lattice constants. Thus, the semi-classical model is applicable to fields that vary very little over this length scale.

- periodic potential varies on a scale < lattice spacing—need quantum mechanical treatment
- external field varies on a scale > lattice spacing—can use classical treatment

The model needs as its only input the energy dispersion $\varepsilon_{nk}$ of the system – no further knowledge of the periodic potential is required.

**Aim of the model:** Relate transport properties to band structure

## 6.2 Semiclassical Electron Dynamics in a Crystal

Consider an electron with position vector $\boldsymbol{r}$, wave vector $\boldsymbol{k}$ (defined in terms of a wave packet), and band index $n$. The energy is given by $\varepsilon_{n\boldsymbol{k}}$.

### Rules of the game

- The band index $n$ is invariant (no inter-band transfer is allowed). We need to consider only these bands that lie within an energy window of $k_BT$ around the Fermi energy.
- The vectors $\boldsymbol{k}$ and $\boldsymbol{r}$ evolve according to:

$$\boldsymbol{v}_{n\boldsymbol{k}} = \frac{d\mathbf{r}}{dt} = \frac{1}{\hbar}\nabla_{\mathbf{k}}E_n(\mathbf{k}) \tag{1}$$

$$\hbar\frac{d\boldsymbol{k}}{dt} = -e\left[\boldsymbol{E}(\boldsymbol{r},t) + \frac{d\boldsymbol{r}}{dt}\times\boldsymbol{B}(\boldsymbol{r},t)\right] \tag{2}$$

- $\boldsymbol{k}$ is uniquely defined only within a Brillouin zone.
- In thermal equilibrium, the number of states in the $n^{th}$ band with wave vectors between $\boldsymbol{k}$ and $\boldsymbol{k}+d\boldsymbol{k}$ is:

$$f(\boldsymbol{k})\frac{d\boldsymbol{k}}{4\pi^3} = \frac{d\boldsymbol{k}}{4\pi^3}\frac{1}{e^{(\varepsilon_{n\boldsymbol{k}}-\mu)/k_BT}+1}$$

## Points to Note

- No inter-band transfer of electrons is allowed. Each band can be treated independently. Only bands within a few $k_BT$ of the Fermi energy $\varepsilon_F$ need to be considered.
- Significance of $\boldsymbol{k}$: The total force on the electron is

$$\boldsymbol{F} = \boldsymbol{F}_{\text{ext}} + \boldsymbol{F}_{\text{periodic potential}}.$$

  The above equations relate the evolution of $\boldsymbol{k}$ only to the *external force*. Thus, $\boldsymbol{k}$ is not the true momentum of Bloch electrons; it is referred to as the **crystal momentum**.

### 6.2.1 Energy Evolution

For Bloch electrons in an external electric field $\mathbf{E}$, the work done is:

$$dW = -e\mathbf{E} \cdot \mathbf{v_{nk}} dt$$

This should equal the change in energy:

$$d\varepsilon_{nk} = \frac{\partial \varepsilon_{nk}}{\partial k} \cdot \frac{d\mathbf{k}}{dt} dt = \hbar \boldsymbol{v_{nk}} \cdot \frac{d\mathbf{k}}{dt} dt$$

yielding:

$$\hbar \frac{d\mathbf{k}}{dt} = -e\mathbf{E} \tag{6.4}$$

This is the same formula as for free electrons.

From now on, we use $\mathbf{v}$ and $\varepsilon$ instead of $\mathbf{v_{nk}}$ and $\varepsilon_{nk}$ for notational simplicity.

### 6.2.2 Acceleration and Effective Mass

$$\mathbf{v} = \frac{1}{\hbar} \nabla_{\mathbf{k}} E \tag{6.5}$$

$$\frac{d\mathbf{v}}{dt} = \frac{1}{\hbar} \frac{d}{dt} \left[ \frac{\partial \varepsilon}{\partial \mathbf{k}} \right] = \frac{1}{\hbar^2} \frac{\partial^2 E}{\partial k^2} \hbar \frac{d\mathbf{k}}{dt} = \frac{1}{m} \mathbf{F} \tag{6.6}$$

Here $F = \hbar d\mathbf{k}/dt$ is the force and $m$ the band mass. In general, for a non-isotropic band,

$$\frac{d\mathbf{v_{ff}}}{dt} = \frac{1}{m^*} \mathbf{F}_\beta$$

with the effective mass tensor:

$$\left( \frac{1}{m^*} \right)_{\alpha\beta} = \frac{1}{\hbar^2} \frac{\partial^2 \varepsilon}{\partial k_\alpha \partial k_\beta}, \text{ with } \alpha,\, \beta = x,\, y,\, z \tag{6.7}$$

### Significance of k

The total force on an electron is

$$\mathbf{F} = \text{force from lattice} + \text{force from external fields.}$$

Eq. 6.6 relates the change of $\mathbf{k}$ to external forces. Thus, $\hbar\mathbf{k}$ is not the true momentum of Bloch electrons — it is called the **crystal momentum**.

## (c) Limit of validity of the semiclassical model

- Must break down as $U \to 0$; goes to the free electron case.
- As $\mathbf{E}$ increases, the energy of the electrons increase electrons may leave the band.

The first restriction implies some strength of $U$ before the model can be applied. The second restriction gives a limit on the strength of applicable fields $\mathbf{E}$.

$$e|\mathbf{E}|a \ll \frac{\varepsilon_g^2(\mathbf{k})}{\varepsilon_F}$$

$$\hbar\omega_c \ll \frac{\varepsilon_g^2(\mathbf{k})}{\varepsilon_F}$$

where

$$\varepsilon_g(\mathbf{k}) = E_n(\mathbf{k}) - E_{n'}(\mathbf{k}), \quad \text{is the band gap}$$

$n, n'$ being the nearest bands. $\hbar\omega_c = eB/m$ is the cyclotron frequency due to a magnetic field $B$.

### Check the conditions

- **Limit on electric field:** Typically smallest gaps $\varepsilon_g \sim 0.01\,\text{eV}$. To violate the condition above, we will need the maximum electric field to satisfy $ea|\mathbf{E}_{\max}| \sim 10^{-2}\,\text{eV}$, or, $|\mathbf{E}_{\max}| \sim 10^6\,\text{V/m}$. This value is exceedingly large — not practical.
- **Limit on magnetic field:** For $B = 1$ T, $\hbar\omega \sim 10^{-4}\,\text{eV}$, condition fails for $\varepsilon_g \sim 0.01\,\text{eV}$. Thus, for narrow bandgap materials, the semiclassical model breaks down.
- **Limit on frequency $\omega$ of radiation:** Need $\hbar\omega \ll \varepsilon_g$; otherwise photon absorption can cause interband transitions.

## 6.3 Results from the semiclassical model

### 6.3.1 Filled bands cannot contribute to transport

Phase space density of filled band states is constant: *Liouville's theorem.* Under evolution according to equations of motion, this remains unchanged.

*Reason:* Liouville's theorem states that the volume element $d^3\mathbf{r}\, d^3\mathbf{k}$ in phase space is unchanged under semiclassical equations of motion. Since $f(\mathbf{r}, \mathbf{k})$ remains unchanged, the density in $\mathbf{k}$-space remains constant.

The macroscopic electrical current, when integrated over a completely filled band, is:

$$\mathbf{j_e} = -e \int \frac{d^3k}{4\pi^3}\, \mathbf{v}(\mathbf{k}) = -e \int \frac{d^3k}{4\pi^3}\, \frac{1}{\hbar} \frac{\partial \varepsilon}{\partial \mathbf{k}} = 0$$

Similarly, the thermal current integrated over a filled band vanishes:

$$\mathbf{j_{th}} = \int \frac{d^3k}{4\pi^3}\, \varepsilon(\mathbf{k}) \frac{1}{\hbar} \frac{\partial \varepsilon}{\partial \mathbf{k}} = 0$$

These results follow from Green's theorem for periodic functions, which states: *the integral over a unit cell of the derivative of a periodic function must vanish.*

**Conclusion:** Completely filled (empty) bands do not contribute to transport or electrical conduction $\Rightarrow$ band insulators.

Only partially filled bands contribute to the thermal or electrical current. The number of electrons in these partially filled bands constitutes an "electron sea" – this is the number $n$ used in the Drude-Sommerfeld model. Also, only solids with an even number of electrons per unit cell can form completely filled bands. From the above reasoning, only they can form insulators. The converse is, of course, not true.

## 6.4 Semiclassical motion in DC electric field

$$\hbar \frac{d\mathbf{k}}{dt} = -e\mathbf{E}.$$

All $\mathbf{k}$-wavevectors change by the same amount. $\mathbf{E}$ field cannot change the density of the filled band — only the Fermi surface shifts to a new center.

$$\mathbf{k}(t) = \mathbf{k}_0 - \frac{e\mathbf{E}t}{\hbar}.$$

**What happens when an E field is applied?**

$$\mathbf{k} \to \mathbf{k} - \frac{e\mathbf{E}t}{\hbar}.$$

The electron velocity $\mathbf{v}$ also changes, but is not proportional to $\mathbf{k}$ as in the free electron case.

$$\mathbf{v}(\mathbf{k}) \;\Rightarrow\; \mathbf{v}\left(\mathbf{k} - \frac{e\mathbf{E}t}{\hbar}\right).$$

For $\mathbf{E}$ parallel to a reciprocal lattice vector, $\mathbf{k} - \frac{e\mathbf{E}t}{\hbar}$ oscillates periodically in the Brillouin zone. Hence $\mathbf{v}$ oscillates with $\mathbf{E}$.

**Important clarification:**

The solution

$$\mathbf{k}(t) = \mathbf{k}_0 - \frac{e\mathbf{E}}{\hbar}t$$

is formally unbounded. However, in a crystal, $\mathbf{k}$ is defined only modulo a reciprocal lattice vector $\mathbf{G}$:

$$\mathbf{k} \equiv \mathbf{k} + \mathbf{G}.$$

Thus, in the reduced zone scheme, $\mathbf{k}(t)$ is periodic in time, even though it evolves linearly in the extended zone picture.

## Bloch oscillations

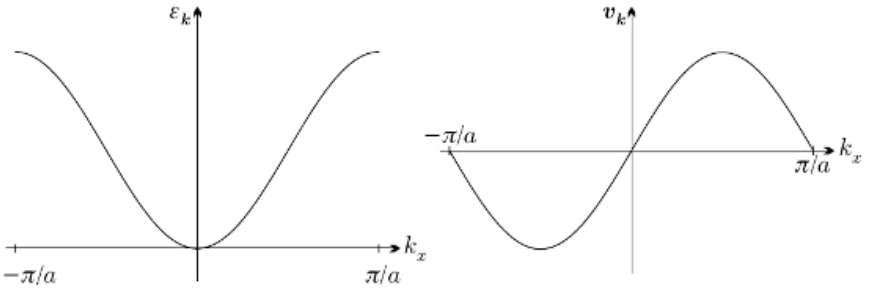


Figure 6.1: Left: Dispersion relation. Right panel: Plot of $\mathbf{v_k}$ versus $\mathbf{k}$.

- $\mathbf{v_k} \propto \sin(ka) \;\Rightarrow$ zero at band edges.
- Sign of acceleration changes halfway from $k = 0$ to $k = \pm\pi/a$.

Near the band edge, the periodic potential has a stronger effect, so it gradually slows down and eventually reverses the velocity $\Rightarrow$ oscillatory behavior.

**General origin of Bloch oscillations:**

The band energy is periodic:

$$E(\mathbf{k}) = E(\mathbf{k} + \mathbf{G}),$$

and hence

$$\mathbf{v}(\mathbf{k}) = \frac{1}{\hbar}\nabla_{\mathbf{k}} E(\mathbf{k})$$

is also periodic in $\mathbf{k}$.

Since $\mathbf{k}(t)$ sweeps across the Brillouin zone, $\mathbf{v}(t) = \mathbf{v}(\mathbf{k}(t))$ becomes periodic in time (Fig. 6.1). Therefore, the electron executes oscillatory motion in real space — this is the **Bloch oscillation**.

**Bloch frequency:**

The time to traverse one Brillouin zone $\Delta k = 2\pi/a$ is

$$T_B = \frac{2\pi/a}{eE/\hbar} = \frac{2\pi\hbar}{eEa},$$

$$\omega_B = \frac{eEa}{\hbar}.$$

**Why don't we see this oscillatory behavior in metals?**

Collisions reset everything — change in wave-vector between collisions is negligible.

Typical estimate:

$$\tau \sim 10^{-14}\,\mathrm{s}$$
$$\Delta k \sim \frac{eE\tau}{\hbar} \sim 10\,\mathrm{m}^{-1}$$

The value of $\Delta k$ is much smaller than the typical Brillouin zone size $\pi/a \sim 10^{10}\,\mathrm{m}^{-1}$.

**Condition for observing Bloch oscillations:**

To observe oscillations, one requires

$$\frac{eE\tau}{\hbar} \sim \frac{\pi}{a},$$

i.e., electrons must traverse a significant fraction of the Brillouin zone before scattering.

This is realized in:

- Very clean systems (large $\tau$)
- Artificial superlattices (small Brillouin zone $\Rightarrow$ small $\Delta k$)
- Cold atom optical lattices

## Concept of holes

**Recall:** The current carried by electrons in a completely filled band is zero. Hence,

$$0 = -e\int_{\text{band}} \frac{d^3k}{4\pi^3}\,\mathbf{v}(\mathbf{k}) = -e\int_{\text{unoccupied}} \frac{d^3k}{4\pi^3}\,\mathbf{v}(\mathbf{k}) - e\int_{\text{occupied}} \frac{d^3k}{4\pi^3}\,\mathbf{v}(\mathbf{k}).$$

Therefore,

$$-e\int_{\text{occupied}} \frac{d^3k}{4\pi^3}\,\mathbf{v}(\mathbf{k}) = e\int_{\text{unoccupied}} \frac{d^3k}{4\pi^3}\,\mathbf{v}(\mathbf{k}).$$

Two equivalent mental pictures are available:

1. The current
$$\mathbf{j} = -\frac{e}{4\pi^3}\int_{\text{occupied}} \mathbf{v}(\mathbf{k})\, d^3k$$
is carried by electrons (charge $-e$) occupying the filled states of the band.

2. The same current
$$\mathbf{j} = \frac{e}{4\pi^3}\int_{\text{unoccupied}} \mathbf{v}(\mathbf{k})\, d^3k$$
can be viewed as being carried by holes (charge $+e$) occupying the empty states.

*Note:* One must not mix the electron and hole descriptions within the same band.

**Equation of motion for holes:**

For electrons:
$$\hbar\frac{d\mathbf{k}}{dt} = -e\mathbf{E}.$$

For holes:
$$\hbar\frac{d\mathbf{k}_h}{dt} = +e\mathbf{E}.$$

Thus, holes respond to external fields as positively charged carriers.

**Effective mass:**

Near the top of the band, expand the dispersion about a maximum at $\mathbf{k}_0$:
$$\varepsilon(\mathbf{k}) \approx \varepsilon_0 - A(\mathbf{k}-\mathbf{k}_0)^2,$$
where the linear term vanishes, and the quadratic coefficient is negative since $\varepsilon(\mathbf{k}_0)$ is a maximum.

Define a positive mass parameter $m_h$ by
$$A = \frac{\hbar^2}{2m_h}.$$

Then, for $\mathbf{k}$ close to $\mathbf{k}_0$,
$$\mathbf{v}(\mathbf{k}) = \frac{1}{\hbar}\frac{\partial\varepsilon}{\partial\mathbf{k}} = -\frac{\hbar}{m_h}(\mathbf{k}-\mathbf{k}_0).$$

The acceleration is:
$$\mathbf{a} = \frac{d\mathbf{v}}{dt} = -\frac{\hbar}{m_h}\frac{d\mathbf{k}}{dt}.$$

Using the semiclassical equation of motion:
$$\hbar\frac{d\mathbf{k}}{dt} = -e\left[\mathbf{E} + \mathbf{v}\times\mathbf{B}\right],$$
we obtain:
$$m_h\mathbf{a} = e\left[\mathbf{E} + \mathbf{v}\times\mathbf{B}\right].$$

Thus, electrons near the top of the band behave as if they have a **negative effective mass**, since their acceleration is opposite to the applied force.

**Geometric interpretation (important):**

The effective mass is determined by the band curvature:

$$\frac{1}{m^*} = \frac{1}{\hbar^2}\frac{\partial^2 \varepsilon}{\partial k^2}.$$

- Near a band **minimum**: $\dfrac{\partial^2 \varepsilon}{\partial k^2} > 0 \Rightarrow m^* > 0$
- Near a band **maximum**: $\dfrac{\partial^2 \varepsilon}{\partial k^2} < 0 \Rightarrow m^* < 0$

Thus, negative effective mass is a direct consequence of negative band curvature at the top of the band.

Alternatively, this motion can be described in terms of holes: quasiparticles with charge $+e$ and positive effective mass $m_h$, obeying

$$\mathbf{F}_h = e\left(\mathbf{E} + \mathbf{v} \times \mathbf{B}\right).$$

**Key idea:**

Transport in a nearly filled band can be equivalently described in terms of holes with positive charge and positive effective mass.

## 6.5 Semiclassical motion in external magnetic field

$$\hbar \frac{d\mathbf{k}}{dt} = -e\,\mathbf{v} \times \mathbf{B} \quad \text{(ignore band index for simplicity)}$$

**Consequences:**

1. We see that $d\mathbf{k}/dt \perp \mathbf{B}$. Hence, only the component of $\mathbf{k}$ perpendicular to $\mathbf{B}$ evolves with time, and $\mathbf{k}$ moves in a plane normal to $\mathbf{B}$.
2. The rate of change of energy is
$$\frac{d\varepsilon}{dt} = \frac{\partial \varepsilon}{\partial \mathbf{k}} \cdot \frac{d\mathbf{k}}{dt} = \hbar \mathbf{v} \cdot \frac{d\mathbf{k}}{dt} = -e\,\mathbf{v} \cdot (\mathbf{v} \times \mathbf{B}) = 0.$$
Thus, the magnetic field does no work on the electron.

**Hence:** The electron energy remains constant, and $\mathbf{k}$ is confined to a constant-energy surface:

$$\varepsilon(\mathbf{k}) = \text{const.}$$

Combining the two results, the electron motion in $\mathbf{k}$-space is restricted to the *intersection* of:

- the constant-energy surface $\varepsilon(\mathbf{k}) = \text{const}$, and
- a plane perpendicular to $\mathbf{B}$.

### 6.5.1 Real space trajectory in B field

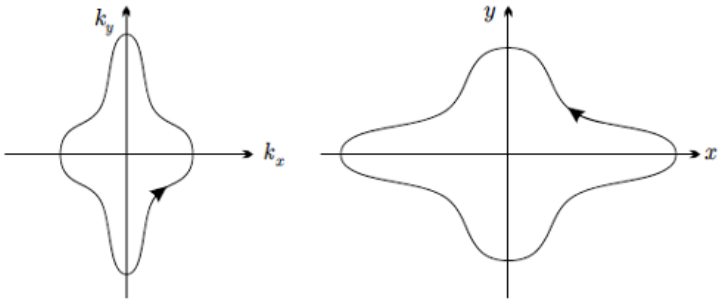


Figure 6.2: Relation between $\mathbf{k}$-space orbit and rela space orbit.

$$\frac{d\mathbf{r}}{dt} = \mathbf{v}, \qquad \hbar\frac{d\mathbf{k}}{dt} = -e\,\mathbf{v}\times\mathbf{B}.$$

Integrating,

$$\mathbf{k}(t) - \mathbf{k}(0) = -\frac{e}{\hbar}\int_0^t \mathbf{v}(t')\times\mathbf{B}\,dt'.$$

Only orbit change takes place in the direction $\perp \mathbf{B}$.

$$[\mathbf{k}(t) - \mathbf{k}(0)]_\perp = -\frac{e}{\hbar}[\mathbf{r}(t) - \mathbf{r}(0)]\times\mathbf{B}.$$

i.e.,

$$\Delta\mathbf{r}(t) = -\frac{\hbar}{eB^2}\,\Delta\mathbf{k}(t)\times\mathbf{B}.$$

**Components:**

$$\Delta x(t) = \frac{\hbar}{eB}\Delta k_y(t), \qquad \Delta y(t) = -\frac{\hbar}{eB}\Delta k_x(t).$$

**Consequences:**

- The real-space path $\mathbf{r}_\perp$ and the $\mathbf{k}$-space path $\mathbf{k}$ are related by a rotation of 90° and a scaling factor $\ell_B^2 = \hbar/(eB)$. The length scale $\ell_B$ is called the **magnetic length**(Fig. 6.2).
- If the $\mathbf{k}$-space orbit is closed $\Rightarrow$ real-space orbit is also closed.
- Motion in real space will be circular only if the motion in $\mathbf{k}$-space is circular, i.e., only if the constant energy surface is spherical.

### 6.5.2 The Onsager Quantization Condition

The quantization of the electron orbit in phase space is given by the Bohr-Sommerfeld Condition:

$$\oint \mathbf{p} \cdot d\mathbf{r} = (n + \gamma)2\pi\hbar \tag{6.8}$$

where $\mathbf{p} = \hbar\mathbf{k} - e\mathbf{A}$ is the canonical momentum, $n$ is an integer (the Landau level index), and $\gamma$ is a phase offset incorporating the Maslov index and the Berry phase.

#### Evaluating the Integral

Expanding the canonical momentum integral:

$$\oint \hbar\mathbf{k} \cdot d\mathbf{r} - \oint e\mathbf{A} \cdot d\mathbf{r} = (n + \gamma)2\pi\hbar \tag{6.9}$$

Using the equation of motion $\hbar d\mathbf{k} = -e(d\mathbf{r} \times \mathbf{B})$, we relate the real-space path to the $\mathbf{k}$-space path:

$$d\mathbf{r} = \frac{\hbar}{eB}(d\mathbf{k} \times \hat{z}) \tag{6.10}$$

For the first term:

$$\oint \hbar\mathbf{k} \cdot d\mathbf{r} = \oint \hbar\mathbf{k} \cdot \left[\frac{\hbar}{eB}(d\mathbf{k} \times \hat{z})\right] = \frac{\hbar^2}{eB}\oint (\mathbf{k} \times d\mathbf{k}) \cdot \hat{z} = \frac{2\hbar^2}{eB}A_k \tag{6.11}$$

where $A_k$ is the area enclosed by the orbit in $\mathbf{k}$-space.

For the second term, using Stokes' Theorem and the relation between real-space area $A_r$ and $\mathbf{k}$-space area $A_k$:

$$\oint e\mathbf{A} \cdot d\mathbf{r} = e\Phi = eBA_r = eBA_k\left(\frac{\hbar}{eB}\right)^2 = \frac{\hbar^2}{eB}A_k \tag{6.12}$$

#### Resulting Quantization Condition

Subtracting the two terms yields:

$$\frac{2\hbar^2}{eB}A_k - \frac{\hbar^2}{eB}A_k = (n + \gamma)2\pi\hbar \tag{6.13}$$

Solving for $A_k$ gives the final expression:

$$A_k(\epsilon_n, k_z) = \frac{2\pi eB}{\hbar}(n + \gamma) \tag{6.14}$$

Increment in $B$ that causes successive allowed orbits in $k$-space of the same area on the Fermi surface is

$$\Delta\left(\frac{1}{B}\right) = \frac{2\pi e}{\hbar A_F},$$

where $A_F$ is the extremal cross-sectional area of the Fermi surface.

The above result implies that any physical properties of the material that depend on the area enclosed by the orbit in **k**-space will oscillate as a function of $1/B$. Thus, measurement of the oscillation period $\Rightarrow$ gives $A_F$. This allows the Fermi surface to be mapped.

**Summary:**

- Electron motion in a magnetic field is along a constant energy surface
- Orbits in **k**-space are quantized
- Quantization condition depends on enclosed area
- Physical quantities oscillate as a function of $1/B$

### 6.5.3 Quantization of Magnetic Flux through Real-Space Orbits

From section 6.5.1, the real-space path and the **k**-space path are related by a rotation of 90° and a scaling factor $\hbar/eB$. This implies that the real-space area $A_r$ enclosed by the electron orbit is related to the **k**-space area $A_k$ by:

$$A_r = \left(\frac{\hbar}{eB}\right)^2 A_k \tag{6.15}$$

The magnetic flux $\Phi$ threading the real-space orbit is given by:

$$\Phi = B \cdot A_r = B \cdot \left(\frac{\hbar}{eB}\right)^2 A_k = \frac{\hbar^2}{e^2 B} A_k \tag{6.16}$$

#### Substituting the Onsager Condition

We substitute the previously derived Onsager quantization condition, $A_k = \frac{2\pi eB}{\hbar}(n+\gamma)$, into our expression for $\Phi$:

$$\Phi = \frac{\hbar^2}{e^2 B}\left[\frac{2\pi eB}{\hbar}(n+\gamma)\right] \tag{6.17}$$

#### Final Quantized Result

Simplifying the terms, we obtain:

$$\Phi = \frac{2\pi\hbar}{e}(n+\gamma) \tag{6.18}$$

Recognizing that the magnetic flux quantum is defined as $\Phi_0 = \frac{h}{e} = \frac{2\pi\hbar}{e}$, we arrive at the final result:

$$\Phi = (n+\gamma)\Phi_0 \tag{6.19}$$

This confirms that the magnetic flux through the real-space orbit is quantized in integer (or semi-integer, depending on $\gamma$) multiples of the fundamental flux quantum $\Phi_0$.

# Chapter 7

# Phonons

## 7.1 Static lattice model

The static lattice model presumes that electrons move in a constant, rigid periodic background potential – not scattered by it except for specific $k$ values at Brillouin zone boundaries – form standing waves – gaps at electronic spectrum – used to explain x-ray spectrum, equilibrium, and transport properties of metals and insulators that are dominated by electrons.

This is an unrealistic model:

- Ions are not infinitely massive – not held by infinite forces – must move about at finite $T$ because of kinetic energy.
- Quantum zero point mean square momentum even at zero $T$ – uncertainty principle.... so large in Helium that it is called a Quantum Fluid.

### 7.1.1 Where does the static lattice model fail?

Some examples are listed below:

1. Equilibrium properties – Specific heat of metals, specific heat of insulators, thermal expansion, and melting of solids.
2. Transport properties – resistance of metals, superconductivity, thermal conduction in insulators, transmission of sound in insulators.
3. Interaction with radiation – Reflectivity of ionic crystals, inelastic scattering of light, X-ray scattering.

## 7.2 Normal modes of lattice vibrations-phonons

Relax the constraint of the static lattice gradually – replace by two weaker constraints:

1. Idea of Bravais lattice still holds - it is now the mean position rather than instantaneous position – ions move about the Bravais lattice site but never diffuse away from it – assumption valid except near melting point of the solid.

2. The displacement of atoms about the equilibrium position is small compared to the inter-atomic distance. Made for analytical convenience – so that harmonic assumption holds – can ignore higher order terms in displacement- again not valid at high temperatures. The assumption fails completely in light elements like solid Helium – need a Quantum theory from scratch.

Consider elastic vibrations of a crystal with a single-atom basis.

**AIM:** Find dispersion relation (relation between frequency and wavevector of the wave – dependence on the elastic constants of the medium).

Start with a one-dimensional case. Valid for high-symmetry planes like [100], [110], [111] of a cubic lattice – for a wave propagating along this direction, entire planes of atoms move in phase either longitudinally or transversely – can describe each plane by a single coordinate – problem reduces to a 1-D case.

**Assume** – linear force-displacement relation (Hooke's law type) –terms linear in relative displacement vanish at equilibrium – next term is quadratic in relative displacements of any two points in lattice – assume only nearest neighbor interactions.

Force on the $n^{th}$ plane caused by the relative displacement of the $(n+p)^{th}$ plane is

$$F \propto (u_{n+p} - u_n) = K\,(u_{n+p} - u_n)$$

$K$ is the force constant. It:

- Relates from now on to a single atom.
- Is direction dependent.

### 7.2.1 1-D chain of ions with one basis

Assume only nearest neighbor interactions, $p = 1$. Force on the $n^{\text{th}}$ ion is (Fig. 7.1):

$$F_n = K[(u_{n+1} - u_n) + (u_{n-1} - u_n)]$$

$$= K(u_{n+1} + u_{n-1} - 2u_n)$$

Equation of motion is: $m\ddot{u}_n = K(u_{n+1} + u_{n-1} - 2u_n)$

Want solutions like (travelling wave solutions): $u_n \propto e^{i(kna-\omega t)}$

$$m\ddot{u}_n = K(u_{n+1} + u_{n-1} - 2u_n)$$

$$-m\omega^2 e^{i(kna-\omega t)} = K(e^{i(ka)} + e^{-ika} - 2)e^{i(kna-\omega t)}$$

$$m\omega^2 = K(2 - e^{i(ka)} - e^{-ika}) = 2K(1 - \cos ka) = 4K\sin^2\left(\frac{ka}{2}\right)$$


Figure 7.1: Linear chain of atoms

$$\omega(k) = 2\sqrt{\frac{K}{m}}\left|\sin\left(\frac{ka}{2}\right)\right|$$

This is the dispersion relation relating the frequency of oscillation to the wavelength of oscillation (Fig. 7.2).

**What are the allowed values of $k$?**

Ratio of the displacements of two neighboring planes is:

$$\frac{u_{n+1}}{u_n} = \frac{e^{ik(n+1)a}}{e^{iknа}} = e^{ika} \tag{7.1}$$

The two planes oscillate with only a phase difference. Phase difference is meaningfully defined to only within $\pm\pi$. So allowed values of $ka$ lie between $\pm\pi$, or

$$-\frac{\pi}{a} < k < \frac{\pi}{a} \tag{7.2}$$

This is just the first Brillouin zone.

Thus, the allowed values of the wave vectors are those that lie within the first Brillouin zone. Any value of $k$ outside this range can be described by subtracting an appropriate reciprocal lattice vector.

**How many modes?**

Total $N$ normal modes – $N$ degrees of freedom – complete solution to the problem!

**Notes:**

- Actual motion will be a linear combination of all the possible $3N$ modes (similar to eigenvalue problems in quantum mechanics).
- Example: consider two balls connected by a spring. The normal modes (2 in number) are

  $$u_1 = u_2 \quad \text{and} \quad u_1 = -u_2 \tag{7.3}$$

  but the real motion is a complex combination of these two modes. The real motion need not be a plane wave propagating through the crystal – it will be a complex wave having contributions from all the $3N$ normal modes which are its Fourier components.
- Solution describes a plane wave propagating through the lattice – phase velocity (velocity at which a particular crest/trough moves) $\omega/k$ and group velocity $\partial\omega/\partial k$ (velocity at which the envelope moves).

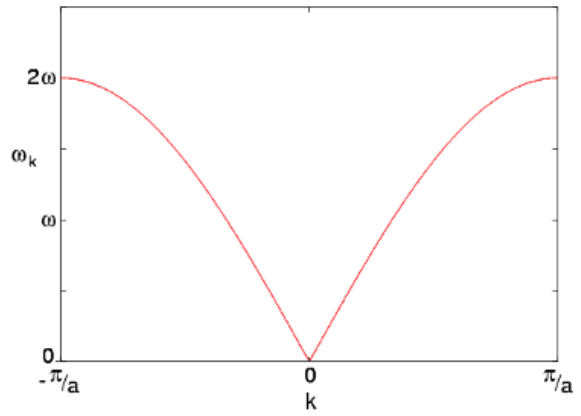


Figure 7.2: Dispersion relation for 1-D chain with single ion

**Features of the simple dispersion relation:**

**Case I – small values of $ka$: Long wavelength response $\lambda \gg a$.**

$$\omega(k) = 2\sqrt{\frac{K}{m}}\left|\sin\left(\frac{ka}{2}\right)\right| = a\sqrt{\frac{K}{m}}\,|k| \tag{7.4}$$

$$v_g = \frac{\partial\omega}{\partial k} = a\sqrt{\frac{K}{m}}\left|\cos\left(\frac{ka}{2}\right)\right| = a\sqrt{\frac{K}{m}} \tag{7.5}$$

Linear dispersion $\omega \propto k$; like for light or sound waves – phase velocity and group velocity are identical and independent of frequency. This is also the result in a continuum where $a = 0 \Rightarrow ka = 0$ identically.

**Case II – $\mathbf{k} = \pm\pi/\mathbf{a}$: At the boundaries of the Brillouin zone**

$$\omega(k) = 2\sqrt{\frac{K}{m}}\left|\sin\left(\frac{ka}{2}\right)\right| = 2\sqrt{\frac{K}{m}} = \text{constant} \tag{7.6}$$

$$v_g = \frac{\partial\omega}{\partial k} = a\sqrt{\frac{K}{m}}\left|\cos\left(\frac{ka}{2}\right)\right| = 0 \tag{7.7}$$

The group velocity $\partial\omega/\partial k = 0$, standing waves. At $ka = \pm\pi$, the ratio of displacement of two neighbouring planes of ions is:

$$\frac{u_{n+1}}{u_n} = \frac{e^{ik(n+1)a}}{e^{ikna}} = e^{ika} = e^{\pm i\pi} = \pm 1 \tag{7.8}$$

The alternate planes oscillate with the same amplitude but out of phase by 180° – the wave moves neither to the left nor to the right – a standing wave.

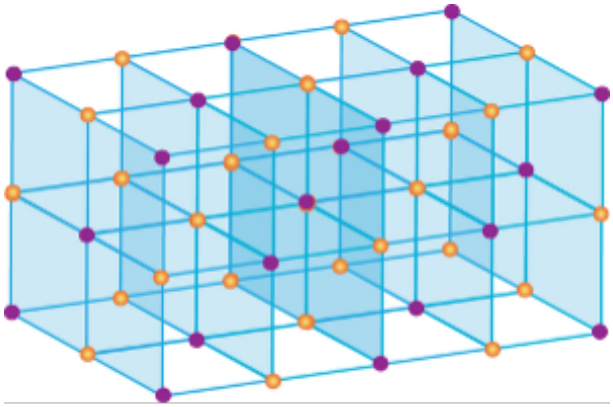

Figure 7.3: Planes in the NaCl crystal

We have seen a similar situation before – Bragg reflection of electrons at the Brillouin zone boundary. Is this the case here? For Bragg reflection $2d\sin(\theta) = n\lambda$. Here the waves are propagating perpendicular to the planes; so $\theta = \pi/2$; $d = a$ (lattice spacing in the particular direction); $n = 1$.

$$2d\sin(\theta) = n\lambda \;\Rightarrow\; \lambda = 2a \quad \text{or} \quad k = \frac{2\pi}{\lambda} = \frac{\pi}{a} \tag{7.9}$$

So the values of $k$ at the Brillouin zone boundary satisfy the condition for Bragg reflection of lattice vibrations, leading to the formation of standing waves.

### 7.2.2 1-D chain of ions with two ions per primitive cell

Consider NaCl – it has an FCC structure with a 2-ion basis. The distance between the Na and Cl ions is $d$ while the distance between two NaCl molecules is $a$.

Equilibrium positions of the ions for the nth unit cell are $na$ and $(na+d)$. The displacements of the ions from their mean positions are: $u_n$ for the ion at $na$ and $v_n$ for the ion at $na+d$.

$$m\ddot{u}_n = K\left(v_n - u_n\right) + G\left(v_{n-1} - u_n\right) \tag{7.10}$$

$$m\ddot{v}_n = K\left(u_n - v_n\right) + G\left(u_{n+1} - v_n\right) \tag{7.11}$$

**Look for solutions of the form:**

$$u_n = \varepsilon_1 e^{i(kna-\omega t)} \tag{7.12}$$

$$v_n = \varepsilon_2 e^{i(kna-\omega t)} \tag{7.13}$$

Substituting Eqn. 7.12 and Eqn. 7.13 in Eqn. 7.10:

$$-m\omega^2\varepsilon_1 e^{i(kna-\omega t)} = K\left(\varepsilon_2 - \varepsilon_1\right)e^{i(kna-\omega t)} + G\left(\varepsilon_2 e^{-ika} - \varepsilon_1\right)e^{i(kna-\omega t)} \tag{7.14}$$

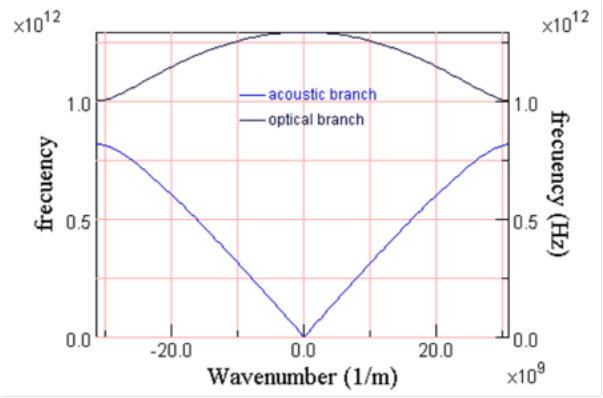


Figure 7.4: Dispersion relation for two-ion basis

$$-m\omega^2\varepsilon_1 = K\left(\varepsilon_2 - \varepsilon_1\right) + G\left(\varepsilon_2 e^{-ika} - \varepsilon_1\right) \tag{7.15}$$

$$\left(m\omega^2 - K - G\right)\varepsilon_1 + \left(K + Ge^{-ika}\right)\varepsilon_2 = 0 \qquad \text{—(5)} \tag{7.16}$$

Substituting Eqn. 7.12 and Eqn. 7.13 in Eqn. 7.11:

$$\left(K + Ge^{ika}\right)\varepsilon_1 + \left(m\omega^2 - K - G\right)\varepsilon_2 = 0 \qquad \text{—(6)} \tag{7.17}$$

A set of homogeneous equations of type $ax + by = 0$ and $cx + dy = 0$ has a solution if and only if the determinant of the coefficients vanishes:

$$\begin{vmatrix} a & b \\ c & d \end{vmatrix} = ad - bc = 0 \tag{7.18}$$

So,

$$\left(m\omega^2 - K - G\right)^2 = \left(K + Ge^{-ika}\right)\left(K + Ge^{ika}\right) \tag{7.19}$$

$$\omega^2 = \frac{K+G}{m} \pm \frac{1}{m}\sqrt{K^2 + G^2 + 2KG\cos(ka)} \tag{7.20}$$

This is the dispersion relation (Fig. 7.4).

The ratio of the displacements of the two ions in a cell given by:

$$\frac{\varepsilon_1}{\varepsilon_2} = \mp\frac{K + Ge^{ika}}{\left|K + Ge^{ika}\right|} \tag{7.21}$$

**How many modes are there?**

Total allowed values of $k$ (again lying in the first Brillouin zone) – for each value of $k$, there are two possible values of $\omega$ – total $2N$ normal modes – $2N$ degrees of freedom for a 1-D lattice with two ions in each cell – complete solution to the problem!

## Features of the dispersion relation

- Lower branch is acoustic branch - so called because the dispersion at long wavelength (small $ka$) is $\omega = vk$; like ordinary sound waves.
- Upper branch is optical branch - at long wavelength (small $k$) optical modes in ionic crystals interact with EM waves and are responsible for many of the optical properties like reflectivity, polarizability, etc.

## Case I – $ka << 1$: Long wavelength response $\lambda >> a$

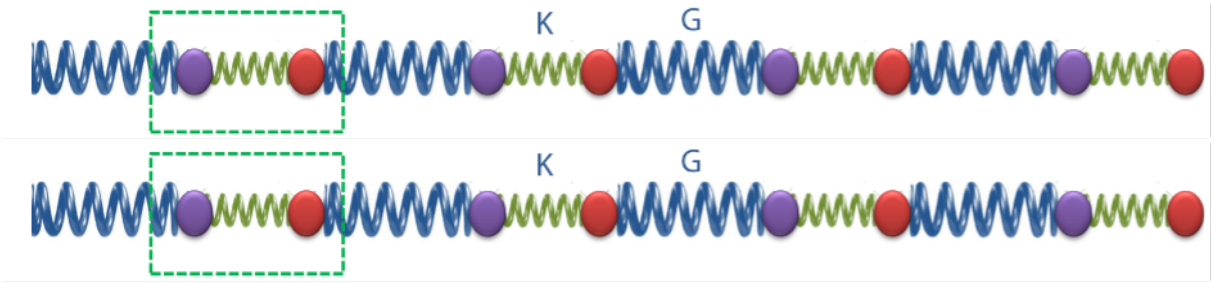


Figure 7.5: Dispersion relation for $ka << 1$. Top panel: Acoustic mode, Bottom panel: Optical mode.

- **Solutions 1:** $\omega = \sqrt{\frac{KG}{2m(K+G)}}\ (ka)$; $\varepsilon_2 = \varepsilon_1$. This is the acoustic mode. The two ions in the cell move in phase; linear sound-wave-like dispersion (top panel of Fig. 7.5).
- **Solutions 2:** $\omega = \sqrt{\frac{2(K+G)}{m}}$ ; $\varepsilon_2 = -\varepsilon_1$; This is the optical mode; the two ions move out of phase (bottom panel of Fig. 7.5).

## Case II – $\mathbf{k = \pm\pi/a}$: At the Brillouin zone boundaries

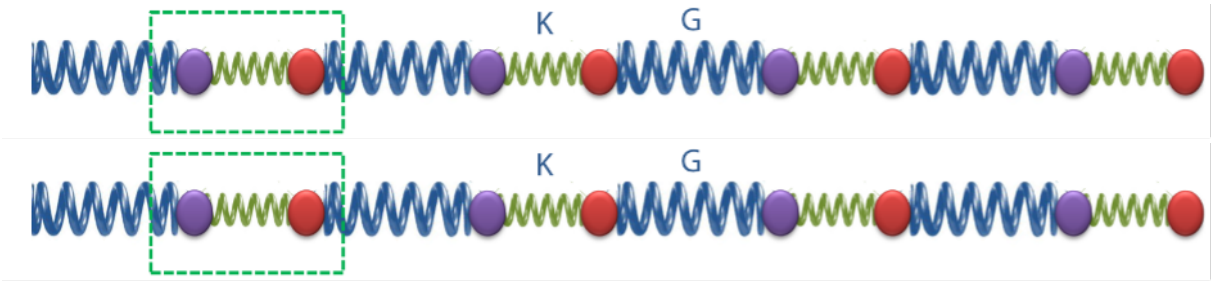


Figure 7.6: Dispersion relation for $k = \pm\pi/a$. Top panel: Acoustic mode, Bottom panel: Optical mode.

- **Solutions 1:** $\omega = \sqrt{\frac{2G}{m}}$ ; $\varepsilon_2 = \varepsilon_1$. This is the acoustic mode. The two ions in the cell move in phase; only the $G$ spring is stretched/compressed. The solution corresponds to a standing wave (top panel of Fig. 7.6).
- **Solutions 2**: $\omega = \sqrt{\frac{2K}{m}}$ ; $\varepsilon_2 = -\varepsilon_1$. This is the higher energy solution, the Optical mode. The two ions in the cell move out of phase; only the harder $K$ spring is stretched/compressed. The solution corresponds to a standing wave – the cells oscillate independent of each other (bottom panel of Fig. 7.6)!

For $K = G$, the two modes are indistinguishable at zone boundaries, and the two branches meet.

### Case III – $K \gg G$: The two ions are connected by a very rigid spring

- **Solutions 1:** $\omega = \sqrt{\frac{2G}{m}}\left|\sin\left(\frac{ka}{2}\right)\right|\left[1 + O\left(\frac{G}{K}\right)\right]$ ; $\varepsilon_2 \approx \varepsilon_1$. This is the acoustic mode; the solution resembles that of a linear chain of ions of mass $2m$ connected by a spring $G$ – each cell behaves like a single unit – low energy oscillations, so a stiff $K$ spring is unperturbed.
- **Solutions II:** $\omega = \sqrt{\frac{2K}{m}}\left[1 + O\left(\frac{G}{K}\right)\right]$ ; $\varepsilon_2 \approx -\varepsilon_1$. This is the optical mode; $\omega$ is approximately independent of $k$. Behaves like a diatomic molecule of masses $m$ connected by a spring of constant $K$. The two masses move approximately out of phase.

**Naive rule of thumb:** Acoustic mode dynamics determined by intercellular interaction, units in the cell move in phase. In optical mode, the ions in each cell execute molecular vibrations; interactions between the different cells broaden out the allowed levels into a band.

## 7.3 Phonon heat capacity

Till now, our treatment of lattice vibrations has been entirely classical—there has been no notion of quantization or uncertainty. This raises a fundamental question: *why do we need a quantum theory of lattice vibrations?*

In the classical picture, the specific heat of a solid is described by the Dulong–Petit law. Since all energy values are allowed, the equipartition theorem applies: each degree of freedom contributes an average energy of $\frac{1}{2}k_BT$ (for both kinetic and potential parts, giving $k_BT$ per mode). For a solid with $3N$ degrees of freedom, the total energy is therefore

$$E = 3Nk_BT,$$

leading to a heat capacity

$$C = \frac{\partial E}{\partial T} = 3Nk_B,$$

which is independent of temperature.

However, experiments show a striking deviation from this prediction. The specific heat is not constant: at low temperatures it vanishes, and more generally follows a behavior of the form

$$C = aT + bT^3.$$

This clear failure of classical theory necessitates a quantum description of lattice vibrations, where energy is quantized, and the population of modes depends on temperature.

## 7.4 Quantum theory of lattice vibrations

Hamiltonian for 1D linear chain

$$\mathcal{H} = \sum_i \frac{p_i^2}{2m} + \text{interaction energy}$$

Interaction energy is simple harmonic type $\sim \frac{1}{2}kx^2$.

Solve it for $N$ coupled harmonic oscillators – $3N$ normal modes – each with a characteristic frequency $\omega_p(k)$ where $p$ is the polarization/branch.

Energy of any given mode is

$$E_{kp} = \left(n_{kp} + \frac{1}{2}\right)\hbar\omega_p(k); \quad n_{kp} = 0, 1, 2, \ldots$$

- $\frac{1}{2}\hbar\omega_p(k)$ is the zero-point energy.
- $n_{kp} = 1/(e^{\beta\hbar\omega_p(k)} - 1)$ is the 'excitation number' of the particular mode of $p$th branch with wavevector $k$. It is the 'Planck distribution' of the occupation number.

Phonons are quanta of the ionic displacement field that describes a classical sound wave. Analogy with black body radiation – $n_i$ is the number of photons of the $i^{th}$ mode of oscillations of the EM wave.

Total energy of the system $E$ is given by:

$$E = \sum_{kp} E_{kp} = \sum_{kp}\left(n_{kp} + \frac{1}{2}\right)\hbar\omega_p(k)$$

or,

$$E = \sum_{kp} E_{kp} = \sum_{kp}\left(n_{kp} + \frac{1}{2}\right)\hbar\omega_p(k) = \sum_{kp}\left(\frac{\hbar\omega_p(k)}{e^{\beta\hbar\omega_p(k)} - 1} + \frac{1}{2}\hbar\omega_p(k)\right)$$

Specific heat

$$C_v = \frac{\partial E}{\partial T} = \sum_{kp}\frac{\partial}{\partial T}\left(\frac{\hbar\omega_p(k)}{e^{\beta\hbar\omega_p(k)} - 1}\right)$$

This is a general expression; actual values will depend upon the frequency spectrum of the normal modes.

### 7.4.1 Phonon heat capacity in the high temperature limit

Writing $\omega_p(k)$ as just $\omega$ for brevity:

$$C_v = \frac{\partial E}{\partial T} = \sum_{kp} \frac{\partial}{\partial T}\left(\frac{\hbar\omega}{e^{\beta\hbar\omega}-1}\right)$$

Replace $x = \beta\hbar\omega = \frac{\hbar\omega}{k_B T} \ll 1$

$$\frac{1}{e^x - 1} = \frac{1}{x + \frac{x^2}{2} + \frac{x^3}{6} + \ldots} = \frac{1}{x}\left(\frac{1}{1 + \frac{x}{2} + \frac{x^2}{6} + \ldots}\right) = \frac{1}{x}\left(1 - \frac{x}{2} + \frac{x^2}{12}\ldots\right)$$

$$E = \sum_{\text{all modes}} \left(\frac{\hbar\omega}{e^{\beta\hbar\omega}-1}\right) + \sum_{kp} \frac{1}{2}\hbar\omega$$

$$E = \sum_{\text{all modes}} \left(\frac{\hbar\omega}{\beta\hbar\omega}\right)\left[1 - \frac{\beta\hbar\omega}{2} + \frac{(\beta\hbar\omega)^2}{12} - \ldots\right] + \sum_{kp} \frac{1}{2}\hbar\omega$$

$$E = \sum_{\text{all modes}} k_B T\left[1 - \frac{\hbar\omega}{2k_B T} + \frac{1}{12}\left(\frac{\hbar\omega}{k_B T}\right)^2 - \ldots\right] + \sum_{kp} \frac{1}{2}\hbar\omega$$

$$C_v = \frac{\partial E}{\partial T} = \sum_{\text{all modes}} k_B\left[1 - \frac{k_B}{12}\left(\frac{\hbar\omega}{k_B T}\right)^2 + \ldots\right]$$

To first order;

$$C_v = \sum_{\text{all modes}} k_B = 3Nk_B;$$

This is the Dulong–Petit law; the other terms ignored in the expansion give the correction to the above result.

### 7.4.2 Phonon heat capacity in the low temperature limit

To get the expression for the heat capacity in the low-$T$ limit, we make certain assumptions:

- Replace the summation by an integral over the first Brillouin zone – justified since $N$ is very large, spacing between allowed values of $k$ is very small, and the summand does not vary much between two consecutive points.

$$C_v = \frac{\partial E}{\partial T} = \sum_{p} \frac{\partial}{\partial T}\int \frac{d\mathbf{k}}{(2\pi)^3}\left(\frac{\hbar\omega_p}{e^{\beta\hbar\omega_p}-1}\right)$$

- Modes with high frequency $\beta\hbar\omega_p \gg 1$ will make a negligible contribution to the integral as these terms die out exponentially – so can completely ignore the optical branches.
- Replace the acoustic branch with $\omega(k) = ck$; valid provided the frequency at which the dispersion deviates from linearity is large compared to the temperature.

$$C_v = \sum_p \frac{\partial}{\partial T} \int \frac{d\mathbf{k}}{(2\pi)^3} \left( \frac{\hbar ck}{e^{\beta\hbar ck} - 1} \right)$$

- Extend the limit of integral to all $k$-space – anyway integrand is negligible everywhere except near $k \to 0$.

$$C_v = \sum_p \frac{\partial}{\partial T} \int_0^\infty \frac{d\mathbf{k}}{(2\pi)^3} \left( \frac{\hbar ck}{e^{\beta\hbar ck} - 1} \right)$$

$$C_v = \sum_p \frac{\partial}{\partial T} \int_0^\infty \frac{4\pi k^2}{(2\pi)^3} \left( \frac{\hbar ck}{e^{\beta\hbar ck} - 1} \right) dk$$

$$x = \beta\hbar ck$$

$$C_v = \frac{\partial}{\partial T} \left[ \frac{3}{2\pi^2} \frac{(k_B T)^4}{(\hbar c)^3} \int_0^\infty dx \left( \frac{x^3}{e^x - 1} \right) \right]$$

The factor 3 is for the three acoustic modes.

$$C_v = \frac{\partial}{\partial T} \left[ \frac{3}{2\pi^2} \frac{(k_B T)^4}{(\hbar c)^3} \cdot \frac{\pi^4}{15} \right] = k_B \frac{2\pi^2}{5} \frac{(k_B T)^3}{(\hbar c)^3} \propto T^3$$

This result matches that obtained experimentally for alkali halides to within 1%!!

### 7.4.3 Specific heat in intermediate temperature range

There is no simple general theory; two good models exist: the Debye model and the Einstein model.

## Debye Model for Specific Heat

**Motivation:** We approximate the phonon spectrum to obtain a tractable expression for the specific heat. We make the following assumptions:

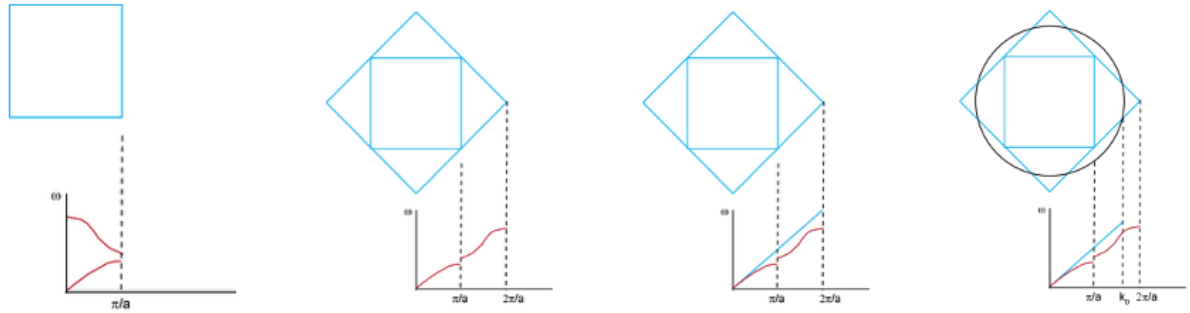

Figure 7.7: Debye model

1. Replace all phonon branches by a linear dispersion:

$$\omega(k) = ck$$

2. Replace the Brillouin zone by a sphere of equal volume (Debye sphere).

3. Choose the cutoff $k_D$ such that the total number of modes is preserved:

$$\frac{V}{(2\pi)^3} \cdot \frac{4}{3}\pi k_D^3 = N \quad \Rightarrow \quad k_D = \left(\frac{6\pi^2 N}{V}\right)^{1/3}$$

4. There are three acoustic branches $\Rightarrow$ total number of modes $= 3N$.

The total energy of phonons is:

$$E = \sum_p \int \frac{d^3k}{(2\pi)^3} \frac{\hbar\omega(k)}{e^{\beta\hbar\omega(k)} - 1}$$

Using $\omega = ck$ and spherical symmetry:

$$E = 3\int_0^{k_D} \frac{4\pi k^2 dk}{(2\pi)^3} \frac{\hbar ck}{e^{\beta\hbar ck} - 1}$$

$$E = \frac{3\hbar c}{2\pi^2}\int_0^{k_D} \frac{k^3}{e^{\beta\hbar ck} - 1}\, dk$$

Define:

$$x = \beta\hbar ck = \frac{\hbar ck}{k_B T}, \qquad T_D = \frac{\hbar ck_D}{k_B}$$

Then:

$$E = \frac{3}{2\pi^2}\frac{(k_B T)^4}{(\hbar c)^3}\int_0^{T_D/T} \frac{x^3}{e^x - 1}\, dx$$

The specific heat is

$$C_v = \frac{\partial E}{\partial T}$$

$$C_v = \frac{3}{2\pi^2}\frac{\partial}{\partial T}\left[\frac{(k_B T)^4}{(\hbar c)^3}\int_0^{T_D/T}\frac{x^3}{e^x-1}dx\right]$$

After differentiation:

$$C_v = 9Nk_B\left(\frac{T}{T_D}\right)^3\int_0^{T_D/T}\frac{x^4 e^x}{(e^x-1)^2}dx$$

**Limiting Cases**

**High temperature:** $T \gg T_D$

$$C_v \to 3Nk_B \quad \text{(Dulong–Petit law)}$$

**Low temperature:** $T \ll T_D$

$$C_v = \frac{12\pi^4}{5}Nk_B\left(\frac{T}{T_D}\right)^3$$

$$C_v \propto T^3$$

**Physical Interpretation**

- $T_D$ sets the energy scale of lattice vibrations.
- For $T \ll T_D$: only long-wavelength modes are excited ⇒ quantum regime.
- For $T \gg T_D$: all modes excited ⇒ classical equipartition recovered.

**Remark**

$T_D$ plays a role analogous to the Fermi temperature $T_F$ for electrons. However:

$$T_F \sim 10^4\,\text{K}, \quad T_D \sim 10^2\text{–}10^3\,\text{K}$$

Thus, phonons exhibit both classical and quantum regimes in accessible temperature ranges, while for electrons, only the quantum regime is encountered.

## Einstein model

The Einstein model differs from the Debye model essentially in the way it treats the optical modes. In this model, we make the following assumptions:

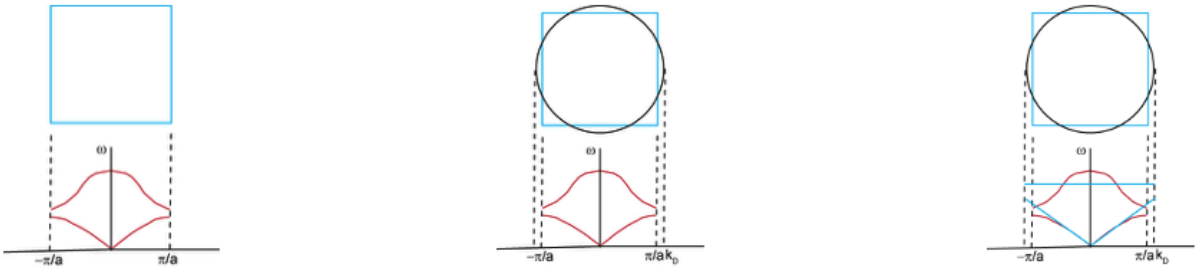


Figure 7.8: Einstein model

Figure 6: Normal dispersion
Figure 7: Replace by Debye sphere
Figure 8: Linearize the dispersion

- The acoustic modes all have a linear dispersion relation.
- The optical modes have a constant frequency $\omega_E$ independent of $k$ (remember the case $G/K \to 0$).

Acoustic mode contribution to the specific heat remains unchanged.

The optical mode energy is (assuming same dispersion for all three modes)

$$E_{\text{opt}} = 3N \frac{\hbar\omega_E}{e^{\beta\hbar\omega_E} - 1}$$

Specific heat due to optical modes is:

$$C_v = 3Nk_B \left(\frac{\hbar\omega_E}{k_B T}\right)^2 \frac{e^{\beta\hbar\omega_E}}{\left(e^{\beta\hbar\omega_E} - 1\right)^2}$$

At temperatures high compared to $\hbar\omega_E$; $C_v = 3Nk_B$. This is the Dulong–Petit result.

At temperatures low compared to $\hbar\omega_E$, $C_v$ dies off exponentially as it is difficult to excite high-energy modes at low temperatures.

## Comparison between electronic and lattice specific heats

Lattice specific heat:

$$C_v^{\text{lat}} = \frac{12\pi^4}{5} n_i k_B \left(\frac{T}{T_D}\right)^3; \quad n_i \text{ is the number of ions}$$

Electronic specific heat:

$$C_v^{\text{elec}} = \frac{\pi^2}{2} n_e k_B \frac{T}{T_F}; \quad n_e = Zn_i \text{ is the number of electrons; } Z \text{ is valence}$$

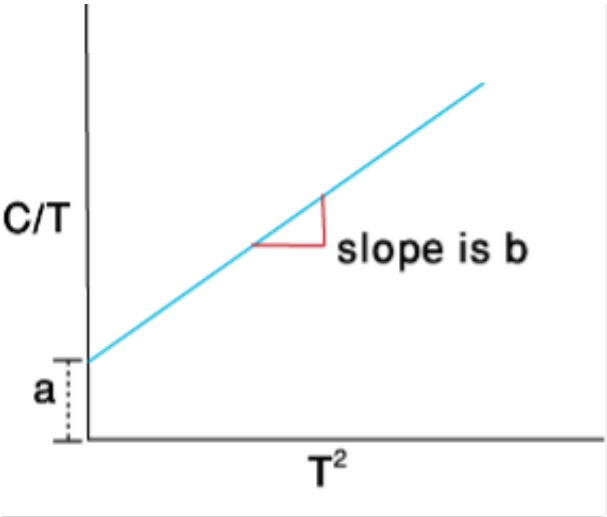


Figure 7.9: Linear and cubic term in specific heat

$$\frac{C_v^{\text{elec}}}{C_v^{\text{lat}}} = \frac{5}{24\pi^2} Z \frac{T_D^3}{T^2 T_F}$$

They will be equal at a temperature $T_0$ where

$$\frac{5}{24\pi^2} Z \frac{T_D^3}{T_0^2 T_F} = 1$$

Using $T_D \sim 300\,\text{K}$ while $T_F \sim 10^4\,\text{K}$,

$$T_0 = \sqrt{\frac{5Z}{24\pi^2}} \sqrt{\frac{T_D}{T_F}}\, T_D \;\sim\; 10\,\text{K}$$

The linear term (electronic contribution) in specific heat is seen only at very low temperatures, above that the cubic term (phonon contribution) begins to dominate. Total specific heat of a crystal is:

$$C = C_v^{\,elec} + C_v^{\,lat} = \frac{\pi^2}{2} n_e k_B \frac{T}{T_F} + \frac{12\pi^4}{5} n_i k_B \left(\frac{T}{T_D}\right)^3 ;\; n_e = Z n_i$$

One can write $C = aT + bT^3$; $C/T = a + bT^2$, where

$$a = \frac{\pi^2}{2} n_e k_B \frac{1}{T_F}$$

and

$$b = \frac{12\pi^4}{5} n_i k_B \left(\frac{1}{T_D}\right)^3$$

Thus, in a plot of $C/T$ as a function of $T^2$, the intercept $a$ on the y-axis gives the value of the Fermi temperature (or equivalently Fermi energy) while the slope of the curve $b$ is a measure of the Debye temperature (Fig. 7.9).

## 7.5 Anharmonicity in phonons

Discussion till now confined to harmonic approximation – potential energy of lattice vibrations had only quadratic terms. We learnt that the lattice waves are normal modes – phonons do not interact with each other; they do not change with time. Its consequences are:

- The heat capacity becomes T independent for $T > T_D$.
- There is no thermal expansion of solids.
- Thermal conductivity of solids is infinite

Conditions not fulfilled in real crystals. Way out: Include higher order terms in potential energy.

$$U(x) = U_{harm}(x) + U_{anharm}(x) = cx^2 - gx^3 - fx^4$$

with $c, g$ and $f > 0$. This is equivalent to having three or more phonon processes in the Hamiltonian. The coefficients $g$ and $f$ are related to the probabilities for having these third order and fourth order processes respectively.

## 7.6 Thermal expansion of solids

Consider the potential energy in terms of the relative displacement $x$ between two ions from their equilibrium position:

$$U(x) = U_{\text{harm}}(x) + U_{\text{anharm}}(x) = cx^2 - gx^3 - fx^4 \quad \text{with } c, g, f > 0$$

Average displacement of the ions is:

$$\langle x \rangle = \frac{\int_{-\infty}^{\infty} dx\ x \exp[-\beta U(x)]}{\int_{-\infty}^{\infty} dx\ \exp[-\beta U(x)]}$$

For small displacements such that $U_{\text{anharm}}/k_B T \ll 1$, we can expand the exponential as:

**Numerator:**

$$\int dx\ x e^{-\beta(cx^2 - gx^3 - fx^4)} = \int dx\ x\ e^{-\beta cx^2} e^{\beta gx^3} e^{\beta fx^4}$$

$$\cong \int dx\ x\ e^{-\beta cx^2} \left(1 + \beta gx^3\right) \left(1 + \beta fx^4\right)$$

$$= \int dx\ e^{-\beta cx^2} \left(x + \beta gx^4 + \beta fx^5\right)$$

$$= \frac{3\pi^{1/2}}{4} \frac{g}{c^{5/2}} \beta^{-3/2}$$

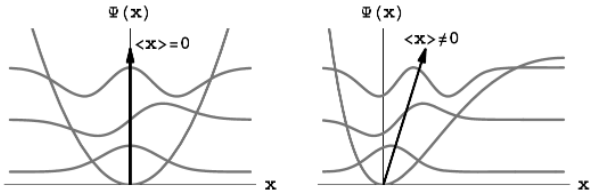


Figure 7.10: Phonon wavefunctions for (Left) harmonic potential (Right) anharmonic potential

**Denominator:**

$$\int dx\ e^{-\beta(cx^2-gx^3-fx^4)} = \int dx\ e^{-\beta cx^2} e^{\beta gx^3} e^{\beta fx^4}$$

$$\cong \int dx\ e^{-\beta cx^2} \left(1+\beta gx^3\right)\left(1+\beta fx^4\right)$$

$$\cong \int dx\ e^{-\beta cx^2} = \left(\frac{\pi}{c}\right)^{1/2} \beta^{-1/2}$$

So,

$$\langle x \rangle = \frac{3g}{4c^2} k_B T$$

Note that the thermal expansion does not involve the symmetric term $x^4$ but only the asymmetric cubic term.

The origin of anharmonicity is explained in Fig. 7.10. The figure on the left shows the phonon wavefunctions when the potential is harmonic. The average displacement of an atom from its mean position, $\langle x \rangle$ is zero for all modes. The right figure shows the same wavefunctions when the potential in anharmonic; in this case the average displacement increases with phonon energy. Therefore anharmonicity is essential for non-zero $\langle x \rangle$, and consequently, for thermal expansion of a solid.

## Dependence of thermal expansion coefficient on specific heat

Helmholtz free energy is defined as:

$$F = U - TS$$

It is related to pressure as:

$$P = -\left(\frac{\partial F}{\partial V}\right)_T$$

From $TdS = dU + PdV$ we get:

$$T\left(\frac{\partial S}{\partial T}\right)_V = \left(\frac{\partial U}{\partial T}\right)_V$$

So,

$$P = -\left(\frac{\partial}{\partial V}[U - TS]\right)_T = -\left(\frac{\partial}{\partial V}\left[U - T\int_0^T dT' \left(\frac{\partial U}{\partial T'}\right)_V\right]\right)_T$$

From calculations based on harmonic approximation:

$$U = \sum_{k,p} \frac{\hbar\omega_p(k)}{e^{\beta\hbar\omega_p(k)} - 1} + \frac{1}{2}\sum_{k,p}\hbar\omega_p(k)$$

Combining (1) and (2):

$$P = -\frac{\partial}{\partial V}\left[\frac{1}{2}\sum_{k,p}\hbar\omega_p(k)\right] + \sum_{k,p}\left(-\frac{\partial}{\partial V}(\hbar\omega_p(k))\right)\frac{1}{e^{\beta\hbar\omega_p(k)} - 1}$$

The first term (only term at zero temperature) is the volume derivative of the ground state energy. The second term is the volume derivative of the phonon energies.

If harmonic approximation is rigidly correct then the second term vanishes, $P$ does not depend on $T$ at all!!

So,

$$\left(\frac{\partial V}{\partial T}\right)_P = -\frac{(\partial P/\partial T)_V}{(\partial P/\partial V)_T} = 0$$

implying the coefficient of linear expansion:

$$\alpha = \frac{1}{3V}\left(\frac{\partial V}{\partial T}\right)_P = \frac{1}{3B}\left(\frac{\partial P}{\partial T}\right)_V = 0$$

The coefficient of thermal expansion for a harmonic lattice is zero!!

Here,

$$B = -V\left(\frac{\partial P}{\partial V}\right)_T$$

is the bulk modulus.

**Many other thermodynamic anomalies:**

- $$C_P = C_v - \frac{T}{V}\frac{[(\partial P/\partial T)_V]^2}{(\partial P/\partial V)_T} = C_v$$

  implying the specific heats at constant pressure and constant volume are identical.

- $$\frac{(\partial P/\partial V)_S}{(\partial P/\partial V)_T} = \frac{C_P}{C_v} = 1$$

  implying the adiabatic and isothermal compressibilities are identical.

Both these go against experimental results.

As a first order correction, assume that the energy for the anharmonic potential is the same as that we got for the harmonic potential approximation, only now the normal modes depend on the volume of the crystal.

$$\alpha = \frac{1}{3B}\left(\frac{\partial P}{\partial T}\right)_V = \frac{1}{3B}\sum_{k,p}\left(-\frac{\partial}{\partial V}(\hbar\omega_p(k))\right)\frac{\partial}{\partial T}\left(\frac{1}{e^{\beta\hbar\omega_p(k)}-1}\right)$$

Compare with the expression for lattice specific heat per unit volume:

$$c_V^{\text{ion}} = \frac{1}{V}\frac{\partial}{\partial T}\sum_{k,p}\left(\frac{\hbar\omega_p(k)}{e^{\beta\hbar\omega_p(k)}-1}\right)$$

$$= \sum_{k,p}\left(\frac{\hbar\omega_p(k)}{V}\right)\frac{\partial}{\partial T}\left(\frac{1}{e^{\beta\hbar\omega_p(k)}-1}\right)$$

Therefore,

$$\alpha = \frac{c_V^{\text{ion}}}{3B}\frac{\sum_{k,p}\left(-\frac{\partial}{\partial V}(\hbar\omega_p(k))\right)}{\sum_{k,p}\left(\frac{\hbar\omega_p(k)}{V}\right)}$$

For simple dispersion relations like Debye model, we can make further simplifications.

Define a parameter called Grüneisen parameter:

$$\gamma \equiv -\frac{\partial(\ln\omega_D)}{\partial(\ln V)}$$

$$\alpha^{\text{ion}} = \frac{\gamma c_V^{\text{ion}}}{3B}$$

**Physical interpretation of the Grüneisen parameter**

The Grüneisen parameter $\gamma$ quantifies how the phonon frequencies shift with volume, and hence provides a direct measure of lattice anharmonicity:

$$\gamma = -\frac{\partial \ln\omega}{\partial \ln V}.$$

In a purely harmonic crystal, the normal mode frequencies are independent of volume, implying $\gamma = 0$ and hence $\alpha = 0$. Thus, a nonzero thermal expansion is a direct consequence of anharmonicity in the interatomic potential.

Physically, when the lattice expands, the interatomic spacing increases and the effective restoring forces weaken, leading to a reduction in phonon frequencies ($\omega$ decreases with increasing $V$). This corresponds to $\gamma > 0$, which is the typical case for most solids and results in positive thermal expansion.

Conversely, materials with anomalous bonding or transverse vibrational modes may exhibit $\gamma < 0$ over certain ranges, leading to negative thermal expansion.

The relation

$$\alpha = \frac{\gamma c_V}{3B}$$

makes this connection explicit: thermal expansion arises from the interplay of (i) lattice anharmonicity ($\gamma$), (ii) the number of thermally excited phonons ($c_V$), and (iii) the mechanical stiffness of the lattice ($B$).

Thus, $\gamma$ serves as a bridge between microscopic lattice dynamics and macroscopic thermodynamic response.

### Electrical contribution to the thermal expansion co-efficient

For electrons the internal energy is related to the pressure by:

$$P = \frac{2U}{3V}\alpha^{el} = \frac{1}{3B}\left(\frac{\partial P}{\partial T}\right)_V = \frac{1}{3B}\frac{2}{3V}\left(\frac{\partial U}{\partial T}\right)_V = \frac{2}{9B}{c_V}^{el}$$

So, the net thermal expansion coefficient is:

$$\alpha = \alpha^{\text{ion}} + \alpha^{\text{el}} = \frac{\gamma\, c_V^{\text{ion}}}{3B} + \frac{2}{9B}\, c_V^{\text{el}} = \frac{1}{3B}\left(\gamma\, c_V^{\text{ion}} + \frac{2}{3} c_V^{\text{el}}\right)$$

$\gamma \sim 1{-}2$, so the electronic term will make a significant contribution only when the electronic specific heat is large as compared to the lattice specific heat, i.e., at temperatures below 10 K. In metals, $\alpha$ vanishes linearly with temperature (dominated by $\alpha_{el}$) while in insulators it vanishes as $T^3$ (determined by $\alpha_{ion}$). These predictions have been experimentally verified.

## 7.7 Thermal conductivity

Without collisions, there will be no thermal equilibrium, and thermal conductivity will be infinite. For a harmonic crystal, there is no collision between phonons; only factors limiting the thermal conductivity are geometrical scattering of phonons by the boundary of the crystal and defects in the crystal. In ordinary gas, two particle collisions lead to equilibrium, so how does phonon 'gas' differ from the ordinary gas of molecules?

The main difference is that phonon number need not be conserved – so the analog of phonon gas is not molecules confined in a vessel (Fig. 7.11 top panel) but rather molecules flowing freely through a tube carrying heat across it without any temperature gradient (Fig. 7.11 bottom panel).

Consider a rod with the two ends maintained at different temperatures. Thermal conductivity $\kappa$ is defined as the energy transmitted per unit time across a unit area per unit temperature gradient.

$$j = -\kappa \frac{dT}{dx}$$

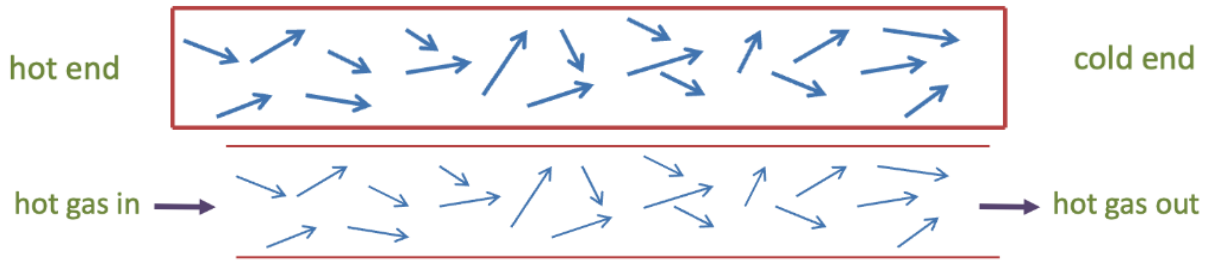


Figure 7.11: Top panel: Gas flow in a closed tube: no mass flow permitted - energy transported from left to right with no thermal gradient - finite thermal conductivity. Bottom panel: Gas flow in open tube: energy transported from left to right with no thermal gradient; thermal conductivity infinite.

Dependence of $\kappa$ on $dT/dx$ implies that the thermal energy transfer is a random process involving scattering, which introduces the mean free path of phonons in the problem. If the process were ballistic, it would involve only the $T$-difference between the two ends and not the gradient.

**We make a relaxation time kind of approximation:** the energy contributed by a phonon at a point is decided by where it has had its last collision. So phonons coming from the high temperature end bring more energy than those coming from the low temperature end. Thus, although there is no net number flux, there can be energy flux traveling from the high $T$ end to the low $T$ end.

Temperature at the two ends of a one-dimensional rod are $(T+\Delta T)$ and $T$. The temperature at point $x$ is $T(x)$, and the energy at that point is $E(T[x])$.

Half the phonons arriving at a point $x$ are from the high temperature side, each carrying an energy $E(T[x - v_x\tau])$, the other half are from the low-$T$ side and carry an energy $E(T[x + v_x\tau])$.

Number of phonons arriving at $x$ per unit time per unit area of cross section is $\frac{1}{2}nv_x$, where $v_x$ is the phonon speed in $x$ direction.

So net energy flux is:

$$j = \frac{1}{2}nv_x \left[E\left(T[x - v_x\tau]\right) - E\left(T[x + v_x\tau]\right)\right] = nv_x^2\tau\frac{dE}{dT}\left(-\frac{dT}{dx}\right) = -\frac{1}{3}v^2\tau C_v\frac{dT}{dx}$$

$$\kappa = \frac{1}{3}C_v v^2\tau = \frac{1}{3}C_v lv \qquad \text{—-(7)}$$

Lattice thermal conductivity of a crystal is determined by two contributions – specific heat and the mean free path of phonons.

The mean free path of phonons is determined by two factors:

- rate of scattering with other phonons
- scattering with static impurities or boundaries of the crystal

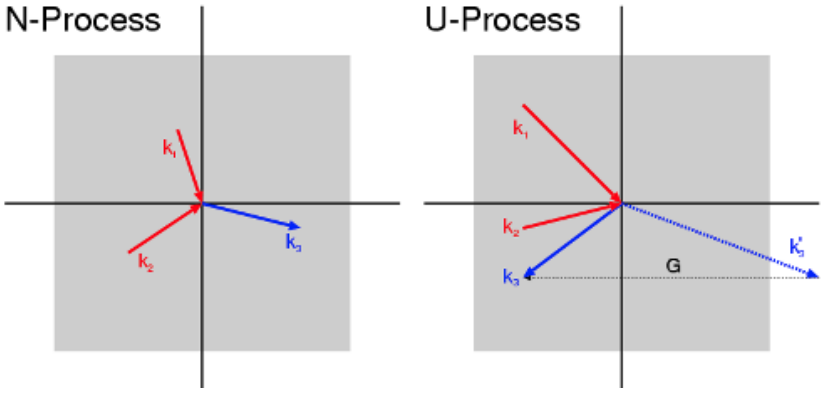


Figure 7.12: (left figure) N-process and (right figure) U-process in phonon scattering

Scattering from other phonons can be classified into two types depending on the energies involved:

**N-process:**

Consider a three-phonon scattering process. If the initial energies of the phonons involved in the process are small as compared to $\hbar\omega_D$, then (since energy is conserved in the process) the final energies of the phonons will also be small as compared to $\hbar\omega_D$.

Thus, all the wave-vectors involved in the process will be small as compared to the reciprocal wave-vector (which is of the same order as the Debye wave-vector). So, in the equation:

$$k_1 + k_2 = k_3 + G$$

the reciprocal lattice vector $G$ is identically zero; crystal momentum is exactly conserved in the process. This is called a normal process or an N-process. Such processes cannot change the crystal momentum.

In equilibrium, the net crystal momentum:

$$\sum_{k,p} \hbar k \, n_p(k) = \sum_{k,p} \frac{\hbar k}{e^{\beta\hbar\omega_p(k)} - 1} = 0$$

Thus, if we start with a non-equilibrium phonon distribution, N-processes cannot bring about thermal equilibrium – it can be shown that if there were only N-processes, the thermal conductivity of a crystal would have been infinite.

Analogous to the flow of gas in a cylinder with open ends– thermal energy is transported from one end to another without a thermal gradient.

**U-process (Umklapp process):**

For scattering events where the initial phonon momenta are not small as compared to $k_D$, the value of the reciprocal lattice vector required to bring back the final phonon state into the first Brillouin zone will be non-zero.

Hence, for such scattering events, crystal momentum is conserved only to within a reciprocal lattice vector, and this gives finite thermal resistance to the crystal.

## N-process vs U-process

| **Feature** | **N-process** | **U-process** |
|---|---|---|
| Momentum conservation | Exact ($\mathbf{G} = 0$) | Only modulo reciprocal lattice vector ($\mathbf{G} \neq 0$) |
| Effect on net phonon momentum | Preserves | Reduces (acts like resistance) |
| Contribution to thermal conductivity | Infinite conductivity if only N-processes | Finite conductivity due to scattering |
| Temperature dependence | Always possible, but ineffective for resistance | Rare at low $T$, dominant at high $T$ |

In short: N-processes shuffle phonons without resistance, while U-processes are the true "brakes" on phonon transport. This distinction explains why thermal conductivity peaks at low temperatures (few U-processes) and decreases at high temperatures (many U-processes).

## Temperature dependence of phonon mean free path

**High temperature limit** ($T/T_D \gg 1$)**:**

The probability that a phonon will suffer a collision is directly proportional to the number of other phonons present. At high $T$, the equilibrium number of phonons is:

$$n = \frac{1}{e^{\beta\hbar\omega} - 1} \simeq \frac{k_B T}{\hbar\omega}$$

So the mean free path should go as $1/T$. Since $C_V$ is constant in this temperature range, the entire temperature dependence of $\kappa$ comes from the temperature dependence of $l$. Thus,

$$\kappa \sim \frac{1}{T}$$

**Low temperature limit** ($T/T_D \ll 1$)**:**

Thermal conductivity of a perfect infinite crystal is finite at low temperatures only because of U-processes. For a U-process, at least one of the initial phonons must have energy comparable to $\hbar\omega_D$. At $T/T_D \ll 1$, the number of such phonons is:

$$n = \frac{1}{e^{\beta\hbar\omega} - 1} \simeq \frac{1}{e^{T_D/T} - 1} \sim e^{-T_D/T}$$

As $T$ decreases, the number of phonons that can take part in the U-process falls exponentially. Thermal conductivity is inversely proportional to the number of U-processes, so the effective relaxation time for thermal scattering goes as:

$$\tau \sim e^{T_D/T}$$

Thus, as $T$ decreases, $\kappa$ shows an exponential increase till the mean free path becomes comparable to that due to scattering from static imperfections or boundaries of the crystal. Below this temperature, $l$ becomes $T$ independent and $\kappa$ is determined solely by the temperature dependence of specific heat.

So, at very low temperatures, thermal conductivity will be determined by $C_V$ and will go as $T^3$. As the temperature increases, U-processes begin to appear and gradually make the mean free path smaller than the sample dimensions. Thermal conductivity at this point reaches a maximum and then begins to fall exponentially with temperature as $e^{T_D/T}$.

At higher temperatures, the exponential fall is replaced by a slower $1/T$ power-law decrease of $\kappa$ with increasing $T$.

## Temperature dependence of lattice thermal conductivity

At low temperatures, the thermal conductivity rises steeply, following $\kappa \propto T^3$. This behavior is consistent with the theoretical expectation that U-processes are rare at low $T$, so phonons scatter primarily from boundaries or defects. The cubic temperature dependence arises from the specific heat contribution of acoustic phonons.

As the temperature increases, the thermal conductivity reaches a maximum. This peak corresponds to the onset of U-processes: a sufficient number of phonons acquire energies high enough to reach the Brillouin zone boundary, enabling Umklapp scattering. These processes reduce the phonon mean free path, thereby lowering $\kappa$.

At high temperatures, the thermal conductivity decreases approximately as $1/T$. This agrees with theoretical predictions: the number of phonons increases linearly with $T$, enhancing the probability of phonon–phonon collisions. Consequently, the mean free path decreases as $1/T$. Since the specific heat is nearly constant in this regime, the entire temperature dependence of $\kappa$ arises from scattering processes.

The plot in Fig, 7.13 shows that $\kappa/T^3$ saturates at different values depending on the crystal size. This demonstrates that at very low temperatures, boundary scattering dominates. N-processes cannot relax momentum, and U-processes are exponentially suppressed. As a result, the phonon mean free path is limited only by the crystal dimensions.

Larger crystals correspond to a longer mean free path and hence higher thermal conductivity. This provides a direct experimental confirmation of the theory: in the absence of U-processes, thermal conductivity remains finite only due to static scattering from boundaries or defects.

**Summary of scaling behavior:**

$$\kappa(T) \sim \begin{cases} T^3 & (T \ll T_D) \quad \text{boundary-limited regime} \\ \text{maximum} & (\text{onset of Umklapp processes}) \\ \dfrac{1}{T} & (T \gg T_D) \quad \text{Umklapp-dominated regime} \end{cases}$$

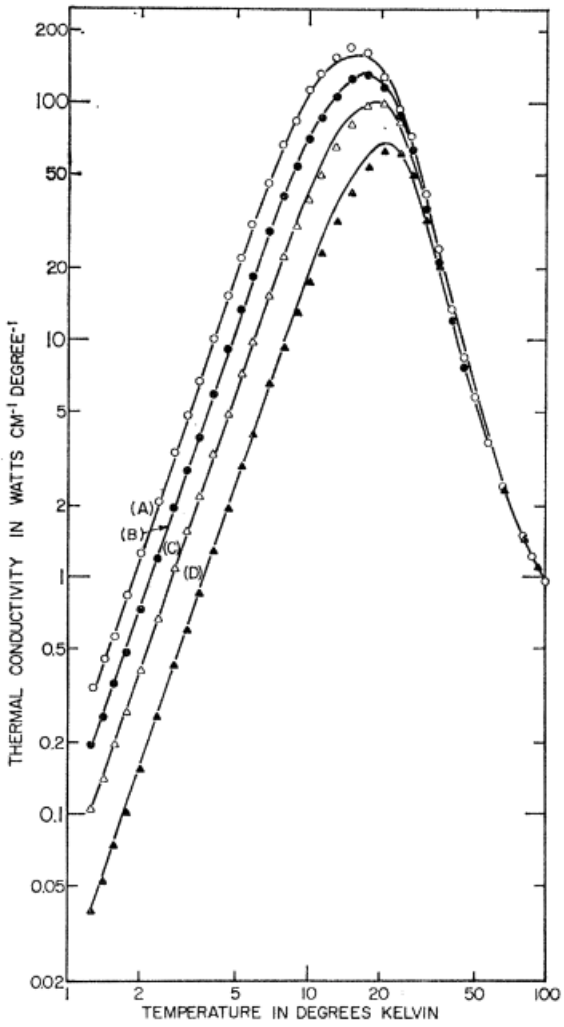


Figure 7.13: Thermal conductivity of LiF; Mean crystal widths: (A) 7.25 mm, (B) 4.00 mm, (C) 2.14 mm, (D) 1.06 mm. Ref: P. D. Thacher Phys. Rev. 156, 975–988 (1967).

**Heuristic derivation (one-line):**

$$\kappa \sim \frac{1}{3} C_v v l, \quad \begin{cases} \text{low } T,\ C_v \sim T^3,\ l \approx \text{const} & \Rightarrow K \sim T^3 \\ \text{high } T,\ C_v \approx \text{const},\ l \sim \frac{1}{T} & \Rightarrow K \sim \frac{1}{T} \end{cases}$$

This compact relation captures the essential physics: the low-temperature behaviour is governed by the phonon population ($C_v$), while the high-temperature behaviour is controlled by phonon scattering (mean free path $l$).

## 7.8 Measuring phonon Dispersion

Phonon dispersion relations can be measured using either neutron scattering or electromagnetic (EM) wave scattering.

For neutrons:

$$E = \frac{p^2}{2m}$$

For phonons:

$$E = \hbar\omega \sim pc$$

**Focus on neutron scattering:**

Neutrons are charge neutral and therefore interact primarily with the ionic cores. Their interaction with electrons occurs only via weak magnetic coupling between their magnetic moments.

Consider neutrons incident with energy:

$$E = \frac{p^2}{2m}$$

and emerging with energy:

$$E' = \frac{p'^2}{2m}.$$

Let the initial phonon occupation be $n_{ks}$ and the final occupation be $n'_{ks}$.

**Energy conservation**

$$E + \hbar \sum_{k,s} \omega_s(k)\, n_{ks} = E' + \hbar \sum_{k,s} \omega_s(k)\, n'_{ks}$$

$$E' = E - \hbar \sum_{k,s} \omega_s(k)\, (n'_{ks} - n_{ks}) = E - \hbar \sum_{k,s} \omega_s(k)\, \Delta n_{ks} \qquad \text{—-(1)}$$

**Momentum conservation**

$$\vec{p}' = \vec{p} - \hbar \sum_{k,s} \vec{k}\, \Delta n_{ks} + \hbar \vec{G} \qquad \text{—-(2)}$$

**Zero-phonon scattering** ($\Delta n = 0$)

$$\vec{p'} = \vec{p} + \hbar\vec{G}$$

$$\vec{K'} = \vec{K} + \vec{G}, \quad p = \hbar K, \quad p' = \hbar K'$$

This corresponds to the Laue condition for elastic scattering of a plane wave from a crystal and provides no information about phonons.

**One-phonon scattering** ($\Delta n = \pm 1$)

Consider absorption of one phonon ($\Delta n = 1$):

$$E' = E + \hbar\omega_s(k)$$

$$\vec{p'} = \vec{p} + \hbar\vec{k} + \hbar\vec{G}$$

Using the dispersion relation:

$$\frac{p'^2}{2m} = \frac{p^2}{2m} + \hbar\omega_s\left(\frac{\vec{p'} - \vec{p}}{\hbar} - \vec{G}\right)$$

Since $\omega_s(k)$ is periodic in reciprocal lattice vectors $\vec{G}$:

$$\omega_s\left(\frac{\vec{p'} - \vec{p}}{\hbar} - \vec{G}\right) = \omega_s\left(\frac{\vec{p'} - \vec{p}}{\hbar}\right)$$

Thus, by measuring $\vec{p'} - \vec{p}$ and $E' - E$, one directly obtains:

$$\omega = \frac{E' - E}{\hbar}, \qquad \vec{k} = \pm\frac{\vec{p'} - \vec{p}}{\hbar}$$

This allows mapping of the full phonon dispersion relation.

**Two-phonon scattering** ($\Delta n = \pm 2$)

$$E' = E + \hbar\omega_s^{(1)}(k) + \hbar\omega_s^{(2)}(k)$$

$$\vec{p'} = \vec{p} + \hbar\vec{k}^{(1)} + \hbar\vec{k}^{(2)} + \hbar\vec{G}$$

There are many unknowns in this case, leading to multiple possible solutions. As a result, multi-phonon processes form a continuous background in the scattering spectrum rather than sharp features.

### Finite linewidth of phonon peaks

The one-phonon scattering peaks have a finite width. This arises because the harmonic approximation is only approximate; phonons are not exact eigenstates of the full Hamiltonian and therefore have a finite lifetime $\tau$.

This finite lifetime leads to an energy uncertainty:

$$\Delta E \sim \frac{\hbar}{\tau},$$

which broadens the observed peaks.

### Key takeaways for scattering processes

- **Zero-phonon scattering ($\Delta n = 0$):** Corresponds to the Laue condition; provides no information about phonons.
- **One-phonon scattering ($\Delta n = \pm 1$):** Produces discrete peaks and allows direct measurement of phonon frequencies and wavevectors.
- **Multi-phonon scattering ($\Delta n \geq 2$):** Leads to a continuous background due to multiple possible energy and momentum combinations.

# Chapter 8

# Paramagnetism and diamagnetism

## 8.1 Magnetization and Magnetic Susceptibility

Magnetization $M(H)$ in the presence of a uniform magnetic field $H$ at $T = 0$ is defined as:

$$M(H) = -\frac{1}{V}\frac{\partial E_0(H)}{\partial H}, \tag{8.1}$$

where $E_0(H)$ is the ground state energy. Note that $H$ is the magnetic field felt by the substance and not the applied magnetic field $B$ ($B = \mu_0 H$).

At finite temperature $T$, higher energy states may be occupied with finite probability. The net magnetization is therefore the thermal equilibrium average of the magnetization of each available state:

$$M(H,T) = -\frac{\sum_n M_n(H)\, e^{-\beta E_n(H)}}{\sum_n e^{-\beta E_n(H)}}, \qquad \beta = (k_B T)^{-1}. \tag{8.2}$$

Here,

$$M_n(H) = -\frac{1}{V}\frac{\partial E_n(H)}{\partial H}. \tag{8.3}$$

This expression can equivalently be written in terms of the Helmholtz free energy:

$$M(H,T) = -\frac{1}{V}\frac{\partial F}{\partial H}, \tag{8.4}$$

where the magnetic Helmholtz free energy is defined through:

$$e^{-\beta F(H)} = \sum_n e^{-\beta E_n(H)}, \qquad \beta = (k_B T)^{-1}. \tag{8.5}$$

The magnetic susceptibility per unit volume is defined as:

$$\chi = \mu_0 \frac{\partial M}{\partial H}. \tag{8.6}$$

## 8.2 Atomic contribution to magnetization

The magnetic moment of a free atom arises due to three main factors:

- Spin of the electrons
- Orbital angular momentum of electrons
- Change of the orbital angular momentum of electrons due to the applied magnetic field

The first two contributions are paramagnetic in nature, while the last contribution is diamagnetic.

### Magnetic perturbation of the Hamiltonian

The kinetic energy of each electron is modified according to:

$$\mathbf{p} \to \mathbf{p} + e\mathbf{A}, \tag{8.7}$$

where $\mathbf{A}$ is the vector potential defined through:

$$\mathbf{H} = \boldsymbol{\nabla} \times \mathbf{A}, \qquad \boldsymbol{\nabla} \cdot \mathbf{A} = 0. \tag{8.8}$$

A commonly used choice for the vector potential is:

$$\mathbf{A} = -\frac{1}{2}\,\mathbf{r} \times \mathbf{H}. \tag{8.9}$$

The kinetic energy of the nucleus remains almost unchanged due its large mass.

The interaction energy of electron spins with the external magnetic field is added to the Hamiltonian:

$$\Delta H = g_0 \mu_B\, \mathbf{H} \cdot \mathbf{S} = g_0 \mu_B H S_z, \tag{8.10}$$

assuming $\mathbf{H}$ is along the $z$-axis and $\mathbf{S}$ is the net electronic spin,

$$\mathbf{S} = \sum_i \mathbf{s}_i. \tag{8.11}$$

$$\mu_B = \frac{\hbar e}{2m} = 9.27 \times 10^{-24}\ \text{J/T} \tag{8.12}$$

is the Bohr magneton, and $g_0 \sim 2$ is the electronic $g$-factor.

The total kinetic energy is now:

$$T = \frac{1}{2m} \sum_i \left(\mathbf{p} + e\mathbf{A}(\mathbf{r}_i)\right)^2 = \frac{1}{2m} \sum_i \left(\mathbf{p} - \frac{e}{2}\mathbf{r}_i \times \mathbf{H}\right)^2 \tag{8.13}$$

$$= \frac{1}{2m}\sum_i p^2 - \frac{e}{2m}\sum_i (\mathbf{p}\times\mathbf{r}_i)\cdot\mathbf{H} + \frac{e^2}{8m}H^2\sum_i\left(x_i^2+y_i^2\right) \tag{8.14}$$

$$= T_0 + \mu_B\,\mathbf{L}\cdot\mathbf{H} + \frac{e^2}{8m}H^2\sum_i\left(x_i^2+y_i^2\right), \tag{8.15}$$

where

$$\hbar\mathbf{L} = \sum_i \mathbf{r}_i\times\mathbf{p} \tag{8.16}$$

is the total electronic orbital angular momentum.

Adding the spin energy to this gives the change in the Hamiltonian:

$$\Delta H = \mu_B\,\mathbf{L}\cdot\mathbf{H} + g_0\mu_B\,\mathbf{S}\cdot\mathbf{H} + \frac{e^2}{8m}H^2\sum_i\left(x_i^2+y_i^2\right) \tag{8.17}$$

The energy shifts in Eqn. 8.17 are of order $\sim 0.1\,\text{meV}$ and are very small compared to atomic energy scales ($\sim$ eV). Therefore, perturbation theory can be used to calculate the change in the energy of the system due to the magnetic perturbation.

Using second-order perturbation theory (keeping terms up to second order in $H$):

$$E_n \to E_n + \Delta E_n, \tag{8.18}$$

where the energy change $\Delta E_n$ is:

$$\Delta E_n = \langle n|\Delta H|n\rangle + \sum_{n'\neq n}\frac{|\langle n'|\Delta H|n\rangle|^2}{E_n - E_{n'}} \tag{8.19}$$

Combining Eqn. 8.17 and Eqn. 8.19, we obtain to second order in $H$:

$$\Delta E_n = \mu_B\,\mathbf{H}\cdot\langle n|\mathbf{L}+g_0\mathbf{S}|n\rangle + \sum_{n'\neq n}\frac{|\langle n'|\mu_B(\mathbf{L}+g_0\mathbf{S})\cdot\mathbf{H}|n\rangle|^2}{E_n - E_{n'}} + \frac{e^2}{8m}H^2\,\langle n|\sum_i(x_i^2+y_i^2)|n\rangle \tag{8.20}$$

From this energy expression, one can calculate the magnetic susceptibility of individual atoms, ions, or molecules, as well as of ionic and molecular solids.

All atomic magnetic responses arise from these mechanisms:

1. alignment of permanent moments (Curie)
2. modification of orbital motion (Larmor/Landau)
3. virtual transitions between states (Van Vleck)

Below, we look at a few of these.

### 8.2.1 Larmor/Langevin diamagnetism

Consider ions/atoms with all shells filled. In the ground state, the net spin and angular momentum are both zero:

$$\mathbf{L}\left|0\right\rangle = \mathbf{S}\left|0\right\rangle = 0,$$

So only the third term in Eqn. 8.20 survives. The change in the ground state energy (and usually only the ground state is appreciably occupied) is:

$$\Delta E_0 = \frac{e^2}{8m} H^2 \sum_i \left(x_i^2 + y_i^2\right) = \frac{e^2}{12m} H^2 \sum_i r_i^2$$

The magnetic susceptibility of $N$ such ions is:

$$\chi = \mu_0 \frac{\partial M}{\partial H} = -\mu_0 \frac{1}{V} \frac{\partial^2 \Delta E_0}{\partial H^2} = -\mu_0 \frac{e^2}{6m} \frac{N}{V} \langle r_i^2 \rangle$$

This is a diamagnetic response: the magnetization is opposite to the external field, opposing it as in Lenz's law.

### 8.2.2 Curie paramagnetism

Consider now atoms/ions with unfilled shells. The first term in Eqn. 8.20 is of order $\mu_B H \sim 0.1\,\text{meV}$ for a 1 Tesla field. The second term is substantially smaller than the first. The third term is about $10^{-5}$ times the first term. Thus, if the first term is non-vanishing, it dominates.

To calculate the first term, we evaluate the expectation value of $\mathbf{L} + g_0\mathbf{S}$ with $\mu_B\mathbf{H}$. From atomic physics:

$$\mathbf{L} + g_0\mathbf{S} = g\mathbf{J}$$

where $g$ is the Landé factor and $\hbar\mathbf{J}$ is the total angular momentum.

Thus:

$$\Delta E_0 = \mu_B \mathbf{H} \cdot (\mathbf{L} + g_0\mathbf{S}) = \mu_B g \mathbf{J} \cdot \mathbf{H}$$

The energy levels are:

$$E = \mu_B g m_J H$$

where $m_J = J, J-1, \ldots, -J$.

#### Spin-1/2 case ($L = 0$)

Then $m_J = \pm\frac{1}{2}$ and $g = 2$, so:

$$\Delta E = \pm \mu_B H$$

Lower energy:

$$E_\downarrow = -\mu_B H \quad \text{(spins anti-parallel to field)}$$

Higher energy:

$$E_\uparrow = \mu_B H \quad \text{(spins parallel to field)}$$

The occupation numbers in the two states are:

$$N_\uparrow = N\frac{e^{-\beta E_\uparrow}}{e^{-\beta E_\uparrow} + e^{-\beta E_\downarrow}} = N\frac{e^{-\beta\mu_B H}}{e^{-\beta\mu_B H} + e^{\beta\mu_B H}}$$

$$N_\downarrow = N\frac{e^{-\beta E_\downarrow}}{e^{-\beta E_\uparrow} + e^{-\beta E_\downarrow}} = N\frac{e^{\beta\mu_B H}}{e^{-\beta\mu_B H} + e^{\beta\mu_B H}}$$

The net magnetic moment is:

$$\boldsymbol{\mu} = -g\mu_B\mathbf{J}, \quad |\mu| = g\mu_B J = \mu_B$$

Consequently, the magnetization is:

$$M = N_\uparrow(-\mu_B) + N_\downarrow\mu_B = (N_\downarrow - N_\uparrow)\mu_B$$

$$M = N\mu_B\frac{e^{\beta\mu_B H} - e^{-\beta\mu_B H}}{e^{\beta\mu_B H} + e^{-\beta\mu_B H}} = N\mu_B\tanh(\beta\mu_B H)$$

In the high temperature limit ($\beta\mu_B H \ll 1$):

$$M = N\mu_B(\beta\mu_B H) = N\frac{\mu_B^2 H}{k_B T}$$

The magnetic susceptibility in this limit is:

$$\chi = \frac{\mu_0}{V}\frac{\partial M}{\partial H} = \frac{N}{V}\frac{\mu_0\mu_B^2}{k_B T} = \frac{C}{T}$$

## General case: angular momentum $J$

Energy levels:

$$E = \mu_B g m_J H$$

Partition function:

$$e^{-\beta F(H)} = \sum_{m_J=-J}^{J} e^{-\beta\mu_B g m_J H}$$

Using:

$$\sum_{k=m}^{n} x^k = \frac{x^m - x^{n+1}}{1-x}$$

$$e^{-\beta F(H)} = \frac{e^{\beta\mu_B gH(J+\frac{1}{2})} - e^{-\beta\mu_B gH(J+\frac{1}{2})}}{e^{\beta\mu_B gH/2} - e^{-\beta\mu_B gH/2}}$$

Magnetization:

$$M(H,T) = -\frac{N}{V}\frac{\partial F}{\partial H} = \frac{N}{V}\mu_B g J\, B_J(\beta\mu_B g J H)$$

Here

$$B_J(x) = \frac{2J+1}{2J}\coth\left(\frac{2J+1}{2J}x\right) - \frac{1}{2J}\coth\left(\frac{x}{2J}\right)$$

is the Brillouin function. In the high temperature limit, $x \ll 1$. One can expand:

$$\coth x \approx \frac{1}{x} + \frac{x}{3} + \mathcal{O}(x^3)$$

$$B_J(x) \approx \frac{J+1}{3J}x + \mathcal{O}(x^3)$$

Thus:

$$M(H,T) = \frac{N}{V}\frac{(g\mu_B)^2}{3}\frac{J(J+1)}{k_B T}H$$

$$\chi = \mu_0\frac{\partial M}{\partial H} = \mu_0\frac{N}{V}\frac{(g\mu_B)^2}{3}\frac{J(J+1)}{k_B T} = \frac{C}{T}$$

This is **Curie's law** of paramagnetic susceptibility, valid at high temperatures.

The paramagnetic susceptibility for ions with non-zero $J$ is typically $\sim 10^3$ times larger than Larmor diamagnetism.

### 8.2.3 Van Vleck paramagnetism

Consider ions for which the ground state has total angular momentum $J = 0$ (for example, shells that are either closed or one electron short of half-filled). In this case, the linear Zeeman term vanishes:

$$\langle 0|\mathbf{L} + g_0\mathbf{S}|0\rangle = 0,$$

and hence there is no first-order (Curie-like) paramagnetic response.

The leading contribution to the energy shift arises from second-order perturbation theory. Using Eqn. 8.20, the ground state energy shift is:

$$\Delta E_0 = \frac{e^2}{8m}H^2\sum_i(x_i^2 + y_i^2) + \sum_{n\neq 0}\frac{\left|\langle 0\left|\mu_B(\mathbf{L} + g_0\mathbf{S})\cdot\mathbf{H}\right|n\rangle\right|^2}{E_0 - E_n}.$$

Rewriting the second term:

$$\Delta E_0 = \frac{e^2}{8m}H^2\sum_i(x_i^2 + y_i^2) - \sum_{n\neq 0}\frac{\left|\langle 0\left|\mu_B(\mathbf{L} + g_0\mathbf{S})\cdot\mathbf{H}\right|n\rangle\right|^2}{E_n - E_0}.$$

The magnetic susceptibility is obtained from:

$$\chi = -\mu_0\frac{N}{V}\frac{\partial^2 E_0}{\partial H^2}.$$

Evaluating the derivatives, we obtain:

$$\chi = -\mu_0\frac{N}{V}\left[\frac{e^2}{4m}\left\langle 0\left|\sum_i(x_i^2 + y_i^2)\right|0\right\rangle + 2\mu_B^2\sum_{n\neq 0}\frac{\left|\langle 0\left|(\mathbf{L} + g_0\mathbf{S})\right|n\rangle\right|^2}{E_n - E_0}\right].$$

**Physical interpretation**

The first term is the familiar **Larmor diamagnetic response**, arising from the modification of orbital motion in the applied field.

The second term is the **Van Vleck paramagnetic susceptibility**. It originates from *virtual transitions* between the ground state and excited states induced by the magnetic field operator $(\mathbf{L}+g_0\mathbf{S})$. Even though the ground state has no permanent magnetic moment $(J = 0)$, the field admixes excited states with nonzero angular momentum, producing a net paramagnetic response.

**Key features**

- The Van Vleck contribution is **temperature independent**, since it does not rely on thermal population of excited states.
- It depends sensitively on the **energy gap** $(E_n - E_0)$ to excited states.
- It is typically **paramagnetic**, competing with the diamagnetic Larmor term.
- It is especially important in **insulators and ionic solids** with non-magnetic ground states.

Thus, in systems with $J = 0$, the magnetic response is governed by a competition between diamagnetic (Larmor) and paramagnetic (Van Vleck) contributions, both arising at second order in the applied field.

## 8.3 Magnetism due to itinerant electrons

Additionally, in solids, particularly metals, electrons are not localized; their magnetic response must be computed using band theory. Below, we look at two major contributions of 'free' electrons in a metal to magnetization.

### 8.3.1 Pauli paramagnetism of electrons in a metal

The magnetic moment and energy of spin 1/2 elements:

For spin parallel to $H$, the contribution to magnetization is $-\mu_B$, while for spin anti-parallel it is $\mu_B$. Thus,

$$M = -\mu_B(n_+ - n_-)$$

The density of states in the absence of a field:

$$g_\pm(E) = \frac{1}{2}g(E)$$

| Spin direction | Magnetic moment | Energy in field $H$ | No. per unit volume | Density of states |
|---|---|---|---|---|
| $+1/2$ | $\boldsymbol{\mu} = -g\mu_B\mathbf{S} = -\mu_B$ | $E = -\boldsymbol{\mu}\cdot\mathbf{H} = \mu_B H$ | $n_+$ | $g_+(E) = \frac{1}{2}g(E - \mu_B H)$ |
| $-1/2$ | $\boldsymbol{\mu} = -g\mu_B\mathbf{S} = \mu_B$ | $E = -\boldsymbol{\mu}\cdot\mathbf{H} = -\mu_B H$ | $n_-$ | $g_-(E) = \frac{1}{2}g(E + \mu_B H)$ |

In the presence of a field:

$$g_+(E) = \frac{1}{2}g(E - \mu_B H)$$

Expanding near $E_F$:

$$g_+(E) = \frac{1}{2}g(E - \mu_B H) = \frac{1}{2}g(E) - \frac{1}{2}\mu_B H\frac{\partial g(E)}{\partial E}$$

Number density:

$$n_+ = \int dE\, f(E)g_+(E) = \frac{1}{2}\int dE\, f(E)g(E) - \frac{\mu_B H}{2}\int dE\, f(E)\frac{\partial g(E)}{\partial E}$$

Similarly,

$$n_- = \frac{1}{2}\int dE\, f(E)g(E) + \frac{\mu_B H}{2}\int dE\, f(E)\frac{\partial g(E)}{\partial E}$$

The net magnetization due to the conduction electrons is:

$$M = -\mu_B(n_+ - n_-)$$

$$M = -\mu_B\left[\frac{1}{2}\int dEfg - \frac{\mu_B H}{2}\int dEf\frac{\partial g}{\partial E} - \frac{1}{2}\int dEfg + \frac{\mu_B H}{2}\int dEf\frac{\partial g}{\partial E}\right]$$

$$M = \mu_B^2 H\int dE\, f(E)\frac{\partial g(E)}{\partial E}$$

Integrating by parts:

$$M = \mu_B^2 H\int g(E)\left(-\frac{\partial f}{\partial E}\right)dE$$

From the Sommerfeld arguments, only states within $\sim k_B T$ of $E_F$ contribute because $\frac{\partial f}{\partial E}$ is sharply peaked. Consequently, one can use:

$$-\frac{\partial f}{\partial E} = \delta(E - E_F)$$

$$\Rightarrow M = \mu_B^2 H\, g(E_F)$$

Thus:

$$\chi = \mu_0 \frac{\partial M}{\partial H} = \mu_0 \mu_B^2 g(E_F) \qquad \text{(independent of temperature)}$$

From the Sommerfeld model:

$$g(E_F) = \frac{3}{2} \frac{n}{E_F}$$

$$\Rightarrow \chi = \frac{3N}{2V} \frac{\mu_0 \mu_B^2}{E_F}$$

Compare this result with Curie's law:

$$\chi = \frac{N}{V} \frac{\mu_0 \mu_B^2}{k_B T}$$

In Pauli susceptibility, $E_F$ plays the role of temperature. Since $E_F \gg k_B T$, the Pauli susceptibility is much smaller.

**Physical interpretation:**

- Pauli paramagnetism is a longitudinal effect (spin alignment).
- Only electrons near $E_F$ contribute.
- Hence weak and temperature-independent.

### 8.3.2 Landau diamagnetism of electrons in a metal

Landau diamagnetism is a transverse effect—it concerns the circular motion of the electron's charge induced by the Lorentz force. It has an orbital origin. We note here only its key features, deferring a derivation to Section 11.7.

- **The Mechanism:** Classically, an electron in a magnetic field moves in a circle (cyclotron motion). Quantum mechanically, this circular motion is quantized into Landau Levels.
- **Energy Increase:** As the magnetic field increases, the "spacing" between these Landau levels grows. This forcing of electrons into higher discrete energy levels increases the system's total kinetic energy.
- **The Response:** According to thermodynamics, a system wants to minimize its energy. Since the energy increases with the field ($dE/dB > 0$), the system develops a magnetization M that opposes the field ($M = -dE/dB$).
- **Physical Insight:** This is essentially the quantum version of Lenz's Law. The electrons "fight" the magnetic field's penetration by adjusting their orbital motion.

| Feature | Pauli Susceptibility $\chi_P$ | Landau Susceptibility $\chi_L$ |
|---|---|---|
| **Source** | Electron **Spin** | Electron **Orbital Motion** |
| **Sign** | Positive (Paramagnetic) | Negative (Diamagnetic) |
| **Magnitude** | $\mu_0 \mu_B^2 g\left(E_F\right)$ | $(-1/3)\mu_0 \mu_B^2 g\left(E_F\right)$ (for free electrons) |
| **Analogy** | Compass needles aligning | Lenz's Law / Eddy currents |

### 8.3.3 Curie vs Pauli Paramagnetism: Classical vs Quantum Statistics

It is instructive to contrast the Curie paramagnetism of localized moments with the Pauli paramagnetism of conduction electrons in metals. Although both arise from spin degrees of freedom, their physical origins and temperature dependence are fundamentally different.

#### Curie Paramagnetism (Localized Moments)

In ionic or molecular systems, magnetic moments are associated with localized electrons (e.g., partially filled $d$ or $f$ shells). These moments behave approximately as independent entities. Thermal fluctuations compete with magnetic field alignment. The magnetization is obtained from Boltzmann statistics:

$$M \propto \tanh(\beta \mu_B H)$$

which, in the high temperature limit ($\beta \mu_B H \ll 1$), reduces to:

$$M \propto \frac{\mu_B^2 H}{k_B T}$$

Thus,

$$\chi \propto \frac{1}{T}$$

**Key feature:** All moments are thermally active, and temperature directly controls the degree of alignment.

#### Pauli Paramagnetism (Itinerant Electrons)

In metals, electrons are delocalized and obey Fermi–Dirac statistics. At zero field, spin-up and spin-down states are equally occupied up to the Fermi energy $E_F$.

When a magnetic field is applied:

- Spin-up and spin-down bands shift by $\mp \mu_B H$
- Only electrons near the Fermi surface can change occupation

The magnetization is:

$$M = \mu_B^2 H \, g(E_F)$$

leading to:

$$\chi = \mu_0 \mu_B^2 g(E_F)$$

**Key feature:** Only a narrow energy window $\sim k_B T$ around $E_F$ contributes.

#### Physical Origin of the Difference

The essential distinction arises from statistics:

- **Curie case:** Classical (Boltzmann) statistics All spins are free to respond independently to the field.
- **Pauli case:** Quantum (Fermi–Dirac) statistics The Pauli exclusion principle restricts spin rearrangement to states near $E_F$.

This leads to a useful interpretation:

$$\chi_{\text{Curie}} \sim \frac{1}{k_B T}, \qquad \chi_{\text{Pauli}} \sim \frac{1}{k_B T_F}$$

Thus, the Fermi energy plays the role of an effective temperature scale. Since $T_F \gg T$ in metals, Pauli paramagnetism is much weaker.

#### Conceptual Summary

- Curie paramagnetism: alignment of *all* localized moments, thermally limited.
- Pauli paramagnetism: redistribution of *states at the Fermi surface*, quantum limited.

## 8.4 Summary

| Mechanism | Origin | Temp. dep. | Sign | System |
|---|---|---|---|---|
| Larmor | orbital | none | $-$ | atoms |
| Curie | spin/orbital | $1/T$ | $+$ | ions |
| Pauli | spin | none | $+$ | metals |
| Landau | orbital | none | $-$ | metals |
| Van Vleck | virtual | none | $+$ | insulators |

# Chapter 9

# Ferromagnetism

## 9.1 Introduction

Ferromagnetism is the phenomenon in which a material exhibits a spontaneous magnetization below a critical temperature known as the Curie temperature $T_C$. In the ferromagnetic phase, the magnetic moments of electrons align parallel to each other even in the absence of an applied magnetic field.

Examples of elemental ferromagnets include Fe, Co, and Ni. Ferromagnetism arises from quantum mechanical exchange interactions between electron spins and cannot be explained by classical magnetic dipole interactions alone.

The central questions addressed in the theory of ferromagnetism are:

- Why do electron spins align spontaneously?
- What microscopic interactions produce this alignment?
- How does magnetization depend on temperature?
- What are the elementary excitations of a ferromagnet?

The magnetic moment of an electron has contributions from both orbital and spin angular momentum.

Orbital magnetic moment:

$$\boldsymbol{\mu}_L = -\mu_B \frac{\mathbf{L}}{\hbar} \tag{9.1}$$

and, spin magnetic moment:

$$\boldsymbol{\mu}_S = -g_s \mu_B \frac{\mathbf{S}}{\hbar} \tag{9.2}$$

where, $\mu_B = \frac{e\hbar}{2m}$ is the Bohr magneton.

In most transition metals, the orbital moment is largely quenched by the crystal field, and magnetism arises primarily from electron spin (see Appendix 9.9).

A naive explanation of ferromagnetism might invoke magnetic dipole interactions.

The dipole-dipole interaction energy is approximately.

$$E_{dd} \sim \frac{\mu_0}{4\pi}\frac{\mu^2}{r^3} \tag{9.3}$$

Using typical atomic parameters

$$\mu \sim \mu_B, \qquad r \sim 3\,\text{Å}$$

gives

$$E_{dd} \sim 10^{-4}\,\text{eV}$$

However, the Curie temperature corresponds to energies

$$k_B T_C \sim 0.1\,\text{eV}$$

Thus, classical dipole interactions are far too weak to explain ferromagnetism.

## 9.2 Exchange Interaction

The fundamental origin of ferromagnetism is the **exchange interaction**. This purely quantum mechanical effect arises from the combination of the Coulomb interaction and the antisymmetry of the electronic wavefunction required by the Pauli exclusion principle.

To understand the origin of exchange, consider two interacting electrons in an external potential $V(\mathbf{r})$. The Hamiltonian is

$$H = \frac{p_1^2}{2m} + \frac{p_2^2}{2m} + V(\mathbf{r}_1) + V(\mathbf{r}_2) + \frac{e^2}{|\mathbf{r}_1 - \mathbf{r}_2|} \tag{9.4}$$

Because electrons are fermions, the total wavefunction must be antisymmetric under particle exchange,

$$\Psi(1,2) = -\Psi(2,1). \tag{9.5}$$

The total wavefunction can be written as a product of spatial and spin parts,

$$\Psi = \psi(\mathbf{r}_1, \mathbf{r}_2)\chi(s_1, s_2). \tag{9.6}$$

The antisymmetry requirement implies that if the spin wavefunction is symmetric, the spatial wavefunction must be antisymmetric, and vice versa.

Two distinct spin configurations are therefore possible.

**Singlet state.** The spin wavefunction is antisymmetric,

$$\chi_s = \frac{1}{\sqrt{2}}(\uparrow\downarrow - \downarrow\uparrow), \tag{9.7}$$

So the spatial wavefunction must be symmetric,

$$\psi_s(\mathbf{r}_1, \mathbf{r}_2) = \frac{1}{\sqrt{2}}\left[\phi_a(\mathbf{r}_1)\phi_b(\mathbf{r}_2) + \phi_a(\mathbf{r}_2)\phi_b(\mathbf{r}_1)\right]. \tag{9.8}$$

**Triplet state.** The spin wavefunction is symmetric,

$$\chi_{t1} = \uparrow\uparrow \tag{9.9}$$

$$\chi_{t0} = \frac{1}{\sqrt{2}}(\uparrow\downarrow + \downarrow\uparrow) \tag{9.10}$$

$$\chi_{t-1} = \downarrow\downarrow, \tag{9.11}$$

and therefore the spatial wavefunction must be antisymmetric,

$$\psi_t(\mathbf{r}_1, \mathbf{r}_2) = \frac{1}{\sqrt{2}}\left[\phi_a(\mathbf{r}_1)\phi_b(\mathbf{r}_2) - \phi_a(\mathbf{r}_2)\phi_b(\mathbf{r}_1)\right]. \tag{9.12}$$

### 9.2.1 Direct and exchange Coulomb integrals

The expectation value of the Coulomb interaction

$$V_C = \frac{e^2}{|\mathbf{r}_1 - \mathbf{r}_2|}$$

contains two distinct contributions.

**Direct Coulomb integral**

$$J_D = \int d^3r_1 d^3r_2 |\phi_a(\mathbf{r}_1)|^2 |\phi_b(\mathbf{r}_2)|^2 \frac{e^2}{|\mathbf{r}_1 - \mathbf{r}_2|}, \tag{9.13}$$

which corresponds to the classical electrostatic interaction between the two charge distributions.

**Exchange integral**

$$J = \int d^3r_1 d^3r_2 \phi_a^*(\mathbf{r}_1)\phi_b^*(\mathbf{r}_2) \frac{e^2}{|\mathbf{r}_1 - \mathbf{r}_2|} \phi_a(\mathbf{r}_2)\phi_b(\mathbf{r}_1). \tag{9.14}$$

This term has no classical analog and arises entirely from the quantum-mechanical symmetry of the electronic wavefunction.

## Energy splitting

Evaluating the expectation value of the Hamiltonian gives

$$E_{\text{singlet}} = E_0 + J_D + J, \tag{9.15}$$
$$E_{\text{triplet}} = E_0 + J_D - J. \tag{9.16}$$

The energy difference between the two states is therefore

$$E_{\text{singlet}} - E_{\text{triplet}} = 2J. \tag{9.17}$$

This energy splitting can be written in the form of an effective spin Hamiltonian,

$$H_{ex} = -2J\,\mathbf{S}_1 \cdot \mathbf{S}_2. \tag{9.18}$$

If $J > 0$, the triplet state is lower in energy and parallel spin alignment is favored, leading to ferromagnetism. If $J < 0$, the singlet state is favored, resulting in antiferromagnetic coupling.

## Physical interpretation of exchange

Although the exchange integral contains no explicit spin variables, it produces an effective interaction between spins because the symmetry of the spin wavefunction determines the symmetry of the spatial wavefunction.

For parallel spins (triplet state), the spatial wavefunction is antisymmetric. In particular,

$$\psi_t(\mathbf{r}, \mathbf{r}) = 0,$$

which means that two electrons with the same spin cannot occupy the same spatial position. As a result, electrons with parallel spins tend to avoid each other, reducing their Coulomb repulsion.

This reduction in Coulomb energy relative to the singlet state is the **exchange energy**. The exchange interaction, therefore, originates from the modification of electron spatial correlations imposed by the Pauli principle. It is not a classical magnetic interaction between spins but a purely quantum mechanical consequence of electron indistinguishability.

The magnitude of the exchange integral depends strongly on the overlap of the electronic orbitals. If the orbitals on neighboring sites overlap weakly, the exchange interaction becomes small. Consequently, exchange interactions in solids are typically short ranged and act primarily between nearest neighbors.

### 9.2.2 The exchange hole picture

A particularly intuitive way to understand exchange is through the concept of the **exchange hole**. The key idea is that an electron with a given spin reduces the probability of finding another electron with the same spin nearby.

Consider placing an electron with spin up at position $\mathbf{r}_0$. Because the spatial wavefunction for two electrons with parallel spins is antisymmetric, the probability of finding another spin-up electron close to $\mathbf{r}_0$ is reduced. In fact,

$$\psi(\mathbf{r}, \mathbf{r}) = 0$$

for identical spins. This creates a region around the electron in which the density of same-spin electrons is suppressed. This region is called the exchange hole.

The exchange hole affects only electrons with the same spin; electrons with opposite spin are not subject to the same Pauli constraint. Because the exchange hole pushes same-spin electrons apart, the average separation between electrons increases, reducing the Coulomb repulsion

$$E_C = \frac{e^2}{|\mathbf{r}_1 - \mathbf{r}_2|}. \tag{9.19}$$

The resulting reduction in Coulomb energy is the physical origin of the exchange interaction. If many electrons align their spins, the exchange hole operates collectively between many pairs of electrons, and the total Coulomb energy of the system decreases. In this way, the system can lower its energy through spin alignment, providing an intuitive explanation of Hund's rule and the tendency toward ferromagnetism in itinerant-electron systems.

The spatial extent of the exchange hole in metals is typically of the order

$$\sim k_F^{-1}, \tag{9.20}$$

where $k_F$ is the Fermi wavevector, the exchange hole has no classical analog and arises entirely from the fermionic statistics of electrons.

### Connection to the Heisenberg Hamiltonian

In a crystal with many localized magnetic moments, the exchange interaction between pairs of spins leads to the Heisenberg model

$$H = -\sum_{ij} J_{ij} \mathbf{S}_i \cdot \mathbf{S}_j \tag{9.21}$$

where $J_{ij}$ depends on the overlap of the electronic orbitals on sites $i$ and $j$. This effective Hamiltonian forms the basis of the theoretical description of magnetically ordered materials.

## 9.3 Heisenberg Model

At energies much smaller than the electronic excitation energies, the microscopic Coulomb interaction between electrons can be replaced by an effective interaction between localized spins. The resulting effective Hamiltonian is the **Heisenberg Hamiltonian**,

$$H = -\sum_{i,j} J_{ij}\, \mathbf{S}_i \cdot \mathbf{S}_j. \tag{9.22}$$

Here $\mathbf{S}_i$ denotes the spin operator associated with the magnetic moment on lattice site $i$, and $J_{ij}$ is the exchange coupling between spins on sites $i$ and $j$. The sign and magnitude of $J_{ij}$ depend on the overlap of the electronic orbitals and the microscopic exchange mechanisms present in the material.

The scalar product of spin operators may be written as

$$\mathbf{S}_i \cdot \mathbf{S}_j = S_i^x S_j^x + S_i^y S_j^y + S_i^z S_j^z. \tag{9.23}$$

This interaction is rotationally invariant in spin space, reflecting the fact that in the absence of spin–orbit coupling, the exchange interaction does not select a preferred spin direction.

### Nearest-neighbour approximation

In most solids, the exchange interaction decreases rapidly with distance because it depends sensitively on orbital overlap. It is therefore often sufficient to retain only nearest-neighbor interactions,

$$H = -J \sum_{\langle ij \rangle} \mathbf{S}_i \cdot \mathbf{S}_j, \tag{9.24}$$

where $\langle ij \rangle$ denotes pairs of nearest-neighbor lattice sites.

### Ground states

The nature of the ground state depends on the sign of the exchange constant $J$.

- **Ferromagnetic coupling ($J > 0$).** The energy is minimized when neighboring spins align parallel to each other. The ground state corresponds to all spins pointing in the same direction, producing a macroscopic magnetization.
- **Antiferromagnetic coupling ($J < 0$).** The energy is minimized when nneighboringspins are antiparallel. On a bipartite lattice, this produces the **Néel state**, in which the lattice divides into two sublattices with opposite spin orientations.

For the ferromagnetic case, the classical ground state may be written as

$$\mathbf{S}_1 = \mathbf{S}_2 = \cdots = \mathbf{S}_N,$$

meaning that all spins are aligned. Because the Hamiltonian is rotationally invariant, the direction of the common spin orientation is arbitrary. This degeneracy reflects the continuous spin-rotation symmetry of the system. Hence, small deviations cost zero energy - this leads to spin waves.

### Physical significance

Despite its apparent simplicity, the Heisenberg model captures many essential features of magnetic materials, including

- ferromagnetic and antiferromagnetic order,
- collective spin excitations (spin waves),
- magnetic phase transitions.

The Heisenberg model, therefore, provides the starting point for the theoretical description of magnetism in solids.

## 9.4 Spin Waves in the Heisenberg Ferromagnet

The ground state of a ferromagnet corresponds to all spins aligned parallel. Small deviations from this ordered state propagate through the lattice as collective excitations known as **spin waves**. The deviated spins precess due to the torque on them from the other spins. The quanta of these excitations are called **magnons**. Each magnon reduces the total magnetization by one unit of $\hbar$.

Introducing spin raising and lowering operators

$$S_i^+ = S_i^x + iS_i^y \tag{9.25}$$
$$S_i^- = S_i^x - iS_i^y, \tag{9.26}$$

the Heisenberg Hamiltonian becomes

$$H = -J \sum_{\langle ij \rangle} \left( S_i^z S_j^z + \frac{1}{2} S_i^+ S_j^- + \frac{1}{2} S_i^- S_j^+ \right). \tag{9.27}$$

Using the Holstein–Primakoff transformation

$$S_i^+ = \sqrt{2S}\, a_i \tag{9.28}$$
$$S_i^- = \sqrt{2S}\, a_i^\dagger \tag{9.29}$$
$$S_i^z = S - a_i^\dagger a_i, \tag{9.30}$$

and retaining terms to leading order in magnon density yields

$$H = E_0 + \sum_k \epsilon(k) a_k^\dagger a_k. \tag{9.31}$$

The magnon dispersion relation is

$$\epsilon(k) = 2JSz(1 - \gamma_k), \tag{9.32}$$

where

$$\gamma_k = \frac{1}{z} \sum_\delta e^{ik\cdot\delta}. \tag{9.33}$$

The sum runs over all nearest-neighbor vectors $\delta$ connecting a lattice site to its neighboring sites, and $z$ is the coordination number of the lattice.

### Long-wavelength limit

For $ka \ll 1$ we obtain

$$\epsilon(k) \approx Dk^2, \tag{9.34}$$

where

$$D = JSa^2 \tag{9.35}$$

is the **spin stiffness**. Thus, ferromagnetic magnons exhibit a **quadratic dispersion**.

## 9.4.1 Bloch's $T^{3/2}$ Law

Thermal excitation of magnons reduces the magnetization of a ferromagnet. The number of thermally excited magnons is

$$N_m = \frac{V}{(2\pi)^3} \int \frac{d^3k}{e^{\epsilon(k)/k_BT} - 1}. \tag{9.36}$$

For ferromagnets $\epsilon(k) = Dk^2$, which leads to

$$N_m \propto T^{3/2}. \tag{9.37}$$

Since each magnon reduces the magnetization by one unit of spin,

$$M(T) = M(0) - AT^{3/2}. \tag{9.38}$$

This result is known as **Bloch's $T^{3/2}$ law**.

## 9.5 Spin Waves in Heisenberg Antiferromagnets

### Linear magnon dispersion in antiferromagnets

The dispersion relation of spin waves in antiferromagnets differs qualitatively from that of ferromagnets. In a ferromagnet, the magnon dispersion is quadratic ($\epsilon_k \propto k^2$), whereas in an antiferromagnet it is linear ($\epsilon_k \propto k$) at long wavelengths. To demonstrate this result, we consider the nearest-neighbor Heisenberg antiferromagnet:

$$H = -J \sum_{\langle ij \rangle} \mathbf{S}_i \cdot \mathbf{S}_j, \tag{9.39}$$

with $J < 0$.

#### Néel ground state

On a bipartite lattice, the classical ground state is the Néel state in which spins on the two sublattices point in opposite directions:

$$\mathbf{S}_i = S\hat{z} \quad (i \in A), \qquad \mathbf{S}_j = -S\hat{z} \quad (j \in B).$$

Because the two sublattices have opposite orientations, we introduce separate bosonic operators for the two sublattices using the Holstein–Primakoff transformation.

For sublattice $A$

$$S_i^z = S - a_i^\dagger a_i \tag{9.40}$$
$$S_i^+ = \sqrt{2S}\, a_i \tag{9.41}$$
$$S_i^- = \sqrt{2S}\, a_i^\dagger \tag{9.42}$$

For sublattice $B$

$$S_j^z = -S + b_j^\dagger b_j \tag{9.43}$$
$$S_j^+ = \sqrt{2S}\, b_j^\dagger \tag{9.44}$$
$$S_j^- = \sqrt{2S}\, b_j. \tag{9.45}$$

### Linear spin-wave Hamiltonian

Substituting these expressions into the Heisenberg Hamiltonian and retaining only terms quadratic in the boson operators yields

$$H = E_0 + JS \sum_{\langle ij \rangle} \left( a_i^\dagger a_i + b_j^\dagger b_j + a_i b_j + a_i^\dagger b_j^\dagger \right). \tag{9.46}$$

We now perform the Fourier transform

$$a_i = \frac{1}{\sqrt{N}} \sum_k a_k e^{ik \cdot r_i} \tag{9.47}$$
$$b_j = \frac{1}{\sqrt{N}} \sum_k b_k e^{ik \cdot r_j}. \tag{9.48}$$

The Hamiltonian becomes

$$H = E_0 + JSz \sum_k \left[ a_k^\dagger a_k + b_k^\dagger b_k + \gamma_k (a_k b_{-k} + a_k^\dagger b_{-k}^\dagger) \right], \tag{9.49}$$

where $z$ is the coordination number and

$$\gamma_k = \frac{1}{z} \sum_\delta e^{ik \cdot \delta}. \tag{9.50}$$

### Diagonalization

The Hamiltonian can be diagonalized using a Bogoliubov transformation. The resulting magnon spectrum is

$$\epsilon(k) = JSz\sqrt{1 - \gamma_k^2}. \tag{9.51}$$

### Long wavelength limit

For small wavevectors ($ka \ll 1$) we expand

$$\gamma_k \approx 1 - \frac{a^2k^2}{2}. \tag{9.52}$$

Substituting into the dispersion relation gives

$$\epsilon(k) \approx JSz\sqrt{1 - \left(1 - \frac{a^2k^2}{2}\right)^2} \tag{9.53}$$

$$\approx JSz\,ak. \tag{9.54}$$

Thus, the long-wavelength magnon dispersion is

$$\epsilon(k) = ck, \tag{9.55}$$

where

$$c = JSza \tag{9.56}$$

is the **spin-wave velocity**.

#### Physical interpretation

The linear dispersion arises because the antiferromagnetic ground state contains two oppositely oriented sublattices. A disturbance of one sublattice immediately affects the other, producing a propagating collective mode analogous to an acoustic wave.

## Low-temperature magnetization in antiferromagnets

For antiferromagnets, the magnon dispersion is linear,

$$\epsilon(k) \propto k.$$

Repeating the same analysis gives

$$N_m \propto T^3 \tag{9.57}$$

and therefore

$$M(T) = M(0) - BT^3. \tag{9.58}$$

### Origin of the different temperature dependences

The difference arises from the long-wavelength magnon dispersion:

| System | Dispersion | Magnetization correction |
|---|---|---|
| Ferromagnet | $\epsilon(k) \propto k^2$ | $T^{3/2}$ |
| Antiferromagnet | $\epsilon(k) \propto k$ | $T^3$ |

Thus, the temperature dependence of the magnetization is directly determined by the dispersion relation of the spin-wave excitations.

## 9.6 Weiss Mean Field Theory

A major step toward understanding ferromagnetism was made by Weiss, who introduced the concept of a **molecular field**. The central idea is that each magnetic moment experiences not only the externally applied magnetic field but also an additional internal field produced by neighboring moments.

Weiss proposed that this internal field is proportional to the magnetization of the material. The effective magnetic field acting on a spin is therefore

$$B_{\text{eff}} = B + \lambda M, \tag{9.59}$$

where $B$ is the external magnetic field, $M$ is the magnetization, and $\lambda$ is the **molecular field constant**. This phenomenological relation incorporates the effect of the exchange interaction in an average way.

### 9.6.1 Magnetization of localized spins

Consider a system of $N$ localized spins of magnitude $S$. In an effective magnetic field $B_{\text{eff}}$, the magnetization is given by

$$M = Ng\mu_B S B_S(x), \tag{9.60}$$

where $g$ is the Landé $g$-factor, $\mu_B$ is the Bohr magneton, and $B_S(x)$ is the **Brillouin function**,

$$B_S(x) = \frac{2S+1}{2S}\coth\!\left(\frac{2S+1}{2S}x\right) - \frac{1}{2S}\coth\!\left(\frac{x}{2S}\right). \tag{9.61}$$

The argument of the Brillouin function is

$$x = \frac{g\mu_B S B_{\text{eff}}}{k_B T}. \tag{9.62}$$

Substituting the expression for the effective field gives the **self-consistency equation**

$$M = Ng\mu_B S B_S\left(\frac{g\mu_B S(B+\lambda M)}{k_B T}\right). \tag{9.63}$$

This equation determines the magnetization as a function of temperature and applied magnetic field.

## Curie temperature

Spontaneous magnetization corresponds to a nonzero solution for $M$ even when the external field $B = 0$. To determine the transition temperature, we consider the limit of small magnetization near the critical point.

For small $x$, the Brillouin function can be expanded as

$$B_S(x) \approx \frac{S+1}{3S}x. \tag{9.64}$$

Substituting this approximation into the self-consistency equation with $B = 0$ gives

$$M = Ng\mu_B S\left(\frac{S+1}{3S}\right)\frac{g\mu_B S\lambda M}{k_B T}. \tag{9.65}$$

Canceling $M$ yields the condition

$$1 = \frac{Ng^2\mu_B^2 S(S+1)}{3k_B T_C}\lambda. \tag{9.66}$$

The temperature at which this equality holds defines the **Curie temperature**

$$T_C = \frac{Ng^2\mu_B^2 S(S+1)}{3k_B}\lambda. \tag{9.67}$$

Below this temperature, the system develops spontaneous magnetization.

### 9.6.2 Curie–Weiss law

Above the Curie temperature, the magnetization is small and proportional to the applied field. Linearizing the self-consistency equation yields

$$M = \chi B, \tag{9.68}$$

where the magnetic susceptibility becomes

$$\chi = \frac{C}{T - T_C}. \tag{9.69}$$

Here

$$C = \frac{Ng^2\mu_B^2 S(S+1)}{3k_B} \tag{9.70}$$

is the **Curie constant**. This result is known as the **Curie–Weiss law**.

## Physical interpretation

The Weiss mean field theory predicts that the exchange interaction produces an internal molecular field that reinforces the alignment of spins. When the temperature is sufficiently low, this internal field is strong enough to maintain spin alignment even in the absence of an external magnetic field, leading to spontaneous magnetization.

Although Weiss theory successfully explains the Curie–Weiss law and the existence of a phase transition, it neglects fluctuations of the spin system. As a result, it overestimates the Curie temperature and predicts mean-field critical exponents. Nevertheless, it provides an important conceptual framework for understanding magnetic phase transitions.

### 9.6.3 Connection to the Heisenberg exchange interaction

The molecular field introduced by Weiss can be understood microscopically by starting from the Heisenberg Hamiltonian

$$H = -J \sum_{\langle ij \rangle} \mathbf{S}_i \cdot \mathbf{S}_j, \tag{9.71}$$

where $J$ is the exchange constant, and the sum runs over nearest-neighbor pairs.

In the mean-field approximation, each spin is assumed to interact with the *average* magnetization of its neighbors rather than their instantaneous fluctuating orientations. Writing the spin operator as

$$\mathbf{S}_j = \langle \mathbf{S}_j \rangle + (\mathbf{S}_j - \langle \mathbf{S}_j \rangle),$$

and neglecting the fluctuation term, we obtain

$$\mathbf{S}_i \cdot \mathbf{S}_j \approx \mathbf{S}_i \cdot \langle \mathbf{S}_j \rangle. \tag{9.72}$$

If each lattice site has $z$ nearest neighbors, the Hamiltonian acting on spin $i$ becomes

$$H_i \approx -Jz\, \mathbf{S}_i \cdot \langle \mathbf{S} \rangle. \tag{9.73}$$

The magnetization per unit volume is related to the average spin by

$$M = ng\mu_B\langle S_z\rangle, \tag{9.74}$$

where $n$ is the number density of spins.

Thus, the mean-field Hamiltonian can be written as

$$H_i = -g\mu_B \mathbf{S}_i \cdot \mathbf{B}_{\text{mf}}, \tag{9.75}$$

where the effective molecular field is

$$B_{\text{mf}} = \frac{2zJ}{(g\mu_B)^2} M. \tag{9.76}$$

Comparing this expression with the Weiss assumption

$$B_{\text{eff}} = B + \lambda M, \tag{9.77}$$

we identify the molecular field constant as

$$\lambda = \frac{2zJ}{(g\mu_B)^2}. \tag{9.78}$$

## Curie temperature in terms of exchange

Substituting this result into the Weiss expression for the Curie temperature gives

$$T_C = \frac{2zJ}{3k_B} S(S+1). \tag{9.79}$$

This relation shows that the Curie temperature is determined by the strength of the exchange interaction and the number of nearest neighbors. Stronger exchange coupling and larger coordination number both increase the ordering temperature.

## Physical interpretation

The Weiss molecular field is therefore not a real magnetic field but rather an effective field arising from exchange interactions with neighboring spins. In the mean-field approximation, each spin experiences an average field produced by the surrounding magnetization, which tends to align it parallel to the existing magnetic order.

This derivation demonstrates that the Weiss mean-field theory can be viewed as the mean-field approximation to the Heisenberg model. The phenomenological parameter $\lambda$ is directly related to the microscopic exchange constant $J$.

## Validity and limitations of mean-field theory

The Weiss mean-field theory provides a remarkably simple description of ferromagnetism and successfully explains several important experimental observations, including the Curie–Weiss law and the existence of a ferromagnetic phase transition. Nevertheless, the theory relies on a strong approximation: each spin is assumed to interact only with the *average* magnetization of its neighbors, while fluctuations of the local spin configuration are neglected.

The accuracy of this approximation depends strongly on the dimensionality of the system and on the number of interacting neighbors.

### Role of coordination number

In a lattice with coordination number $z$, each spin interacts with $z$ neighbors. When $z$ is large, the fluctuations in the local environment of a spin tend to average out, making the mean-field approximation more accurate. In this sense, mean-field theory becomes exact in the limit of infinite coordination number.

This explains why the Weiss theory often gives a reasonable estimate of the Curie temperature in three-dimensional magnetic materials.

### Importance of fluctuations

Near the critical temperature $T_C$, fluctuations of the magnetization become large and long-ranged. These fluctuations are not captured by mean-field theory, which assumes a spatially uniform magnetization. As a result, Weiss theory predicts incorrect critical exponents for the magnetic phase transition.

For example, mean-field theory predicts that the spontaneous magnetization near $T_C$ behaves as

$$M(T) \propto (T_C - T)^{1/2}, \tag{9.80}$$

corresponding to a critical exponent $\beta = 1/2$. In real materials, however, experiments typically find smaller values, such as

$$\beta \approx 0.33$$

for three-dimensional Heisenberg magnets.

### Effect of dimensionality

The importance of fluctuations increases dramatically in lower dimensions. In fact, the Mermin–Wagner theorem shows that continuous spin-rotation symmetry cannot be

spontaneously broken at a finite temperature in one- or two-dimensional systems with short-range interactions.

As a consequence:

- One-dimensional Heisenberg magnets do not exhibit long-range magnetic order at finite temperature.
- Two-dimensional isotropic Heisenberg magnets also lack long-range order at finite temperature.

Thus, mean-field theory greatly overestimates the tendency toward magnetic ordering in low-dimensional systems.

**Summary**

Despite its limitations, the Weiss mean-field theory remains extremely important because it captures the essential physics of magnetic ordering in a simple framework. More sophisticated approaches, such as renormalization-group theory and numerical simulations, are required to describe the critical behavior near the transition temperature.

## 9.7 Ferromagnetic Hysteresis

One of the most characteristic experimental signatures of ferromagnetism is the existence of **magnetic hysteresis**. When an external magnetic field is applied and cycled, the magnetization does not follow the same path during increasing and decreasing field. Instead, the system exhibits a history-dependent response, forming a closed loop known as the **hysteresis loop**.

### Basic phenomenology

Consider a ferromagnet initially in a demagnetized state. As the external magnetic field $H$ is increased, the magnetization $M$ increases and eventually saturates at a value $M_s$ known as the **saturation magnetization**. If the field is now reduced to zero, the magnetization does not return to zero but instead retains a finite value $M_r$, called the **remanent magnetization**.

To reduce the magnetization to zero, a finite reverse field $H_c$ must be applied. This field is called the **coercive field**. Continuing to increase the negative field leads to saturation in the opposite direction. Reversing the field again completes the hysteresis loop.

### Hysteresis loop

The magnetization curve therefore, forms a loop characterized by three important quantities:

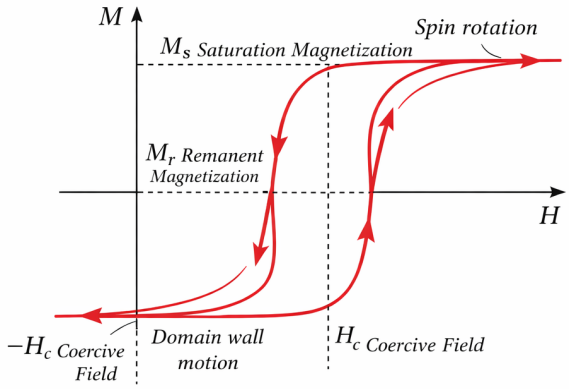


Figure 9.1: Origin of hysteresis in ferromagnets

- **Saturation magnetization** $M_s$: maximum magnetization at large field.
- **Remanence** $M_r$: magnetization at zero applied field.
- **Coercivity** $H_c$: field required to reduce $M$ to zero.

The area enclosed by the hysteresis loop represents the **energy loss per cycle** due to irreversible processes in the material.

## Origin of hysteresis: magnetic domains

The microscopic origin of hysteresis lies in the existence of **magnetic domains**. A uniformly magnetized crystal produces a large magnetostatic energy due to stray fields. To minimize this energy, the system breaks into domains within which the magnetization is uniform but oriented in different directions.

In a zero applied field, domains are arranged so that the net magnetization is small or zero. When a magnetic field is applied, magnetization increases through two main processes:

1. **Domain wall motion**: domains aligned with the field grow at the expense of others.
2. **Domain rotation**: spins within domains gradually rotate toward the field direction.

These mechanisms dominate in different regions of the hysteresis curve.

### (1) Initial magnetization: domain wall motion

Starting from a demagnetized state, the material consists of many domains with different orientations. As a small external field is applied, magnetization increases primarily through **domain wall motion**.

Domains whose magnetization is aligned with the field grow at the expense of unfavorable domains. This process requires relatively little energy because it involves shifting domain boundaries rather than rotating all spins.

As a result:

- The initial part of the $M$–$H$ curve is steep.
- Magnetization increases rapidly with a small applied field.

This regime is largely reversible at very small fields but becomes irreversible once domain walls encounter pinning centers.

### (2) Intermediate region: irreversible domain wall motion

As the field increases further, domain walls move through the crystal, but are hindered by defects, impurities, and grain boundaries.

Overcoming these pinning centers requires finite energy, leading to:

- irreversible jumps in magnetization,
- hysteresis and energy loss.

This regime contributes significantly to the width of the hysteresis loop and to the coercive field.

### (3) Approach to saturation: spin rotation

Once domains aligned with the field have grown to occupy most of the sample, further increase in magnetization cannot occur through domain wall motion. Instead, the magnetization increases through **rotation of spins within domains** toward the direction of the applied field.

This process involves overcoming magnetic anisotropy energy and is therefore more gradual.

As a result:

- The $M$–$H$ curve becomes less steep.
- Magnetization approaches saturation smoothly.

#### (4) Saturation regime

In large fields, all spins are nearly aligned with the field, and the system reaches the **saturation magnetization** $M_s$. Further increases in field produce a negligible change in magnetization.

#### (5) Field reversal and coercivity

When the field is reduced from saturation, the reverse process does not retrace the same path because domain walls remain pinned.

- Initially, small changes are dominated by **spin rotation**.
- As the reverse field increases, **domain walls begin to move**, but only after overcoming pinning barriers.

The field required to reduce the magnetization to zero is the **coercive field** $H_c$, which is primarily determined by the strength of the domain wall pinning.

#### Summary

Different regions of the hysteresis loop are dominated by different mechanisms:

| Region of loop | Dominant mechanism |
|---|---|
| Initial slope | Domain wall motion (easy, reversible) |
| Mid region | Domain wall motion (pinned, irreversible) |
| Near saturation | Spin rotation |
| High field | Saturated state |
| Reversal near $H_c$ | Domain wall depinning |

Thus, hysteresis reflects the interplay between domain wall dynamics, spin rotation, and pinning effects in real materials.

## Irreversibility and coercivity

Hysteresis arises because domain wall motion is not perfectly reversible. Defects, impurities, and lattice imperfections act as **pinning centers** that impede the motion of domain walls. As a result, additional energy is required to move domain walls, leading to hysteresis and a finite coercive field.

The strength of pinning determines the magnetic hardness of the material:

- **Soft ferromagnets**: small $H_c$, narrow hysteresis loop.
- **Hard ferromagnets**: large $H_c$, wide hysteresis loop.

## Connection to microscopic theory

The existence of magnetic domains and hysteresis reflects a competition between several energy scales:

- **Exchange energy**: favors parallel alignment of spins.
- **Magnetostatic energy**: favors formation of domains to reduce stray fields.
- **Anisotropy energy**: favors alignment along specific crystallographic directions.
- **Domain wall energy**: penalizes spatial variation of magnetization.

The domain wall width is determined by the balance between exchange and anisotropy,

$$\delta \sim \sqrt{\frac{A}{K}}, \tag{9.81}$$

The constant $K$ is the magnetic anisotropy energy density, which arises from spin–orbit coupling and determines the preferred direction of magnetization. The exchange stiffness $A$ is related to the spin-wave stiffness $D$ introduced earlier; Both originate from the same microscopic exchange interaction, but appear in real-space and momentum-space descriptions, respectively. Intuitively, $A$ is a measure of the cost to bend magnetization in space.

## Energy loss and applications

The area of the hysteresis loop corresponds to the energy dissipated per cycle:

$$W = \oint H\, dM. \tag{9.82}$$

This energy loss is important in applications such as transformers and magnetic storage devices. Materials with small hysteresis losses are used in transformer cores, while materials with large coercivity are used for permanent magnets.

## Physical interpretation

Hysteresis demonstrates that ferromagnets are inherently **non-equilibrium systems** on experimental time scales. The magnetization depends not only on the instantaneous external field but also on the history of the system. This behavior arises from the complex energy landscape associated with domain structures and pinning effects. Thus, while the Heisenberg model and spin-wave theory describe equilibrium properties, hysteresis reflects the dynamics of domain evolution in real materials.

## 9.8 Magnetization Dynamics: Landau–Lifshitz–Gilbert Equation

So far, we have described the *equilibrium properties* of ferromagnets using the Heisenberg model and micromagnetic energy. We now turn to the **dynamics of magnetization**, which governs how the system evolves in time under an effective magnetic field.

### Torque on a magnetic moment

A magnetic moment $\boldsymbol{\mu}$ in a magnetic field $\mathbf{B}$ experiences a torque

$$\boldsymbol{\tau} = \boldsymbol{\mu} \times \mathbf{B}. \tag{9.83}$$

Using the relation $\boldsymbol{\mu} = -\gamma \mathbf{S}$, where $\gamma$ is the gyromagnetic ratio, the equation of motion becomes

$$\frac{d\mathbf{S}}{dt} = -\gamma \mathbf{S} \times \mathbf{B}. \tag{9.84}$$

In a continuous medium, this translates into an equation for the magnetization $\mathbf{M}(\mathbf{r}, t)$,

$$\frac{d\mathbf{M}}{dt} = -\gamma \mathbf{M} \times \mathbf{H}_{\text{eff}}. \tag{9.85}$$

This describes **precession** of magnetization around the effective field.

### Effective magnetic field

The effective field is obtained from the variation of the total energy:

$$\mathbf{H}_{\text{eff}} = -\frac{1}{\mu_0} \frac{\delta E}{\delta \mathbf{M}}. \tag{9.86}$$

It includes contributions from all micromagnetic energy terms:

- Exchange field
- Anisotropy field
- External field
- Demagnetizing field

Thus, $\mathbf{H}_{\text{eff}}$ encodes all interactions discussed previously.

### 9.8.1 Landau–Lifshitz equation

The precession equation alone conserves energy and cannot describe relaxation toward equilibrium. To include dissipation, Landau and Lifshitz introduced a phenomenological damping term:

$$\frac{d\mathbf{M}}{dt} = -\gamma \mathbf{M} \times \mathbf{H}_{\text{eff}} - \lambda \mathbf{M} \times (\mathbf{M} \times \mathbf{H}_{\text{eff}}), \tag{9.87}$$

where $\lambda$ is a damping parameter.

The second term drives $\mathbf{M}$ toward alignment with $\mathbf{H}_{\text{eff}}$.

### 9.8.2 Gilbert form of damping

A more commonly used form is the **Landau–Lifshitz–Gilbert (LLG) equation**,

$$\frac{d\mathbf{M}}{dt} = -\gamma \mathbf{M} \times \mathbf{H}_{\text{eff}} + \frac{\alpha}{M_s} \mathbf{M} \times \frac{d\mathbf{M}}{dt}, \tag{9.88}$$

where $\alpha$ is the **Gilbert damping constant**.

Rewriting this gives

$$\frac{d\mathbf{M}}{dt} = -\frac{\gamma}{1+\alpha^2} \left[ \mathbf{M} \times \mathbf{H}_{\text{eff}} + \frac{\alpha}{M_s} \mathbf{M} \times (\mathbf{M} \times \mathbf{H}_{\text{eff}}) \right]. \tag{9.89}$$

### Physical interpretation

The LLG equation contains two distinct terms:

- **Precession term** $(-\gamma \mathbf{M} \times \mathbf{H}_{\text{eff}})$
  - causes magnetization to rotate around the field
  - conserves energy
- **Damping term**
  - aligns $\mathbf{M}$ with $\mathbf{H}_{\text{eff}}$
  - dissipates energy

Thus, magnetization follows a **spiral trajectory** toward equilibrium.

## Connection to hysteresis

The LLG equation provides a dynamical basis for hysteresis:

- Domain wall motion is governed by LLG dynamics under pinning forces.
- Spin rotation near saturation corresponds to coherent LLG evolution.
- Energy dissipation (loop area) arises from damping ($\alpha$).

Thus, hysteresis reflects **non-equilibrium solutions** of the LLG equation.

## Characteristic time scale

The precession frequency is

$$\omega = \gamma H_{\text{eff}}. \tag{9.90}$$

Typical values:

- GHz range for laboratory magnetic fields
- ultrafast dynamics in nanomagnets and spintronic devices

## Small-angle dynamics and spin waves

Linearizing the LLG equation around a uniform magnetization direction recovers the spin-wave dispersion derived earlier.

Thus:

- Heisenberg model $\rightarrow$ static exchange
- Spin-wave theory $\rightarrow$ normal modes
- LLG equation $\rightarrow$ full time-dependent dynamics

## Summary

The Landau–Lifshitz–Gilbert equation provides a unified description of magnetization dynamics:

- describes precession and damping of spins
- connects microscopic interactions to macroscopic dynamics

- underlies modern magnetism, including spintronics and magnetic switching

It forms the foundation for understanding dynamic phenomena such as ferromagnetic resonance, domain wall motion, and ultrafast magnetization switching.

## 9.9 Appendix A: Orbital Quenching in Transition Metals

In isolated atoms, the electronic states possess spherical symmetry and are eigenstates of orbital angular momentum. In crystalline solids, however, the orbital contribution to the magnetic moment of most $3d$ transition metals is strongly suppressed. This phenomenon is known as *orbital quenching*. In this appendix, we give a simple demonstration of how this occurs.

### Atomic orbitals and angular momentum

In a central potential, the electron wavefunction separates as

$$\psi(r, \theta, \phi) = R(r) Y_{\ell m}(\theta, \phi), \tag{9.91}$$

where $Y_{\ell m}$ are spherical harmonics. These functions are eigenstates of the angular momentum operator,

$$L_z Y_{\ell m} = m\hbar Y_{\ell m}. \tag{9.92}$$

For $d$ orbitals we have $\ell = 2$ and therefore five degenerate states

$$m = -2, -1, 0, 1, 2. \tag{9.93}$$

Because these states are degenerate, electrons can occupy states with well-defined orbital angular momentum and therefore carry an orbital magnetic moment.

### Phase winding and orbital angular momentum

The spherical harmonics contain an azimuthal phase factor

$$Y_{\ell m}(\theta, \phi) \propto e^{im\phi}. \tag{9.94}$$

This factor means that the complex phase of the wavefunction changes as one moves around the nucleus in the azimuthal direction. If the electron circles the nucleus once,

$$\phi \to \phi + 2\pi, \tag{9.95}$$

the wavefunction transforms as

$$\psi \to e^{i2\pi m} \psi. \tag{9.96}$$

Thus, the phase changes by

$$\Delta\text{phase} = 2\pi m. \tag{9.97}$$

This behavior is called *phase winding*. The wavefunction winds $m$ times around the nucleus when the electron completes one full loop.

The connection to angular momentum follows from

$$L_z = -i\hbar \frac{\partial}{\partial \phi}. \tag{9.98}$$

Acting on the phase factor gives

$$L_z e^{im\phi} = -i\hbar \frac{\partial}{\partial \phi} e^{im\phi} = m\hbar e^{im\phi}. \tag{9.99}$$

Thus, the orbital angular momentum is directly associated with the azimuthal phase winding of the wavefunction.

## Circulating probability current

Phase winding produces a circulating probability current. The quantum probability current density is

$$\mathbf{j} = \frac{\hbar}{m_e} \operatorname{Im}\left(\psi^* \nabla \psi\right). \tag{9.100}$$

For a wavefunction containing the factor $e^{im\phi}$,

$$\nabla \psi \propto \frac{im}{r} \hat{\phi} \psi, \tag{9.101}$$

so that

$$\mathbf{j} \propto m\hat{\phi}. \tag{9.102}$$

Thus, the electron probability flows azimuthally around the nucleus. This circulating current produces an orbital magnetic moment

$$\boldsymbol{\mu}_L = -\mu_B \mathbf{L}. \tag{9.103}$$

## Real $d$ orbitals in solids

In crystalline solids, the five $d$ orbitals are usually expressed as real orbitals

$$d_{xy},\ d_{xz},\ d_{yz},\ d_{x^2-y^2},\ d_{z^2}. \tag{9.104}$$

These orbitals are linear combinations of spherical harmonics. For example

$$d_{x^2-y^2} = \frac{1}{\sqrt{2}} \left( Y_{2,2} + Y_{2,-2} \right), \tag{9.105}$$

$$d_{xy} = \frac{1}{i\sqrt{2}} \left( Y_{2,2} - Y_{2,-2} \right). \tag{9.106}$$

Substituting the phase factors gives

$$Y_{2,2} + Y_{2,-2} \propto e^{i2\phi} + e^{-i2\phi} = 2\cos(2\phi). \tag{9.107}$$

The complex phases cancel, leaving a purely real wavefunction with no azimuthal phase winding.

## Expectation value of angular momentum

Consider the orbital

$$d_{x^2-y^2} = \frac{1}{\sqrt{2}} \left( Y_{2,2} + Y_{2,-2} \right). \tag{9.108}$$

Applying the angular momentum operator,

$$L_z Y_{2,m} = m\hbar Y_{2,m}, \tag{9.109}$$

gives

$$L_z d_{x^2-y^2} = \frac{1}{\sqrt{2}} \left( 2\hbar Y_{2,2} - 2\hbar Y_{2,-2} \right). \tag{9.110}$$

The expectation value becomes

$$\langle L_z \rangle = 0. \tag{9.111}$$

Similarly

$$\langle L_x \rangle = \langle L_y \rangle = 0, \tag{9.112}$$

so that

$$\langle \mathbf{L} \rangle = 0. \tag{9.113}$$

Thus, electrons occupying these real orbitals do not carry orbital angular momentum.

### Role of the crystal field

In transition metal solids, the surrounding ions generate an anisotropic electrostatic potential known as the crystal field. This potential removes the degeneracy of the atomic $d$ levels and selects orbitals that are spatially oriented relative to the ligands.

For example, in an octahedral crystal field

$$t_{2g} = (d_{xy}, d_{xz}, d_{yz}), \qquad e_g = (d_{x^2-y^2}, d_{z^2}). \tag{9.114}$$

Because these orbitals are real spatial orbitals fixed relative to the lattice, the degeneracy required to form complex combinations with phase winding is removed. Consequently, the orbital angular momentum becomes quenched.

For this reason, the magnetic moments of most $3d$ transition metals are well approximated by the *spin-only* expression

$$\mu \approx g\sqrt{S(S+1)}\,\mu_B, \tag{9.115}$$

with $g \approx 2$.

## 9.10 Appendix B: Mermin–Wagner Theorem

The Mermin–Wagner theorem states that continuous symmetries cannot be spontaneously broken at finite temperature in one- or two-dimensional systems with sufficiently short-range interactions. As a consequence, long-range magnetic order is forbidden in strictly one- and two-dimensional systems isotropic Heisenberg magnets at any finite temperature.

This result was first established by N. D. Mermin and H. Wagner (Phys. Rev. Lett. 17, 1133 (1966)).

### Statement of the theorem

Consider a system with a continuous symmetry, such as the rotational symmetry of the Heisenberg Hamiltonian

$$H = -J \sum_{\langle ij \rangle} \mathbf{S}_i \cdot \mathbf{S}_j. \tag{9.116}$$

The Mermin–Wagner theorem states that for systems with dimension

$$d \leq 2 \tag{9.117}$$

and short-range interactions, a spontaneous long-range order associated with the breaking of a continuous symmetry cannot occur at finite temperature. In particular,

- No ferromagnetic or antiferromagnetic long-range order exists in a 1D or 2D isotropic Heisenberg magnet at $T > 0$.

- Long-range order can occur only at $T = 0$.

## Physical origin: low-energy spin waves

The physical origin of the theorem lies in the large number of low-energy long-wavelength fluctuations present in low-dimensional systems.

Consider a ferromagnet with magnetization aligned along the $z$ direction. Low-energy excitations correspond to slowly varying rotations of the spin direction. These excitations are spin waves (magnons).

For a Heisenberg ferromagnet, the spin-wave energy is

$$\epsilon(\mathbf{k}) = Dk^2, \tag{9.118}$$

where $D$ is the spin stiffness.

## Thermal population of spin waves

At finite temperature, the number of thermally excited magnons is

$$n_{\mathbf{k}} = \frac{1}{e^{\beta\epsilon_{\mathbf{k}}} - 1}. \tag{9.119}$$

Each magnon reduces the magnetization by one unit of spin. The reduction in magnetization due to thermal fluctuations is therefore

$$\Delta M \propto \int \frac{d^d k}{(2\pi)^d} \frac{1}{e^{\beta D k^2} - 1}. \tag{9.120}$$

For small $k$, we can approximate

$$n_{\mathbf{k}} \approx \frac{T}{Dk^2}. \tag{9.121}$$

Thus, the magnetization correction behaves as

$$\Delta M \propto \int \frac{d^d k}{k^2}. \tag{9.122}$$

## Infrared divergence in low dimensions

The behavior of this integral depends on the spatial dimension.

**Three dimensions**

$$\Delta M \propto \int_0 dk\, k \tag{9.123}$$

which converges. Therefore, long-range order survives at finite temperature.

**Two dimensions**

$$\Delta M \propto \int_0 \frac{dk}{k}. \tag{9.124}$$

This integral diverges logarithmically as $k \to 0$. Long-wavelength fluctuations destroy the magnetization.

**One dimension**

$$\Delta M \propto \int_0 \frac{dk}{k^2}, \tag{9.125}$$

which diverges even more strongly.

Thus, in $d \leq 2$, the thermal population of long-wavelength spin waves diverges and completely destroys long-range order.

## Consequences

The theorem implies that strictly two-dimensional isotropic Heisenberg magnets cannot exhibit spontaneous magnetic order at finite temperature. However, several mechanisms can stabilize magnetic order in real materials:

- Magnetic anisotropy (breaking continuous symmetry)
- Dipolar interactions
- Interlayer coupling
- Finite sample size

For example, if an easy-axis anisotropy reduces the symmetry from continuous $SU(2)$ to discrete Ising symmetry, long-range order becomes possible even in two dimensions.

## Relation to two-dimensional magnetism

The Mermin–Wagner theorem plays an important role in modern condensed matter physics, particularly in the study of two-dimensional materials. In systems such as monolayer magnetic crystals or ultra-thin magnetic films, long-range order can occur only when anisotropy or spin–orbit coupling breaks the continuous rotational symmetry. This explains why magnetic ordering in atomically thin materials such as $CrI_3$ or $Fe_3GeTe_2$ relies on strong magnetic anisotropy.

# Chapter 10

# Boltzmann Transport Equations

## 10.1 Introduction

### Distribution Function and Transport

Transport refers to the flow of currents in response to applied fields. These include:

- Electrical current $j$
- Thermal current $j_Q$

The driving forces are:

- Electric field $E$
- Temperature gradient $\nabla T$

We assume the system is always close to equilibrium, so responses are linear. The central object is the distribution function:

$$f(x, k, t) \tag{10.1}$$

which gives the probability of finding an electron near $(x, k)$ at time $t$.

At equilibrium:

$$f_0(\varepsilon) = \frac{1}{e^{\beta(\varepsilon-\mu)} + 1} \tag{10.2}$$

A key identity:

$$\frac{df_0}{d\varepsilon} = -\frac{1}{k_B T} \frac{e^{\beta(\varepsilon-\mu)}}{(e^{\beta(\varepsilon-\mu)} + 1)^2} \tag{10.3}$$

At low temperature:

$$-\frac{df_0}{d\varepsilon} \to \delta(\varepsilon - E_F) \tag{10.4}$$

Thus, transport is governed by states near $E_F$. More precisely, transport is governed by states within an energy window of order $k_B T$ around $E_F$.

### 10.1.1 Semiclassical Dynamics

Electron motion in a band:

$$\varepsilon = \varepsilon(k) \tag{10.5}$$

Velocity:

$$v_k = \frac{1}{\hbar}\frac{d\varepsilon}{dk} \tag{10.6}$$

Equation of motion:

$$\hbar\frac{dk}{dt} = F \tag{10.7}$$

For electric field:

$$F = -eE \tag{10.8}$$

**Effective Mass Tensor** In general band structures, the response to forces is not isotropic. The effective mass tensor governs the acceleration:

$$M_{ij}^{-1} = \frac{1}{\hbar^2}\frac{\partial^2\varepsilon}{\partial k_i \partial k_j}. \tag{10.9}$$

This generalizes the concept of mass to anisotropic bands and becomes essential for describing transport in real crystals. This means the acceleration of an electron **a** and the applied force **F** are generally not parallel. This is critical for understanding transport in low-symmetry crystals.

## 10.2 Phase Space and Boltzmann Equation

### What leads to non-equilibrium distribution?

The distribution function $f(\boldsymbol{r}, \boldsymbol{k}, t)$ deviates from the equilibrium distribution $f_0$ because the system is subjected to **external perturbations** that "push" particles out of their statistically most probable, uniform state.

In equilibrium, the forces acting on the system are perfectly balanced, the chemical potential and temperature are uniform, and scattering events exactly cancel each other out. When you apply an external influence, this balance is broken.

The deviation occurs due to the following factors:

### External Driving Forces (Drift)

The Boltzmann Transport Equation (BTE) contains terms that represent the motion of particles through phase space due to external fields. These are the "driving" terms:

- **Electric Fields ($\boldsymbol{E}$):** An electric field exerts a force on charged particles (electrons), accelerating them. This changes their momentum ($\boldsymbol{k}$), causing the distribution to shift in momentum space.
- **Thermal Gradients ($\nabla T$):** If one end of a sample is hotter than the other, particles on the hot side have higher average energy. This creates a natural tendency for particles to diffuse toward the colder region, shifting the distribution in both position ($\boldsymbol{r}$) and momentum ($\boldsymbol{k}$) space.
- **Chemical Potential Gradients ($\nabla \mu$):** Differences in particle concentration (or electrochemical potential) drive particles to flow from regions of high concentration to low concentration.

These terms act as a "wind" that constantly drags the distribution function away from the symmetric, stationary equilibrium state.

### The Competition: Drift vs. Scattering

The reason the distribution function does not grow infinitely away from equilibrium is the **collision integral** ($I_{\boldsymbol{k}}\{f\}$).

- **Scattering as a Restoring Force:** Collisions (with impurities, phonons, or other electrons) act to randomize the momentum of the particles. Every time an electron scatters, it "forgets" some of the acceleration it received from the external field.
- **Steady State:** In a steady-state system, the distribution function stops changing ($\frac{\partial f}{\partial t} = 0$). This happens because the **drift** caused by external fields is exactly balanced by the **redistribution** caused by collisions.

### Summary

You can think of the equilibrium distribution ($f_0$) as a **calm, still pond**.

- **External fields** act like a paddle, creating a current in that pond (the drift).
- **Collisions** act like the viscosity of the water, resisting the current and trying to bring the pond back to a still state.

## 10.2.1 Evolution of distribution function

The deviation ($\delta f = f - f_0$) is the net result of this tug-of-war. It is the "ripple" in the distribution function that allows for the transport of charge and heat, which we then measure as electrical current or heat flow.

The distribution evolves in the phase space $(x, k)$. Total derivative:

$$\frac{df(x,k,t)}{dt} = \frac{\partial f}{\partial t} + \frac{dx}{dt}\frac{\partial f}{\partial x} + \frac{dk}{dt}\frac{\partial f}{\partial k} = \frac{\partial f}{\partial t} + v_k\frac{\partial f}{\partial x} + \frac{F}{\hbar}\frac{\partial f}{\partial k} \tag{10.10}$$

In the absence of collisions:

$$\frac{df}{dt} = 0 \tag{10.11}$$

Thus:

$$\frac{\partial f}{\partial t} + v_k\frac{\partial f}{\partial x} + \frac{F}{\hbar}\frac{\partial f}{\partial k} = 0 \tag{10.12}$$

This expresses conservation of particles in phase space. This result follows from the continuity equation in phase space:

$$\frac{\partial f}{\partial t} + \nabla \cdot (\mathbf{u}f) = 0 \tag{10.13}$$

where $\mathbf{u} = (\dot{x}, \dot{k})$ and $\nabla = (\frac{\partial}{\partial x}, \frac{\partial}{\partial k})$. In 3-D, these are six-dimensional vectors. Because phase-space flow is incompressible ($\nabla \cdot u = 0$), the distribution function is conserved along trajectories. This is a statement of Liouville's theorem and forms the foundation of the Boltzmann equation.

$$\frac{\partial f}{\partial t} + \mathbf{u} \cdot \nabla f = 0 \tag{10.14}$$

## 10.3 Inclusion of Collisions

In reality, collisions modify the distribution function. We therefore write the full Boltzmann equation as:

$$\frac{\partial f}{\partial t} + v_k\frac{\partial f}{\partial x} + \frac{F}{\hbar}\frac{\partial f}{\partial k} = \left(\frac{\partial f}{\partial t}\right)_{\text{coll}} \equiv I_k\{f\} \tag{10.15}$$

The quantity $I_k\{f\}$ is called the **collision integral**. It represents the rate of change of the distribution function at momentum $k$ due to scattering processes.

**Physical meaning:**

$$I_k\{f\} = (\text{rate of scattering into state } k) - (\text{rate of scattering out of state } k) \tag{10.16}$$

Thus, it describes the net flow of probability in momentum space.

## Microscopic Collision Integral

The microscopic form of the collision integral is:

$$I_k\{f\} = \sum_{k'} [W_{k'\to k} f(k')(1 - f(k)) - W_{k\to k'} f(k)(1 - f(k'))] \tag{10.17}$$

where $W_{k\to k'}$ is the transition rate from $k$ to $k'$.

**Interpretation of terms:**

- $W_{k'\to k} f(k')(1 - f(k))$ : scattering into state $k$
- $W_{k\to k'} f(k)(1 - f(k'))$ : scattering out of state $k$
- $(1 - f)$ factors encode Pauli blocking.

## Origin of Transition Rates

The transition rates are determined by microscopic physics, typically via Fermi's Golden Rule:

$$W_{k\to k'} \propto |\langle k'|U|k\rangle|^2 \delta(\varepsilon_k - \varepsilon_{k'}) \tag{10.18}$$

where $U$ is the scattering potential (e.g., impurities, phonons).

Thus, $I_k\{f\}$ contains the full microscopic information about scattering.

## Functional Nature of $I_k\{f\}$

The notation $\{f\}$ emphasizes that:

$$I_k\{f\} \text{ depends on } f(k) \text{ and also on } f(k') \text{ for all } k'. \tag{10.19}$$

Hence, it is not a simple function but a **functional** of the entire distribution.

## General Properties

**1. Particle conservation:**

$$\int dk\, I_k\{f\} = 0 \tag{10.20}$$

Collisions do not change the total number of particles.

**2. Collisional invariants:**

For any conserved quantity $\mathcal{F}(k)$,

$$\int dk\, \mathcal{F}(k)\, I_k\{f\} = 0 \tag{10.21}$$

Examples:

- $\mathcal{F} = 1$ : particle number
- $\mathcal{F} = \varepsilon(k)$ : energy

**3. Equilibrium condition:**

$$I_k\{f_0\} = 0 \tag{10.22}$$

The equilibrium distribution is a fixed point of the collision dynamics.

## Physical Picture

The collision integral describes how scattering redistributes electrons:

- electrons arrive into $k$ from other states
- electrons leave $k$ to other states

Thus, transport can be viewed as a competition between:

- drift in phase space (left-hand side)
- redistribution via collisions (right-hand side)

## Why We Approximate $I_k\{f\}$

The exact collision integral is:

- nonlinear in $f$
- coupled across all $k$
- difficult to solve analytically

Therefore, we replace it with a simpler form in the relaxation time approximation.

## 10.4 Local Equilibrium and Linearization

Collisions act on short time scales and tend to establish a **local equilibrium** distribution:

$$f_0(x,k) = \frac{1}{e^{(\varepsilon(k)-\mu(x))/k_B T(x)} + 1} \tag{10.23}$$

Here, both the chemical potential $\mu(x)$ and temperature $T(x)$ are allowed to vary slowly in space.

However, $f_0(x,k)$ is *not* an exact solution of the Boltzmann equation because spatial gradients generate drift in phase space.

We therefore write:

$$f(x,k,t) = f_0(x,k) + \delta f(x,k,t) \tag{10.24}$$

where $\delta f$ is a small deviation.

### Derivatives of the Local Equilibrium Distribution

We now compute the derivatives of $f_0$, which are needed in the Boltzmann equation.

Since $f_0 = f_0(\varepsilon, \mu(x), T(x))$, we compute its total differential:

$$df_0 = \frac{\partial f_0}{\partial \varepsilon} d\varepsilon + \frac{\partial f_0}{\partial \mu} d\mu + \frac{\partial f_0}{\partial T} dT \tag{10.25}$$

### Useful identities

From the definition of the Fermi function:

$$\frac{\partial f_0}{\partial \mu} = -\frac{\partial f_0}{\partial \varepsilon} \tag{10.26}$$

$$\frac{\partial f_0}{\partial T} = \frac{\varepsilon - \mu}{T} \frac{\partial f_0}{\partial \varepsilon} \tag{10.27}$$

### Spatial derivative of $f_0$

Using

$$d\mu = \frac{\partial \mu}{\partial x} dx, \quad dT = \frac{\partial T}{\partial x} dx, \tag{10.28}$$

we obtain:

$$\frac{\partial f_0}{\partial x} = \frac{\partial f_0}{\partial \mu} \frac{\partial \mu}{\partial x} + \frac{\partial f_0}{\partial T} \frac{\partial T}{\partial x} \tag{10.29}$$

Substituting:

$$\frac{\partial f_0}{\partial x} = \left(-\frac{\partial f_0}{\partial \varepsilon}\right)\left[\frac{\partial \mu}{\partial x} + \frac{\varepsilon - \mu}{T}\frac{\partial T}{\partial x}\right] \tag{10.30}$$

## Momentum derivative of $f_0$

Since $f_0$ depends on $k$ only through $\varepsilon(k)$:

$$\frac{\partial f_0}{\partial k} = \frac{df_0}{d\varepsilon}\frac{d\varepsilon}{dk} \tag{10.31}$$

Using

$$\frac{d\varepsilon}{dk} = \hbar v_k \tag{10.32}$$

we obtain:

$$\frac{\partial f_0}{\partial k} = \hbar v_k \frac{\partial f_0}{\partial \varepsilon} \tag{10.33}$$

## Substitution into the Boltzmann Equation

We now substitute:

$$f = f_0 + \delta f \tag{10.34}$$

into:

$$\frac{\partial f}{\partial t} + v_k \frac{\partial f}{\partial x} + \frac{F}{\hbar}\frac{\partial f}{\partial k} = I_k\{f\} \tag{10.35}$$

to get:

$$\frac{\partial \delta f}{\partial t} + v_k \frac{\partial \delta f}{\partial x} + \frac{F}{\hbar}\frac{\partial \delta f}{\partial k} + v_k \frac{\partial f_0}{\partial x} + \frac{F}{\hbar}\frac{\partial f_0}{\partial k} = I_k\{f_0 + \delta f\} \tag{10.36}$$

## Evaluate the driving terms

The two driving terms are (see Eqn. 10.30 and Eqn. 10.33):

$$v_k \frac{\partial f_0}{\partial x} = v_k\left(-\frac{\partial f_0}{\partial \varepsilon}\right)\left[\frac{\partial \mu}{\partial x} + \frac{\varepsilon - \mu}{T}\frac{\partial T}{\partial x}\right] \tag{10.37}$$

$$\frac{F}{\hbar}\frac{\partial f_0}{\partial k} = F v_k \frac{\partial f_0}{\partial \varepsilon} \tag{10.38}$$

With $F = -eE$, this becomes:

$$\frac{F}{\hbar}\frac{\partial f_0}{\partial k} = -eEv_k\frac{\partial f_0}{\partial \varepsilon} \tag{10.39}$$

The net driving term is:

$$v_k\frac{\partial f_0}{\partial x} + \frac{F}{\hbar}\frac{\partial f_0}{\partial k} = v_k\left(-\frac{\partial f_0}{\partial \varepsilon}\right)\left[eE + \frac{\partial \mu}{\partial x} + \frac{\varepsilon-\mu}{T}\frac{\partial T}{\partial x}\right] \tag{10.40}$$

**Electrochemical field** It is useful to define an effective field:

$$E^* = E + \frac{1}{e}\frac{\partial \mu}{\partial x}. \tag{10.41}$$

Then the driving term becomes:

$$v_k\left[eE^* + \frac{\varepsilon-\mu}{T}\frac{\partial T}{\partial x}\right]\left(-\frac{\partial f_0}{\partial \varepsilon}\right). \tag{10.42}$$

This shows that transport is driven by gradients of the electrochemical potential. Combining all the terms, we get the final **Linearized Boltzmann equation (LBE)**:

$$\frac{\partial \delta f}{\partial t} + v_k\frac{\partial \delta f}{\partial x} + v_k\left[eE^* + \frac{\varepsilon-\mu}{T}\frac{\partial T}{\partial x}\right]\left(-\frac{\partial f_0}{\partial \varepsilon}\right) = I_k\{\delta f\} \tag{10.43}$$

Note that we have used

$$I_k\{f_0 + \delta f\} \approx I_k\{\delta f\} \tag{10.44}$$

because:

$$I_k\{f_0\} = 0 \tag{10.45}$$

and we keep only first-order terms in $\delta f$. Also, all terms that are products of two small quantities (like $F \cdot \delta f$) are neglected. This is the **Linear Response** approximation.

## Physical interpretation

The equation has three components:

- Drift of $\delta f$ in phase space
- Driving terms from:
  - electric field $E$
  - temperature gradient $\nabla T$
- Relaxation via collisions (right-hand side)

Thus, $\delta f$ is generated by external fields and opposed by scattering. In other words:

- external fields distort $f$
- collisions restore equilibrium
- steady state = balance of the two

## 10.5 Relaxation Time Approximation

The exact form of $I_k\{\delta f\}$ is unknown. To make progress, we use an approach called **phenomenological closure**. We replace the exact collision integral by a simpler phenomenological model, in this case, a relaxation time approximation. The microscopic scattering is not explicitly computed. Explicitly, we replace the collision integral by:

$$I_k\{\delta f\} = -\frac{f - f_0}{\tau} \tag{10.46}$$

This assumes that in the absence of any fields or temperature and electrochemical potential gradients, the Boltzmann equation becomes:

$$\delta f(t) = \delta f(0) e^{-t/\tau} \tag{10.47}$$

The distribution thereby relaxes to the equilibrium one on the scale of $\tau$.

**Dominant scattering mechanisms** The relaxation time depends on the microscopic scattering processes:

- Impurity scattering: $\tau \sim$ const (dominates at low temperature)
- Phonon scattering: $\tau^{-1} \propto T$ (high temperature regime)
- Electron-electron scattering: $\tau^{-1} \propto T^2$ (Fermi liquid behavior)

The net scattering time is determined by Matthiessen's Rule:

$$\frac{1}{\tau_{total}} = \frac{1}{\tau_{imp}} + \frac{1}{\tau_{ph}} + \frac{1}{\tau_{ee}}$$

## 10.6 Electrical and Thermoelectric Transport

This section details the derivation of transport properties by solving the Boltzmann equation in the presence of an electric field $E$ and a temperature gradient $\nabla T$.

### 10.6.1 Solution for $\delta f$

The Linear Boltzmann Equation (LBE) under the relaxation time approximation

$$\frac{\partial \delta f}{\partial t} + v_k \frac{\partial \delta f}{\partial x} + v_k \left[ eE^* + \frac{\varepsilon - \mu}{T} \frac{\partial T}{\partial x} \right] \left( -\frac{\partial f_0}{\partial \varepsilon} \right) = I_k\{\delta f\} = -\frac{f - f_0}{\tau} \tag{10.48}$$

is used to find the deviation from equilibrium, $\delta f = f - f_0$.

Assuming a steady state ($\frac{\partial \delta f}{\partial t} = 0$) and spatial uniformity of $\delta f$ ($\frac{\partial \delta f}{\partial x} = 0$), the equation simplifies to:

$$v_k \left[ eE^* + \frac{\epsilon - \mu}{T} \frac{\partial T}{\partial x} \right] \left( -\frac{\partial f_0}{\partial \epsilon} \right) = -\frac{\delta f}{\tau} \tag{10.49}$$

Where $E^*$ is the **electrochemical field**, defined as $E^* = E + \frac{1}{e}\frac{\partial \mu}{\partial x}$. Solving for $\delta f$ gives:

$$\delta f = \tau v_k \left( -\frac{\partial f_0}{\partial \epsilon} \right) \left[ eE^* + \frac{\epsilon - \mu}{T} \frac{\partial T}{\partial x} \right] \tag{10.50}$$

### 10.6.2 Electrical Current

The electrical current density $j$ is defined by the integral of the velocity over the occupied states (in 1D, for simplicity):

$$j = -e \int \frac{dk}{2\pi} v_k f(k) \tag{10.51}$$

Since the equilibrium distribution $f_0$ carries no net current, the expression reduces to the contribution from $\delta f$:

$$j = -e \int \frac{dk}{2\pi} v_k \delta f \tag{10.52}$$

Substituting the expression for $\delta f$ derived above yields:

$$j = e \int \frac{dk}{2\pi} v_k^2 \tau \left( -\frac{\partial f_0}{\partial \epsilon} \right) \left[ eE^* + \frac{\epsilon - \mu}{T} \frac{\partial T}{\partial x} \right] \tag{10.53}$$

### Separation of Contributions and General Transport Equation

The total current $j$ is a sum of the response to the electrochemical field and the response to the temperature gradient:

$$j = j_{E^*} + j_T \tag{10.54}$$

We define the transport coefficients as:

- **Electrical Conductivity ($\sigma$)**:

$$\sigma = e^2 \int \frac{dk}{2\pi} v_k^2 \tau \left( -\frac{\partial f_0}{\partial \epsilon} \right) \tag{10.55}$$

- **Thermoelectric Response ($\alpha$)**:

$$\alpha = \frac{e}{T} \int \frac{dk}{2\pi} v_k^2 \tau (\epsilon - \mu) \left( -\frac{\partial f_0}{\partial \epsilon} \right) \tag{10.56}$$

The **General Transport Equation** is written as:

$$j = \sigma E^* - \alpha \frac{\partial T}{\partial x} \tag{10.57}$$

## Energy Representation and Key Results

We define the **transport distribution function** $\Sigma(\epsilon)$ in 3-D (this is a second-rank tensor):

$$\Sigma(\varepsilon) = \int \frac{d\mathbf{k}}{4\pi^3} \mathbf{v_k} \mathbf{v_k} \, \tau(\varepsilon) \, \delta(\varepsilon - \varepsilon_{\mathbf{k}}) \tag{10.58}$$

**Physical interpretation** The transport distribution function $\Sigma(\varepsilon)$ encodes:

- band structure via $\mathbf{v_k}$
- scattering via $\tau(\varepsilon)$
- density of states via phase-space integration

All transport coefficients are determined by the behavior of $\Sigma(\varepsilon)$ near the Fermi energy:

$$\sigma = e^2 \int d\epsilon \Sigma(\epsilon) \left( -\frac{\partial f_0}{\partial \epsilon} \right) \tag{10.59}$$

$$\alpha = \frac{e}{T} \int d\epsilon \Sigma(\epsilon)(\epsilon - \mu) \left( -\frac{\partial f_0}{\partial \epsilon} \right) \tag{10.60}$$

The **Seebeck Coefficient** $S$ is defined under open-circuit conditions ($j = 0$) as $S = \alpha/\sigma$. Explicitly:

$$S = \frac{1}{eT} \frac{\int d\varepsilon \, \Sigma(\varepsilon)(\varepsilon - \mu) \left( -\frac{\partial f_0}{\partial \varepsilon} \right)}{\int d\varepsilon \, \Sigma(\varepsilon) \left( -\frac{\partial f_0}{\partial \varepsilon} \right)} \tag{10.61}$$

In the low-temperature limit (using Sommerfeld expansion), this yields the **Mott Formula**:

$$S = \frac{\pi^2 k_B^2 T}{3e} \frac{d}{d\epsilon} \ln \Sigma(\epsilon) \Big|_{\epsilon = E_F} \tag{10.62}$$

The relaxation time $\tau(\epsilon)$ is often energy dependent (e.g., $\tau \propto \epsilon^{3/2}$ for ionized impurity scattering). This energy dependence is what ultimately drives a non-zero Seebeck coefficient in the Mott Formula.

- **The Seebeck Coefficient ($S$) as a Probe of Asymmetry:** The Seebeck coefficient is a direct measure of the **particle-hole asymmetry** of the transport distribution function $\Sigma(\epsilon)$ near the Fermi level. Physically, a temperature gradient drives both high-energy "hot" carriers and low-energy "cold" carriers in the same direction.
- **Cancellation in Symmetric Bands:** If the band structure and scattering mechanisms are perfectly symmetric around the Fermi energy, the electron-like contributions from states above $\mu$ and the hole-like contributions from states below $\mu$ generate equal and opposite currents that exactly cancel. In such a case, the net thermal voltage is zero ($S = 0$).
- **The Mott Insight:** As captured by the Mott formula, $S \propto \frac{d}{d\epsilon} \ln \Sigma(\epsilon)|_{E_F}$, a non-zero Seebeck effect only arises when there is a gradient in the material's ability to transport charge across the Fermi surface. This makes $S$ an incredibly sensitive tool for detecting subtle changes in the density of states or energy-dependent scattering rates that conductivity ($\sigma$) alone might mask.

Finally, the **Wiedemann-Franz Law** relates thermal and electrical conductivity:

$$\frac{\kappa}{\sigma T} = \frac{\pi^2}{3} \left( \frac{k_B}{e} \right)^2 \tag{10.63}$$

This reflects that the same quasiparticles carry both heat and charge.

## 10.7 Magnetic Field and Hall Conductivity

We now include a magnetic field within the semiclassical Boltzmann framework. We begin with the general Boltzmann equation in phase space:

$$\frac{\partial f}{\partial t} + \frac{d\mathbf{r}}{dt} \cdot \nabla_{\mathbf{r}} f + \frac{d\mathbf{k}}{dt} \cdot \nabla_{\mathbf{k}} f = I_k\{f\} \tag{10.64}$$

The semiclassical equations of motion give:

$$\frac{d\mathbf{r}}{dt} = \mathbf{v}_k, \qquad \frac{d\mathbf{k}}{dt} = -\frac{e}{\hbar} \left( \mathbf{E} + \mathbf{v}_k \times \mathbf{B} \right). \tag{10.65}$$

Substituting into the Boltzmann equation:

$$\frac{\partial f}{\partial t} + \mathbf{v}_k \cdot \nabla_{\mathbf{r}} f - \frac{e}{\hbar} \left( \mathbf{E} + \mathbf{v}_k \times \mathbf{B} \right) \cdot \nabla_{\mathbf{k}} f = I_k\{f\} \tag{10.66}$$

## Steady-State and Uniform Limit

For transport, we assume:

$$\frac{\partial f}{\partial t} = 0, \qquad \nabla_{\mathbf{r}} f = 0, \tag{10.67}$$

which gives:

$$-\frac{e}{\hbar}\left(\mathbf{E} + \mathbf{v}_k \times \mathbf{B}\right) \cdot \nabla_{\mathbf{k}} f = I_k\{f\}. \tag{10.68}$$

Using the relaxation time approximation,

$$I_k\{f\} = -\frac{f - f_0}{\tau}, \tag{10.69}$$

we obtain:

$$\boxed{-\frac{e}{\hbar}\left(\mathbf{E} + \mathbf{v}_k \times \mathbf{B}\right) \cdot \nabla_{\mathbf{k}} f = -\frac{f - f_0}{\tau}} \tag{10.70}$$

## Systematic Expansion in Fields

We expand the distribution function around the equilibrium:

$$f = f_0 + \delta f, \qquad \delta f = \delta f^{(0)} + \delta f^{(1)} + \cdots, \tag{10.71}$$

where:

- $\delta f^{(0)} \sim E$ (longitudinal response),
- $\delta f^{(1)} \sim EB$ (Hall response).

Substituting into the Boltzmann equation:

$$-\frac{e}{\hbar}\left(\mathbf{E} + \mathbf{v}_k \times \mathbf{B}\right) \cdot \nabla_{\mathbf{k}}(f_0 + \delta f) = -\frac{\delta f}{\tau}. \tag{10.72}$$

Expanding:

$$-\frac{e}{\hbar}\left(\mathbf{E} + \mathbf{v}_k \times \mathbf{B}\right) \cdot \nabla_{\mathbf{k}} f_0 - \frac{e}{\hbar}\left(\mathbf{E} + \mathbf{v}_k \times \mathbf{B}\right) \cdot \nabla_{\mathbf{k}} \delta f = -\frac{\delta f}{\tau}. \tag{10.73}$$

## Zeroth-Order Solution

At leading order, we retain terms linear in $\mathbf{E}$:

$$-\frac{e}{\hbar}\mathbf{E}\cdot\nabla_{\mathbf{k}}f_0 = -\frac{\delta f^{(0)}}{\tau}. \tag{10.74}$$

Using:

$$\nabla_{\mathbf{k}}f_0 = \hbar\mathbf{v}_k\frac{\partial f_0}{\partial\varepsilon}, \tag{10.75}$$

we obtain:

$$\boxed{\delta f^{(0)} = e\tau\left(\frac{\partial f_0}{\partial\varepsilon}\right)\mathbf{v}_k\cdot\mathbf{E}.} \tag{10.76}$$

The magnetic field does not contribute at this order, since:

$$(\mathbf{v}_k\times\mathbf{B})\cdot\nabla_{\mathbf{k}}f_0 = \hbar(\mathbf{v}_k\times\mathbf{B})\cdot\mathbf{v}_k\frac{\partial f_0}{\partial\varepsilon} = 0. \tag{10.77}$$

## First-Order Correction (Hall Term)

At the next order, we retain terms proportional to $EB$. The Boltzmann equation gives:

$$-\frac{e}{\hbar}\mathbf{E}\cdot\nabla_{\mathbf{k}}\delta f^{(0)} - \frac{e}{\hbar}(\mathbf{v}_k\times\mathbf{B})\cdot\nabla_{\mathbf{k}}f_0 - \frac{e}{\hbar}(\mathbf{v}_k\times\mathbf{B})\cdot\nabla_{\mathbf{k}}\delta f^{(0)} = -\frac{\delta f^{(1)}}{\tau}. \tag{10.78}$$

The second term vanishes identically, while the first term contributes at order $E^2$ and is neglected in linear response. Thus:

$$\boxed{\delta f^{(1)} = \frac{e\tau}{\hbar}(\mathbf{v}_k\times\mathbf{B})\cdot\nabla_{\mathbf{k}}\delta f^{(0)}.} \tag{10.79}$$

## Evaluating $\nabla_{\mathbf{k}}\delta f^{(0)}$

From Eqn 10.76, we compute:

$$\nabla_{\mathbf{k}}\delta f^{(0)} = e\tau\left[(\nabla_{\mathbf{k}}(\mathbf{v}_k\cdot\mathbf{E}))\left(-\frac{\partial f_0}{\partial\varepsilon}\right) + (\mathbf{v}_k\cdot\mathbf{E})\nabla_{\mathbf{k}}\left(-\frac{\partial f_0}{\partial\varepsilon}\right)\right]. \tag{10.80}$$

The second term vanishes upon integration by symmetry. Thus:

$$\nabla_{\mathbf{k}}\delta f^{(0)} \approx e\tau\left(-\frac{\partial f_0}{\partial\varepsilon}\right)\nabla_{\mathbf{k}}(\mathbf{v}_k\cdot\mathbf{E}). \tag{10.81}$$

For a parabolic band:

$$\mathbf{v}_k = \frac{\hbar \mathbf{k}}{m} \quad \Rightarrow \quad \nabla_{\mathbf{k}}(\mathbf{v}_k \cdot \mathbf{E}) = \frac{\hbar}{m}\mathbf{E}. \tag{10.82}$$

Thus:

$$\boxed{\nabla_{\mathbf{k}} \delta f^{(0)} = e\tau \frac{\hbar}{m}\left(-\frac{\partial f_0}{\partial \varepsilon}\right)\mathbf{E}.} \tag{10.83}$$

## Hall Correction to Distribution

Substituting into Eqn. 10.79:

$$\boxed{\delta f^{(1)} = e^2\tau^2 \frac{1}{m}\left(-\frac{\partial f_0}{\partial \varepsilon}\right)(\mathbf{v}_k \times \mathbf{B}) \cdot \mathbf{E}.} \tag{10.84}$$

## Hall Current

$$\mathbf{j}^{(H)} = -e \int \frac{d^d k}{(2\pi)^d} \mathbf{v}_k \delta f^{(1)}, \tag{10.85}$$

$$\mathbf{j}^{(H)} = -e^3\tau^2 \frac{1}{m} \int \frac{d^d k}{(2\pi)^d} \mathbf{v}_k \left(-\frac{\partial f_0}{\partial \varepsilon}\right)(\mathbf{v}_k \times \mathbf{B}) \cdot \mathbf{E}. \tag{10.86}$$

Using:

$$(\mathbf{v} \times \mathbf{B}) \cdot \mathbf{E} = \mathbf{v} \cdot (\mathbf{E} \times \mathbf{B}), \tag{10.87}$$

and isotropy:

$$\langle v_i v_j \rangle = \frac{v_F^2}{d}\delta_{ij}, \tag{10.88}$$

we obtain:

$$\boxed{\mathbf{j}^{(H)} = \sigma_0(\omega_c\tau)(\mathbf{E} \times \hat{z}).} \tag{10.89}$$

with $\sigma_0 = ne^2\tau/m$.

### 10.7.1 Hall Conductivity

The conductivity tensor is $\boldsymbol{\sigma} = \boldsymbol{\rho}^{-1}$.:

$$\boldsymbol{\sigma} = \frac{\sigma_0}{1 + (\omega_c\tau)^2}\begin{pmatrix} 1 & \omega_c\tau \\ -\omega_c\tau & 1 \end{pmatrix}$$

where $\omega_c = eB/m$ is the cyclotron frequency.

The Hall coefficient is:

$$\boxed{R_H = \frac{1}{ne}.} \tag{10.90}$$

### 10.7.2 Physical Picture

- The electric field distorts the Fermi surface.
- The magnetic field rotates this distortion in momentum space.
- The resulting transverse current gives rise to the Hall effect.
- The response appears at order $EB$.

## 10.8 Berry Curvature and Anomalous Transport

In crystals with broken time-reversal or inversion symmetry, the semiclassical equations of motion acquire an additional term due to Berry curvature. The modified equations of motion are:

$$\hbar \frac{d\mathbf{r}}{dt} = \frac{\partial \varepsilon}{\partial \mathbf{k}} + e\frac{d\mathbf{k}}{dt} \times \mathbf{\Omega}(\mathbf{k}) \tag{10.91}$$

$$\hbar \frac{d\mathbf{k}}{dt} = -e\frac{\partial \phi}{\partial \mathbf{r}} + e\frac{d\mathbf{r}}{dt} \times \mathbf{B} \tag{10.92}$$

where, $\mathbf{\Omega}(\mathbf{k})$ is the Berry curvature defined as:

$$\mathbf{\Omega}_n(\mathbf{k}) = \nabla_k \times \mathbf{A}_n(\mathbf{k})$$

with the Berry connection:

$$\mathbf{A}_n(\mathbf{k}) = i\langle u_{n\mathbf{k}} | \nabla_k | u_{n\mathbf{k}} \rangle$$

Here $|u_{n\mathbf{k}}\rangle$ is the periodic part of the Bloch wavefunction.

Symmetries constrain the Berry curvature: $\mathbf{\Omega}(\mathbf{k})$ is an odd function of $\mathbf{k}$ under time-reversal symmetry (TRS) and an even function under inversion symmetry (IS). For $\mathbf{\Omega}(\mathbf{k})$ to contribute to net transport, at least one of these symmetries must be broken.

The additional term $\dot{\mathbf{k}} \times \mathbf{\Omega}$ in Eqn 10.91 is an 'anomalous' velocity–it is the velocity contribution that does not depend on the band's slope, but rather on the geometric phase accumulated by the electron wavepacket.

Thus, Berry curvature acts as an effective magnetic field in momentum space, functioning as a "momentum-space monopole":

- It modifies electron trajectories by exerting a pseudo-Lorentz force.
- It leads to transverse motion even without an external magnetic field. In other words, it generates an *anomalous velocity*.

### 10.8.1 Intrinsic Anomalous Hall Effect

The intrinsic anomalous Hall current results from the band structure itself:

$$\mathbf{j}_{\text{AH}} = -e \int \frac{d^d k}{(2\pi)^d} \left( \frac{e}{\hbar} \mathbf{E} \times \boldsymbol{\Omega}(\mathbf{k}) \right) f_0(\varepsilon_k)$$

$$\mathbf{j}_{\text{AH}} = \frac{e^2}{\hbar} \mathbf{E} \times \int \frac{d^d k}{(2\pi)^d} \boldsymbol{\Omega}(\mathbf{k}) f_0(\varepsilon_k)$$

Thus, the Hall conductivity is:

$$\sigma_{xy} = \frac{e^2}{\hbar} \int \frac{d^d k}{(2\pi)^d} \Omega_z(\mathbf{k}) f_0(\varepsilon_k)$$

Note that real materials may also include extrinsic contributions such as skew scattering or side jump.

### 10.8.2 Key Insight

- Hall response can arise without a magnetic field.
- It is an intrinsic property of the band structure.
- It depends on the Berry curvature of occupied states.

### 10.8.3 Topological Interpretation

For 2D insulators, the Hall conductivity is related to the global topological properties of the band:

$$\sigma_{xy} = \frac{e^2}{h} C$$

where $C$ is the Chern number:

$$C = \frac{1}{2\pi} \int_{\text{BZ}} d^2 k \, \Omega_z(\mathbf{k})$$

This quantization, representing the integral of the Berry curvature over the entire Brillouin zone, underlies the quantum Hall effect.

# 10.9 Hydrodynamic Transport Regime

## 10.9.1 Transport Regimes

Electron transport can be classified based on the hierarchy of scattering length scales:

- **Ballistic regime:** $l \gg L$.
- **Diffusive regime:** $l \ll L$.
- **Hydrodynamic regime:** $l_{ee} \ll W \ll l_{\text{imp}}, L$.

where $l$ is the mean free path, $l_{ee}$ is the electron-electron scattering length, $l_{\text{imp}}$ is the impurity scattering length, and $W$ is the sample width.

## 10.9.2 Physical Picture

In the hydrodynamic regime:

- Electron-electron ($e$-$e$) scattering is very strong.
- Momentum is conserved locally because $e$-$e$ collisions do not relax total momentum.
- Electrons behave like a viscous fluid where "resistance" arises from internal friction and boundary scattering.

Thus, transport is governed by collective flow rather than independent single-particle motion.

## 10.9.3 Boltzmann Equation Perspective

The collision integral separates into momentum-conserving and momentum-relaxing parts:

$$I = I_{ee} + I_{\text{imp}}$$

Electron-electron collisions:

- Conserve total momentum.
- Rapidly establish a moving local equilibrium.

Thus the distribution takes the form:

$$f(\mathbf{r}, \mathbf{k}) = f_0 \left( \varepsilon_k - \mathbf{u}(\mathbf{r}) \cdot \mathbf{k} \right)$$

where $\mathbf{u}(\mathbf{r})$ is the local drift velocity.

## 10.10 Hydrodynamic Equations

Taking moments of the Boltzmann equation yields fluid equations.

**Continuity equation:**

$$\frac{\partial n}{\partial t} + \nabla \cdot (n\mathbf{u}) = 0$$

**Momentum equation (Navier–Stokes form):**

$$mn\left(\frac{\partial \mathbf{u}}{\partial t} + \mathbf{u} \cdot \nabla \mathbf{u}\right) = -\nabla P + ne\mathbf{E} + \eta \nabla^2 \mathbf{u} - \frac{mn}{\tau_{\text{imp}}}\mathbf{u}$$

where $P$ is pressure and $\eta$ is the viscosity, which acts as a momentum diffusion coefficient.

### 10.10.1 Viscous Flow

In steady state and linear response:

$$\eta \nabla^2 \mathbf{u} - \nabla P + ne\mathbf{E} = 0$$

This is analogous to classical viscous fluid flow.

### Poiseuille Flow

In a channel of width $W$, the velocity profile becomes parabolic:

$$u(y) \sim y(W - y)$$

leading to:

- Non-uniform current density across the channel.
- Enhanced conductivity compared to the diffusive regime because $e$-$e$ collisions allow electrons to avoid impurities by flowing collectively.

### Gurzhi Effect

A key signature of hydrodynamic transport is a decrease in resistivity as temperature increases:

$$\rho(T) \sim \frac{1}{\tau_{ee}} \sim T^{-2}$$

This occurs because higher $T$ reduces $l_{ee}$, making the fluid more “viscous" and better able to flow through the channel without being stopped by impurities, which is opposite to the behavior of normal metals.

### Key Insight

- Transport is a collective fluid phenomenon.
- Momentum-conserving collisions ($e$-$e$) dominate the dynamics.
- Viscosity and boundary conditions control the total resistance.

### Experimental Relevance

Hydrodynamic transport has been observed in high-mobility materials:

- Graphene.
- Ultrapure metals (e.g., $PdCoO_2$).
- Two-dimensional electron systems.

## 10.11 Limits of Boltzmann Theory

The semiclassical Boltzmann framework breaks down in the following regimes:

- **Quantum oscillations:** Landau quantization (Shubnikov–de Haas) is not captured
- **Localization:** Boltzmann theory assumes electrons are point particles and ignores their wave nature. Hence, phase-coherent interference effects are neglected
- **Strong magnetic fields:** when $\hbar\omega_c \gtrsim k_B T$, semiclassical transport fails.

# Chapter 11

# Landau Quantization

## 11.1 Introduction

We consider a charged particle (electron, charge $-e$) moving in a uniform magnetic field $\mathbf{B} = B\hat{z}$. Classically, the electron undergoes circular cyclotron motion with frequency:

$$\omega_c = \frac{eB}{m}.$$

Quantum mechanically, this motion is quantized, leading to discrete energy levels known as **Landau levels**.

### 11.1.1 Hamiltonian in a Magnetic Field

We ignore the spin of the electron for now. The single-particle Hamiltonian is obtained via minimal coupling:

$$\mathbf{p} \to \mathbf{p} - e\mathbf{A},$$
$$\mathcal{H} = \frac{1}{2m}\left(\mathbf{p} - e\mathbf{A}\right)^2.$$

We choose the **Landau gauge**:

$$\mathbf{A} = (0, Bx, 0),$$

so that:

$$\mathbf{B} = \nabla \times \mathbf{A} = B\hat{z}.$$

The Hamiltonian becomes:

$$\mathcal{H} = \frac{1}{2m}\left[p_x^2 + (p_y - eBx)^2 + p_z^2\right].$$

### 11.1.2 Reduction to Harmonic Oscillator

Since $p_y$ and $p_z$ commute with the Hamiltonian:

$$[p_y, \mathcal{H}] = 0, \quad [p_z, \mathcal{H}] = 0,$$

we can label eigenstates by $k_y$ and $k_z$:

$$p_y \to \hbar k_y, \quad p_z \to \hbar k_z.$$

We use the Landau ansatz:

$$\psi(x, y, z) = u(x) e^{ik_y y} e^{ik_z z}.$$

Substituting this into the Schrödinger equation $\mathcal{H}\psi = E\psi$, with

$$\mathcal{H} = \frac{1}{2m}\left[p_x^2 + (p_y - eBx)^2 + p_z^2\right],$$

we obtain an effective one-dimensional equation for $u(x)$:

$$\left[\frac{p_x^2}{2m} + \frac{1}{2m}(eBx + \hbar k_y)^2 + \frac{\hbar^2 k_z^2}{2m}\right] u(x) = E u(x).$$

Define the shifted coordinate:

$$x_0 = \frac{\hbar k_y}{eB},$$

so that:

$$eBx + \hbar k_y = eB(x - x_0).$$

Then the equation reduces to:

$$\left[\frac{p_x^2}{2m} + \frac{1}{2}m\omega_c^2(x - x_0)^2\right] u(x) = \left(E - \frac{\hbar^2 k_z^2}{2m}\right) u(x),$$

where the cyclotron frequency is:

$$\omega_c = \frac{eB}{m}.$$

This is precisely the Schrödinger equation of a harmonic oscillator centered at $x_0$.

Therefore, the eigenfunctions are:

$$u_n(x) = \frac{1}{\sqrt{2^n n!\,\sqrt{\pi}\,\ell_B}} \exp\left[-\frac{(x - x_0)^2}{2\ell_B^2}\right] H_n\left(\frac{x - x_0}{\ell_B}\right),$$

where $H_n$ are Hermite polynomials and

$$\ell_B = \sqrt{\frac{\hbar}{eB}} = \frac{25.6}{\sqrt{B[\mathrm{T}]}}\ \mathrm{nm}$$

is the magnetic length. In the semiclassical approximation, an electron with energy $\hbar\omega_C/2$ moves in real space in a circular orbit of radius $\ell_B$. The magnetic length is of the order of a few nm at $B \sim 10$ T and is thus much larger than the lattice constant.

The corresponding energy eigenvalues are:

$$E_{n,k_z} = \hbar\omega_c\left(n + \frac{1}{2}\right) + \frac{\hbar^2 k_z^2}{2m}, \qquad n = 0, 1, 2, \ldots$$

The kinetic energy of electrons in a 2-D system in the presence of a perpendicular magnetic field thus has two terms:

1. The first term is due to motion perpendicular to $B$ and is quantized in units of $\hbar\omega_C$.

2. The second term is the kinetic energy due to motion parallel to $B$, this is the same as at $B = 0$.

**Key observations**

- The energy is independent of $k_y$, implying a large degeneracy (see section 11.3).
- The center of the wavefunction, $x_0$, depends on $k_y$:

$$x_0 = -\frac{\hbar k_y}{eB}.$$

- Different $k_y$ values correspond to different guiding centers of the cyclotron orbit.
- The motion along $z$ is constrained by the physical dimensions of the material.
- Gauge choice changes wavefunctions, not energies.

## 11.2 Degeneracy of Landau Levels

A striking feature of the Landau level spectrum,

$$E_{n,k_z} = \hbar\omega_c \left(n + \frac{1}{2}\right) + \frac{\hbar^2 k_z^2}{2m},$$

is that it is independent of $k_y$. This implies that for a given Landau level index $n$ (and $k_z$), there exists a large number of distinct quantum states labeled by different values of $k_y$ that all share the same energy. This leads to a macroscopic degeneracy of each Landau level.

**Note:** Although the wavefunctions depend on the choice of gauge, the degeneracy is **gauge invariant**.

**Guiding center interpretation**

From the solution of the Schrödinger equation, the wavefunction is localized in the $x$-direction around $x_0 = k_y \ell_B^2$. Thus, different values of $k_y$ correspond to different guiding center positions $x_0$ of the cyclotron orbit. While the energy depends only on the Landau level index $n$, the degeneracy arises because the center of the orbit can be placed anywhere within the sample.

### Counting the degeneracy

Consider a rectangular sample of dimensions $L_x \times L_y$. Imposing periodic boundary conditions along $y$, the allowed values of $k_y$ are:

$$k_y = \frac{2\pi}{L_y} n_y, \qquad n_y \in \mathbb{Z}.$$

The corresponding spacing between adjacent guiding centers is:

$$\Delta x_0 = \frac{\hbar}{eB} \Delta k_y = \frac{\hbar}{eB} \frac{2\pi}{L_y}.$$

The guiding center must lie within the sample:

$$0 \leq x_0 \leq L_x.$$

This restricts the allowed values of $k_y$, and hence the number of distinct states in a Landau level is:

$$N = \frac{L_x}{\Delta x_0} = \frac{L_x L_y}{2\pi} \frac{eB}{\hbar}.$$

Thus, the degeneracy of each Landau level is:

$$N = \frac{A\, eB}{h}, \qquad A = L_x L_y.$$

Equivalently, the degeneracy per unit area is:

$$\frac{N}{A} = \frac{eB}{h}.$$

Including spin degeneracy (if Zeeman splitting is neglected), the total degeneracy becomes:

$$\frac{2eB}{h}.$$

### Flux quantum interpretation

The above result can be written in a particularly illuminating form:

$$N = \frac{\Phi}{\Phi_0}, \qquad \Phi = BA, \quad \Phi_0 = \frac{h}{e}.$$

Thus,

*The number of available states in a Landau level = the number of magnetic flux quanta threading the sample.*

Each quantum state occupies an area of order $2\pi\ell_B^2$. The degeneracy is **macroscopic**, scaling linearly with both system size and magnetic field. It reflects the fact that the cyclotron orbit can be centered anywhere in the sample without changing the energy.

As we shall see later, this degeneracy is at the heart of many phenomena, including the Quantum Hall effect (through the filling factor $\nu$) and Shubnikov–de Haas and de Haas–van Alphen oscillations.

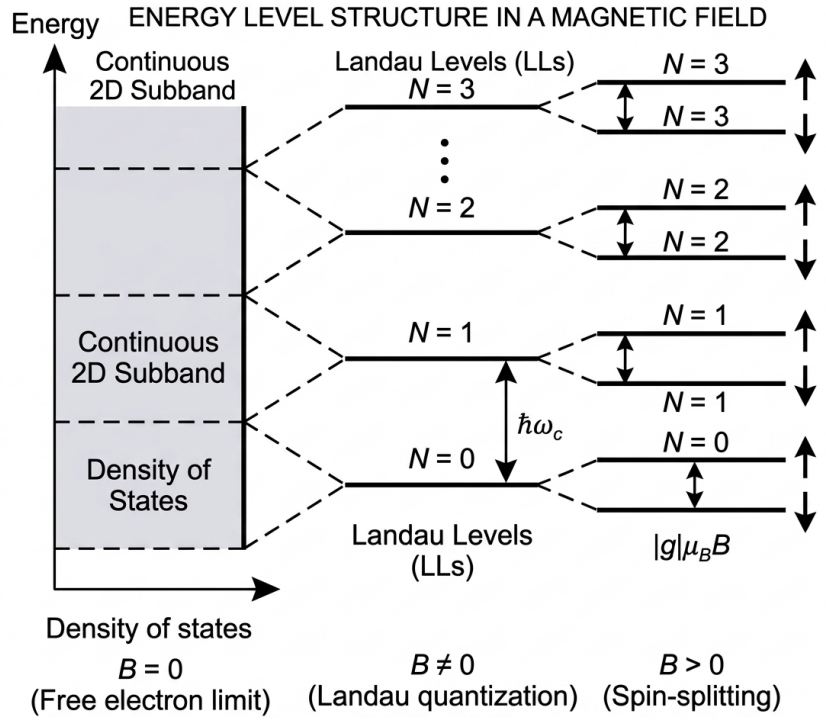


Figure 11.1: Landau levels

## 11.3 Density of States

In 2-D (no $k_z$ dispersion), the density of states is:

$$g(E) = \frac{eB}{h} \sum_n \delta\left(E - \hbar\omega_c\left(n + \frac{1}{2}\right)\right).$$

Thus, the continuous DOS is replaced by a series of delta-function peaks (Fig. 11.1). Including spin, each Landau level is split by the Zeeman energy

$$E_Z = g\mu_B B,$$

leading to two spin-resolved sublevels.

### 11.3.1 Effect of Disorder on DOS and Quantum Oscillations

In real systems, impurities, lattice imperfections, and interface roughness introduce disorder. As a result, the electron states acquire a finite lifetime $\tau$, leading to an energy uncertainty

$$\Gamma \sim \frac{\hbar}{2\tau}.$$

This replaces the delta-function peaks in the DOS by broadened Landau levels. A common phenomenological description is to replace the delta function by a normalized broadening function. Two widely used models are:

*(i) Lorentzian broadening:*

$$\delta(E - E_n) \;\to\; \frac{1}{\pi}\frac{\Gamma}{(E - E_n)^2 + \Gamma^2}.$$

*(ii) Gaussian broadening:*

$$\delta(E - E_n) \;\to\; \frac{1}{\sqrt{2\pi}\Gamma}\exp\left[-\frac{(E - E_n)^2}{2\Gamma^2}\right].$$

The density of states then becomes

$$g(E) = \frac{eB}{h}\sum_n D_\Gamma(E - E_n),$$

where $D_\Gamma$ is the chosen broadening function.

### Physical picture

Disorder converts each discrete Landau level into a *Landau band* of width $\Gamma$. Within each band, states near the band center are typically **extended** and contribute to transport, while those in the tails are **localized** due to disorder.

This distinction is crucial for understanding the quantum Hall effect: transport occurs only when the Fermi energy lies in extended states, while localized states do not contribute to longitudinal conductivity.

### Regimes

The relative magnitude of $\Gamma$ and the Landau level spacing $\hbar\omega_c$ determines the physics:

- $\Gamma \ll \hbar\omega_c$: well-separated Landau levels; strong quantum oscillations.
- $\Gamma \sim \hbar\omega_c$: overlapping levels; oscillations are damped.
- $\Gamma \gg \hbar\omega_c$: Landau quantization is washed out; DOS approaches the zero-field limit.

### Connection to quantum oscillations

The finite width $\Gamma$ leads to damping of oscillatory phenomena. In particular, the amplitude of Shubnikov–de Haas oscillations acquires the Dingle factor:

$$R_D = \exp\left(-\frac{\pi}{\omega_c\tau}\right) = \exp\left(-2\pi^2\frac{k_B T_D}{\hbar\omega_c}\right),$$

where $T_D = \Gamma/\pi k_B$ is the Dingle temperature. Measuring the decay of the amplitude of quantum oscillations with varying $B$ (or equivalently, varying $\omega_C$) at a given $T$ yields the value of disorder broadening $\Gamma$.

**Note:** Disorder broadening not only smoothens the density of states but also controls the visibility of quantum oscillations and the structure of quantum Hall plateaus.

### 11.3.2 Effect of Temperature on DOS and Quantum Oscillations

Thus far, we have treated the density of states as a function of energy alone. However, experimentally measurable quantities depend on how these states are occupied, which is controlled by temperature through the Fermi–Dirac distribution:

$$f(E) = \frac{1}{e^{(E-E_F)/k_BT} + 1}.$$

**Thermal broadening**

At finite temperature, sharp features in the density of states are smeared by the derivative of the Fermi function:

$$-\frac{\partial f}{\partial E} = \frac{1}{4k_BT} \operatorname{sech}^2\left(\frac{E - E_F}{2k_BT}\right).$$

Any experimentally relevant quantity (such as conductivity or magnetization) involves an energy average of the DOS weighted by $-\partial f/\partial E$. This introduces an effective thermal broadening of order $\sim k_BT$. Thus, even in a perfectly clean system ($\Gamma \to 0$), temperature alone can smear the Landau level structure.

**Effect on quantum oscillations**

Temperature reduces the amplitude of quantum oscillations through thermal averaging over the broadened distribution near the Fermi energy. This leads to the Lifshitz–Kosevich thermal damping factor:

$$R_T = \frac{X}{\sinh X}, \qquad X = \frac{2\pi^2 k_BT}{\hbar\omega_c}.$$

The factor $R_T$ quantifies the suppression of quantum oscillations due to finite temperature. It arises from thermal averaging of the oscillatory density of states with the derivative of the Fermi–Dirac distribution:

$$-\frac{\partial f}{\partial E}.$$

This derivative acts as a window function of width $\sim k_BT$, which smoothens the oscillatory structure.

**Limiting behavior**

- **Low temperature** ($k_BT \ll \hbar\omega_c$):

  $$R_T \approx 1,$$

  quantum oscillations are essentially unaffected.

- **High temperature** ($k_BT \gg \hbar\omega_c$):

  $$R_T \sim 2Xe^{-X},$$

  leading to exponential suppression of oscillations.

**Physical interpretation**

Thermal smearing mixes contributions from multiple Landau levels within an energy window $\sim k_B T$ around $E_F$. When this window becomes comparable to or larger than the Landau level spacing $\hbar\omega_c$, the oscillatory structure is averaged out.

### Combined effect of disorder and temperature

There are thus two independent sources of broadening:

- Disorder broadening: $\Gamma \sim \hbar/2\tau$
- Thermal broadening: $\sim k_B T$

In real systems, both disorder and temperature contribute multiplicatively to the suppression of oscillations. The dominant broadening mechanism is set by the larger of the two:

$$\text{Effective width} \sim \max(\Gamma,\, k_B T).$$

The oscillatory part of measurable quantities, such as resistivity or magnetization, thus typically takes the form:

$$\Delta R_{xx} \propto R_T\, R_D\, \cos\!\left(2\pi \frac{E_F}{\hbar\omega_c}\right),$$

Thus, by measuring the decay of oscillation amplitude with $T$, one can extract the effective mass via

$$\omega_c = \frac{eB}{m^*}.$$

## 11.4 Semiclassical Interpretation of Landau Quantization

While Landau quantization was derived exactly from the Schrödinger equation, it admits a powerful semiclassical interpretation that provides deeper physical insight and forms the basis for understanding quantum oscillations. (Some of what follows is a repeat of Section 11.4.1). The semiclassical equation of motion in the presence of a magnetic field $B$ is:

$$\hbar \frac{d\mathbf{k}}{dt} = -e\,\mathbf{v} \times \mathbf{B} \quad \text{(ignore band index for simplicity)}$$

**Consequences:**

1. We see that $d\mathbf{k}/dt \perp \mathbf{B}$. Hence, only the component of $\mathbf{k}$ perpendicular to $\mathbf{B}$ evolves with time, and $\mathbf{k}$ moves in a plane normal to $\mathbf{B}$.

2. The rate of change of energy is

$$\frac{d\varepsilon}{dt} = \frac{\partial\varepsilon}{\partial\mathbf{k}} \cdot \frac{d\mathbf{k}}{dt} = \hbar\mathbf{v} \cdot \frac{d\mathbf{k}}{dt} = -e\,\mathbf{v} \cdot (\mathbf{v} \times \mathbf{B}) = 0.$$

   Thus, the magnetic field does no work on the electron.

The consequences relevant to our discussion are:

- The electron energy remains constant.
- $\mathbf{k}$ is confined to a constant-energy surface $\varepsilon(\mathbf{k}) = \text{const}$, and to a plane perpendicular to $\mathbf{B}$.
- The real-space path $\mathbf{r}_\perp$ and the $\mathbf{k}$-space path $\mathbf{k}$ are related by a rotation of 90° and a scaling factor $\ell_B^2 = \hbar/(eB)$. The length scale $\ell_B$ is called the **magnetic length**(Fig. 6.2).

### 11.4.1 The Onsager Quantization Condition

The quantization of the electron orbit in phase space is given by the Bohr-Sommerfeld Condition:

$$\oint \mathbf{p} \cdot d\mathbf{r} = (n + \gamma)2\pi\hbar \tag{11.1}$$

where $\mathbf{p} = \hbar\mathbf{k} - e\mathbf{A}$ is the canonical momentum, $n$ is an integer (the Landau level index), and $\gamma$ is a phase offset incorporating the Maslov index and the Berry phase.

#### Evaluating the Integral

Expanding the canonical momentum integral:

$$\oint \hbar\mathbf{k} \cdot d\mathbf{r} - \oint e\mathbf{A} \cdot d\mathbf{r} = (n + \gamma)2\pi\hbar \tag{11.2}$$

Using the equation of motion $\hbar d\mathbf{k} = -e(d\mathbf{r} \times \mathbf{B})$, we relate the real-space path to the $\mathbf{k}$-space path:

$$d\mathbf{r} = \frac{\hbar}{eB}(d\mathbf{k} \times \hat{z}) \tag{11.3}$$

For the first term:

$$\oint \hbar\mathbf{k} \cdot d\mathbf{r} = \oint \hbar\mathbf{k} \cdot \left[\frac{\hbar}{eB}(d\mathbf{k} \times \hat{z})\right] = \frac{\hbar^2}{eB}\oint (\mathbf{k} \times d\mathbf{k}) \cdot \hat{z} = \frac{2\hbar^2}{eB}A_k \tag{11.4}$$

where $A_k$ is the area enclosed by the orbit in $\mathbf{k}$-space.

For the second term, using Stokes' Theorem and the relation between real-space area $A_r$ and $\mathbf{k}$-space area $A_k$:

$$\oint e\mathbf{A} \cdot d\mathbf{r} = e\Phi = eBA_r = eBA_k\left(\frac{\hbar}{eB}\right)^2 = \frac{\hbar^2}{eB}A_k \tag{11.5}$$

### Resulting Quantization Condition

Subtracting the two terms yields:

$$\frac{2\hbar^2}{eB}A_k - \frac{\hbar^2}{eB}A_k = (n+\gamma)2\pi\hbar \tag{11.6}$$

Solving for $A_k$ gives the final expression:

$$A_k(\epsilon_n, k_z) = \frac{2\pi eB}{\hbar}(n+\gamma) \tag{11.7}$$

Increment in $B$ that causes successive allowed orbits in $k$-space of the same area on the Fermi surface is

$$\Delta\left(\frac{1}{B}\right) = \frac{2\pi e}{\hbar A_F},$$

where $A_F$ is the extremal cross-sectional area of the Fermi surface.

The above result implies that any physical properties of the material that depend on the area enclosed by the orbit in **k**-space will oscillate as a function of $1/B$. Thus, measurement of the oscillation period $\Rightarrow$ gives $A_F$. This allows the Fermi surface to be mapped.

**Summary:**

- Electron motion in a magnetic field is along a constant energy surface
- Orbits in **k**-space are quantized
- Quantization condition depends on enclosed area
- Physical quantities oscillate as a function of $1/B$

## 11.4.2 Quantization of Magnetic Flux through Real-Space Orbits

From section 6.5.1, the real-space path and the **k**-space path are related by a rotation of 90° and a scaling factor $\hbar/eB$. This implies that the real-space area $A_r$ enclosed by the electron orbit is related to the **k**-space area $A_k$ by:

$$A_r = \left(\frac{\hbar}{eB}\right)^2 A_k \tag{11.8}$$

The magnetic flux $\Phi$ threading the real-space orbit is given by:

$$\Phi = B \cdot A_r = B \cdot \left(\frac{\hbar}{eB}\right)^2 A_k = \frac{\hbar^2}{e^2 B}A_k \tag{11.9}$$

### Substituting the Onsager Condition

We substitute the previously derived Onsager quantization condition, $A_k = \frac{2\pi eB}{\hbar}(n+\gamma)$, into our expression for $\Phi$:

$$\Phi = \frac{\hbar^2}{e^2 B}\left[\frac{2\pi eB}{\hbar}(n+\gamma)\right] \tag{11.10}$$

## Final Quantized Result

Simplifying the terms, we obtain:

$$\Phi = \frac{2\pi\hbar}{e}(n+\gamma) \tag{11.11}$$

Recognizing that the magnetic flux quantum is defined as $\Phi_0 = \frac{h}{e} = \frac{2\pi\hbar}{e}$, we arrive at the final result:

$$\Phi = (n+\gamma)\Phi_0 \tag{11.12}$$

This confirms that the magnetic flux through the real-space orbit is quantized in integer (or semi-integer, depending on $\gamma$) multiples of the fundamental flux quantum $\Phi_0$.

### Free electron case

For free electrons:

$$\varepsilon = \frac{\hbar^2 k^2}{2m}, \quad A_k(\epsilon_n, k_z) = \pi k^2 = \frac{2\pi m E}{\hbar^2}.$$

Substituting into the quantization condition:

$$\frac{2\pi m E}{\hbar^2} = 2\pi\frac{eB}{\hbar}\left(n+\gamma\right),$$

which gives:

$$E_n = \hbar\omega_c\left(n+\gamma\right), \qquad \omega_c = \frac{eB}{m}.$$

Comparison with the exact quantum result:

$$E_n = \hbar\omega_c\left(n+\frac{1}{2}\right),$$

shows that:

$$\gamma = \frac{1}{2}.$$

This 1/2 shift arises from the zero-point motion of the harmonic oscillator.

### Connection to quantum oscillations

As the magnetic field is varied, the condition for a Landau level to cross the Fermi energy $E_F$ is:

$$A_k(\epsilon_F) = 2\pi\frac{eB_n}{\hbar}\left(n+\gamma\right).$$

Rewriting:

$$\Delta\left(\frac{1}{B}\right) = \frac{2\pi e}{\hbar A_F},$$

where $A_F$ is the extremal cross-sectional area of the Fermi surface. Thus, physical quantities oscillate periodically in $1/B$ with frequency:

$$F = \frac{\hbar}{2\pi e} A_F.$$

This semiclassical framework provides the foundation for analyzing quantum oscillations in real materials as $F$ is the fundamental frequency of:

- de Haas–van Alphen effect (magnetization oscillations)
- Shubnikov–de Haas effect (transport oscillations)

**Physical interpretation**

- Landau quantization corresponds to the quantization of closed orbits in momentum space.
- The spacing between Landau levels reflects the area increment $\Delta A_k(\epsilon_n, k_z) = 2\pi eB/\hbar$.
- Only orbits near the Fermi surface contribute to observable oscillations.
- The phase factor $\gamma$ encodes topological information (e.g., Berry phase corrections in Dirac systems).

### 11.4.3 Landau Levels in 2D Electron Gas

**Landau levels in two dimensions and filling factor**

In a two-dimensional electron system, the motion along the magnetic field is absent, and the energy spectrum reduces to a discrete set of Landau levels:

$$E_n = \hbar\omega_c \left(n + \frac{1}{2}\right), \qquad n = 0, 1, 2, \ldots$$

Each Landau level is highly degenerate. As shown earlier, the number of available states in a given Landau level is proportional to the magnetic flux through the sample:

$$N = \frac{eB}{h} A,$$

where $A$ is the area of the system. Thus, the degeneracy per unit area is $eB/h$, reflecting the fact that each Landau level can accommodate one electron per magnetic flux quantum.

For a system with electron density $n_e = N_e/A$, it is useful to define the dimensionless **filling factor**:

$$\nu = \frac{n_e}{(eB/h)} = \frac{n_e h}{eB}.$$

The filling factor $\nu$ represents the number of completely filled Landau levels. When $\nu$ is an integer, an integer number of Landau levels are fully occupied, while higher levels remain empty. When $\nu$ is non-integer, the highest occupied Landau level is only partially filled.

**Physical meaning:** The filling factor directly counts how many Landau levels are occupied by the electrons and therefore provides a natural measure of the electronic state in a magnetic field. It plays a central role in magnetotransport phenomena, particularly in the quantum Hall effect.

## 11.5 Introduction to the Symmetric Gauge

In previous discussions, we utilized the **Landau gauge** (e.g., $\mathbf{A} = (0, Bx, 0)$ or $\mathbf{A} = (-By, 0, 0)$). While these are useful for systems with translational symmetry, the **Symmetric Gauge** is preferred for systems exhibiting circular symmetry. Furthermore, this gauge is essential for the later studies of the **Integer Quantum Hall Effect (IQHE)** and the **Fractional Quantum Hall Effect (FQHE)**.

For a constant magnetic field $B$ in the $\hat{z}$ direction, the vector potential in the symmetric gauge is defined as:

$$\mathbf{A} = \frac{1}{2}(\mathbf{r} \times \mathbf{B}) \tag{11.13}$$

In Cartesian components, this is expressed as:

$$\mathbf{A} = \left(-\frac{1}{2}By, \frac{1}{2}Bx, 0\right) \tag{11.14}$$

The validity of this potential is verified by taking the curl, $\nabla \times \mathbf{A} = B\hat{z}$, confirming a uniform magnetic field while maintaining rotational symmetry.

### 11.5.1 Hamiltonian and Operator Algebra

The Hamiltonian for an electron in a magnetic field is given by:

$$H = \frac{(\mathbf{p} - e\mathbf{A})^2}{2m} = \frac{\boldsymbol{\pi}^2}{2m} \tag{11.15}$$

where $\boldsymbol{\pi} = \mathbf{p} - e\mathbf{A}$ represents the **mechanical (canonical) momentum**. Unlike the components of the standard linear momentum, the components of $\boldsymbol{\pi}$ do not commute:

$$[\pi_x, \pi_y] = \frac{i\hbar^2}{l_B^2} \tag{11.16}$$

where $l_B = \sqrt{\frac{\hbar}{eB}}$ is the **magnetic length**. Expanding the Hamiltonian in terms of these components:

$$H = \frac{1}{2m}\left[\left(p_x + \frac{eBy}{2}\right)^2 + \left(p_y - \frac{eBx}{2}\right)^2\right] \tag{11.17}$$

To solve for the energy spectrum, we define ladder operators analogous to the quantum harmonic oscillator:

$$a = \frac{l_B}{\sqrt{2}\hbar}(\pi_x - i\pi_y), \quad a^\dagger = \frac{l_B}{\sqrt{2}\hbar}(\pi_x + i\pi_y) \tag{11.18}$$

These operators satisfy the bosonic commutation relation $[a, a^\dagger] = 1$. The Hamiltonian transforms into:

$$H = \hbar\omega_c \left(a^\dagger a + \frac{1}{2}\right) \tag{11.19}$$

where $\omega_c = \frac{eB}{m}$ is the cyclotron frequency. The energy eigenvalues are $E_n = \hbar\omega_c(n + \frac{1}{2})$, demonstrating that the energy spectrum is gauge-invariant.

## 11.6 Degeneracy and Angular Momentum

In the Landau gauge, the degeneracy of Landau levels is associated with linear momentum. In the symmetric gauge, the **Angular Momentum** $L_z$ is the conserved quantity, as $[H, L_z] = 0$. We define $L_z$ in terms of coordinates and mechanical momenta:

$$L_z = -\frac{\hbar}{2l_B^2}(x^2 + y^2) + \frac{l_B^2}{2\hbar}(\pi_x^2 + \pi_y^2) \tag{11.20}$$

In terms of the ladder operators $a$ and a second set of operators $b, b^\dagger$ (which act within the degenerate subspace), $L_z$ is:

$$L_z = \hbar(a^\dagger a - b^\dagger b) \tag{11.21}$$

The eigenstates are labeled by $|n, m\rangle$, where $n$ is the Landau level index and $m$ is the angular momentum quantum number. The wavefunctions for the **Lowest Landau Level (LLL)** ($n = 0$) in terms of the complex coordinate $z = x + iy$ are:

$$\psi_{LLL}(z) \propto z^m e^{-|z|^2/4l_B^2} \tag{11.22}$$

The total degeneracy $G$ per Landau level is determined by the number of flux quanta $\Phi_0 = \frac{h}{e}$ threading the area $A$:

$$G = \frac{\Phi}{\Phi_0} = \frac{BA}{h/e} \tag{11.23}$$

The filling fraction is defined as $\nu = \frac{N}{G} = \frac{nh}{eB}$, where $n$ is the electron density.

## 11.7 Landau Diamagnetism

We now use the Landau level spectrum to calculate the magnetic response of a free electron gas. The central idea is that, in a magnetic field, the electronic density of states becomes quantized into Landau levels, and the total energy is obtained by filling these levels up to the Fermi energy $E_F$.

For a three-dimensional electron gas in a magnetic field $\mathbf{B} = B\hat{z}$, the energy spectrum is:

$$E_{n,k_z} = \hbar\omega_c \left(n + \frac{1}{2}\right) + \frac{\hbar^2 k_z^2}{2m}, \qquad \omega_c = \frac{eB}{m}.$$

Each Landau level has a degeneracy per unit area $eB/h$, so that the total number of states is proportional to $B$. As a result, both the density of states and the total energy become functions of the magnetic field.

### Total energy

At zero temperature, all states are filled up to the Fermi energy. The total energy per unit volume can be written as:

$$U(B) = \frac{eB}{h} \sum_n \int \frac{dk_z}{2\pi} E_{n,k_z}\, \Theta(E_F - E_{n,k_z}),$$

where $\Theta$ is the step function.

The presence of the discrete Landau levels introduces an oscillatory structure in $U(B)$ as a function of $B$, since the condition for a Landau level to cross the Fermi energy depends periodically on $1/B$. These oscillations give rise to the well-known:

- **de Haas–van Alphen effect**: oscillations in magnetization,
- **Shubnikov–de Haas effect**: oscillations in transport.

### Separation into smooth and oscillatory parts

The total energy can be separated into a smooth (average) part and an oscillatory part:

$$U(B) = U_0 + \Delta U_{\text{smooth}}(B) + \Delta U_{\text{osc}}(B).$$

The oscillatory contribution is responsible for quantum oscillations, while the smooth part gives the average magnetic response, known as **Landau diamagnetism**.

To extract the smooth part, we replace the discrete sum over Landau levels by an integral using the Euler–Maclaurin formula. This amounts to averaging over the oscillations and retaining only the leading correction in $B$.

### Evaluation of the smooth energy shift

Carrying out this procedure (details omitted here), one finds that the leading field-dependent correction to the energy density is quadratic in $B$:

$$\Delta U_{\text{smooth}}(B) = \frac{1}{2}\chi_L B^2.$$

The magnetization is then obtained from:

$$M = -\frac{\partial U}{\partial B},$$

and the magnetic susceptibility is:

$$\chi = \mu_0 \frac{\partial M}{\partial B}.$$

Evaluating the derivatives, one finds that the orbital motion of electrons produces a diamagnetic response:

$$\chi_L = -\frac{1}{3}\mu_0 \mu_B^2 g(E_F),$$

where $g(E_F)$ is the density of states at the Fermi energy.

### Relation to Pauli paramagnetism

Recall that the Pauli spin susceptibility is:

$$\chi_P = \mu_0 \mu_B^2 g(E_F).$$

Thus, for free electrons:

$$\chi_L = -\frac{1}{3}\chi_P.$$

### Physical interpretation

Landau diamagnetism arises from the quantization of orbital motion in a magnetic field. As the magnetic field increases, the spacing between Landau levels increases, which raises the total kinetic energy of the electron gas. The system responds by developing a magnetization that opposes the applied field, in accordance with Lenz's law.

In contrast to Pauli paramagnetism, which originates from spin alignment near the Fermi surface, Landau diamagnetism is an orbital effect involving all occupied states. However, due to cancellations in the bulk of the Fermi sea, the net response is governed by states near the Fermi energy.